



Crystallization of the Glassy Grain Boundary Phase in Silicon Nitride Ceramics

Charles H. Drummond, III
Department of Materials Science and Engineering

National Aeronautics and Space Administration
Lewis Research Center

Grant No. NAG3-824, Supp. 1 & 2
Final Report

August 1991

111-16-02R
111-16-02R
(144)
30452

p. 77





Crystallization of the Glassy Grain Boundary Phase in Silicon Nitride Ceramics

Charles H. Drummond, III
Department of Materials Science and Engineering

National Aeronautics and Space Administration
Lewis Research Center

Grant No. NAG3-824, Supp. 1 & 2
Final Report
RF Project No. 766445/720238

August 1991

During the time period of the grant (October 15, 1987 - December 31, 1990) four students completed Master's Theses, six presentations were made, six papers were published, and three are in the process of being submitted for publication. The lists of the students and their theses, the presentations and the publications are shown on the attached pages. The reprints of the papers and the drafts of the papers to be submitted are also attached. Copies of the theses have been given to Mr. William A. Sanders at NASA Lewis Research Center.

The work conducted under this grant has concentrated on understanding the role of the intergranular glassy phase in silicon nitride as-processed with yttria as a sintering aid at Lewis Research Center. The microstructure, crystallization, and viscosity of the glassy phase were the areas studied. Crystallization of the intergranular glassy phase to more refractory crystalline phases should improve the high temperature mechanical properties of the silicon nitride. The addition of a nucleating agent will increase the rate of crystallization. The measurement of the viscosity of the glassy phase will permit the estimation of the high temperature deformation of the silicon nitride.

Summarizing the results, a study of the crystallization of the various polymorphs of $Y_2Si_2O_7$ may have provided more questions than answers. The phases that formed at various heat treatments were not always in agreement with the phases reported by other investigators. Some of the factors which complicated the analysis were the different quench rates used after melting the material, the role of dissolved nitrogen in the melts, the presence of W from the crucibles used to melt the material, and the partial crystallization of the melts prior to the heat treatment studies. Furthermore, when comparing the results from melts with those from crystallization of the intergranular glassy phase in as-processed silicon nitride, the possible differences in composition, the role of nitrogen dissolved in the glass and the possible nucleation effects of the silicon nitride grains provided additional complications.

In general, the expected polymorphs crystallized. The transformation to other phases with heat treatment again generally followed the expected form, but in both cases there were exceptions and the formation of metastable polymorphs in temperature ranges outside the reported ranges occurred. In silicon nitride the crystallization resulted in the formation of dislocations which were subsequently annealed out. The addition of zirconia as a nucleating agent favored the crystallization of the beta phase and this result is analogous to the same result in the crystallization of the intergranular glass in silicon nitride in which the beta phase is formed. The measurements of the viscosity of silicon



nitride with varying amounts of glassy phase provided an estimate of the viscosity of the intergranular glass. However, the results are clouded by the partial crystallization of the glass during measurement, the high volume fraction of the crystalline phase, and the use of a model system, a borosilicate glass with alumina, to calculate the viscosity. Regardless of these limitations, the viscosity values obtained are the first ones reported and give an order of magnitude estimate for these yttrium-silicate glasses.



STUDENTS AND THE TITLES OF THESES

1. Gregory E. Hilmas, "Crystallizing the Grain Boundary Glass in Silicon Nitride Ceramics" (1989).
2. Kathryn Kuechelmann, "Crystallization of the Yttria Silicate Intergranular Phases in Silicon Nitride with Zirconia Additions" (1990).
3. Suresh Kumar, "Crystallization in Yttrium Silicate Glasses" (1989).
4. Mark B. Dittmar, "Viscosity Measurement of Silicon Nitride using a Beam Bending Viscometer" (1990).



PRESENTATIONS

1. W. E. Lee, C. H. Drummond, III, G. E. Hilmas, J. D. Kiser and W. A. Sanders, "Microstructural Evolution on Crystallizing the Glassy Phase in 6.6 Weight % $Y_2O_3-Si_3N_4$ Ceramics," 12th Annual Conference on Composites and Advanced Ceramic Materials, Cocoa Beach, FL January 17-22, 1988.
2. C. H. Drummond, III, W. E. Lee, W. A. Sanders, and J. D. Kiser, "Crystallization and Characterization of $Y_2O_3-SiO_2$ Glasses," 12th Annual Conference on Composites and Advanced Materials, Cocoa Beach, FL January 17-22, 1988.
3. S. Kumar, W. E. Lee and C. H. Drummond, III, "Crystallization in Yttrium Silicate Glasses in Si_3N_4 ," Bull. Am. Ceram. Soc. 67 [3] 624 (1988).



4. C. H. Drummond, III, "Glass Formation and Crystallization in High-Temperature Glass-Ceramics and Si_3N_4 ," XV International Congress on Glass, Leningrad, USSR 1989.
5. K. A. Kuechelmann and C. H. Drummond, III, "Crystallization of the Intergranular Glassy Phase in Si_3N_4 with 6wt% Y_2O_3 and Added ZrO_2 ," 92nd Annual Meeting, American Ceramic Society, Dallas, TX, April 22-26, 1990.
6. Mark B. Dittmar and Charles H. Drummond, III, "Measurement of the Viscosity of the Intergranular Glass Phase in Yttria-Sintered Silicon Nitride," Second International Ceramic Science and Technology Congress, Orlando, FL November 12-15, 1990.



PUBLICATIONS

1. C. H. Drummond, III, W. E. Lee, W. A. Sanders, and J. D. Kiser, "Crystallization and Characterization of Y_2O_3 - SiO_2 Glasses," *Ceram. Eng. Sci. Proc.*, **9** [9-10] 1343-54 (1988).
2. W. E. Lee, C. H. Drummond, III, G. E. Hilmas, J. D. Kiser and W. A. Sanders, "Microstructural Evolution on Crystallizing the Glassy Phase in 6.6 Weight % Y_2O_3 - Si_3N_4 Ceramics," *Ceram. Eng. Sci. Proc.*, **9** [9-10] 1355-65 (1988).
3. G. E. Hilmas and W.E. Lee, "Crystallizing $Y_2Si_2O_7$ at the Grain Boundaries of a Si_3N_4 Ceramic," pp 608-9 in *Proceedings of 46th Annual Meeting of Electron Microscopy Society of America*, ed. G. W. Bailey, San Francisco Press, San Francisco, CA (1988).
4. W. E. Lee and G. Hilmas, "Microstructural Changes in Beta Silicon Nitride Grains Upon Crystallization in the Intergranular Glass," *J. Am. Ceram. Soc.* **72**[10] 1931-37 (1989).



5. W. E. Lee, C. H. Drummond, III, G. E. Hilmas, and S. Kumar, "Microstructural Evolution in Near-Eutectic Yttrium Silicate Compositions Fabricated from a Bulk Melt and as an Intergranular Phase in Silicon Nitride," J. Am. Ceram. Soc., **73** [12] 3575-79 (1990).

6. C. H. Drummond, III, "Glass Formation and Crystallization in High-Temperature Glass-Ceramics and Si_3N_4 ," J. Non-Cryst. Solids, **123** 114-28 (1990).



PUBLICATIONS TO BE SUBMITTED

1. Suresh Kumar and Charles H. Drummond, III, "Crystallization of Various Compositions in the Y_2O_3 - SiO_2 System."
2. Mark B. Dittmar and Charles H. Drummond, III, "Indirect Measurement of the Viscosity of the Intergranular Glass Phase in Yttria-Sintered Silicon Nitride."
3. Kathryn A. Kuechelmann and Charles H. Drummond, III, "Crystallization of the Yttria Silicate Intergranular Phase in Silicon Nitride with Zirconia Additions."





Publications



110 110
N91-31962

Ceram. Eng. Sci. Proc., 9 [9-10] pp. 1343-1354 (1988)

Crystallization and Characterization of Y_2O_3 - SiO_2 Glasses

C. H. DRUMMOND III AND W. E. LEE

The Ohio State University
Columbus, OH

W. A. SANDERS AND J. D. KISER

NASA Lewis Research Center
Cleveland, OH

Results of crystallization studies on glasses with 20-40 mol% Y_2O_3 in the Y_2O_3 - SiO_2 system are presented. Glasses were melted in W crucibles at 1900°C-2100°C in 1 and 50 atm N_2 . Phase identification by X-ray diffraction and TEM indicated crystallization of the δ , γ , γ' and β - $Y_2Si_2O_7$, depending on melting and quenching conditions. Characterization of glasses was by differential thermal analysis (DTA), thermal gravimetric analysis (TGA) and chemical analysis including energy dispersive spectroscopy in the TEM. Heat treatment in an air atmosphere from 1100°-1600°C increased the amount of crystallization and resulted in formation of $Y_2Si_2O_7$, cristobalite and polymorphs of $Y_2Si_2O_7$. The effect of 5 and 10 wt% ZrO_2 additions on crystallization was also studied.

Introduction

The use of high-temperature materials in applications such as gas turbine engines requires that the material not only be able to withstand the high temperatures, but also maintain acceptable mechanical properties during use at these temperatures, but also maintain acceptable mechanical properties during use at these temperatures or in cycling to these temperatures. Silicon nitride continues to receive extensive study as one possible material. We report here results on the crystallization of bulk glasses similar in composition to those found in the intergranular glassy grain boundary phases of sintered silicon nitride with yttria as the sintering aid. The silicon nitride composition studied contained a 6% by weight addition of Y_2O_3 to the starting silicon nitride powder as processed by NASA Lewis.¹ This composition lies in the Si_3N_4 - $Y_2Si_2O_7$ - Si_2N_2O triangle of the phase diagram² in Fig. 1. Since this powder contains silica present as a thin layer on each Si_3N_4 grain plus that resulting from addition to the starting powders or from possible oxidation during grinding, the exact composition of the intergranular glassy phase is difficult to determine.

Improvement in the high-temperature mechanical properties may result upon crystallization of a higher-melting-point crystalline phase from the glassy grain boundary phase. Crystallization of the glassy phase may be facilitated by the addition of a nucleating agent or by the alteration of the composition.

Review of Y_2O_3 - SiO_2 Crystalline Phases

The diffraction data on $Y_2Si_2O_7$ crystalline polymorphs have been summarized by Liddel and Thompson.³ A review of the available data and some



of their own indicated that there are four polymorphs: α , β , γ , and δ . The low temperature polymorph, α , transforms to β as the temperature is increased. Figure 2 gives the temperature of the transformations and the densities of the various polymorphs of $Y_2Si_2O_7$. The structure of all polymorphs consists of $Si_2O_7^{4-}$ units. The X-ray powder diffraction file indicates that there are two different patterns of the γ phase, which are designated γ (JCPDS: 20-1416) and γ' (32-1448) in this paper. There are several polymorphs of the $Y_2Si_2O_7$ phase as discussed by Liddel and Thompson.³ The existence of the $2Y_2O_3 \cdot 3SiO_2$ phase as shown in the published phase diagram⁴ has not been confirmed, and, in fact, the existence of such a phase has been questioned.³ The volume change associated with the polymorphic inversions of $Y_2Si_2O_7$ is as large as 6.7% and may be significant in the crystallization of intergranular glassy grain boundary phases in silicon nitride (see these proceedings).⁵ The density of these glasses has not been reported.

Experimental Procedure

Reagent grade silica and yttrium oxide were ball milled for four hours with HSPN grinding media in dry alcohol and dried. The powder was dry milled for two hours then pressed into pellets and placed in tungsten crucibles for melting in a high-pressure nitrogen furnace.⁶ Powders were melted from 1900° to 2100°C, depending on the composition, and were held for four hours under 50 atm nitrogen. Additional melts were also made in 1 atm nitrogen. No difference in properties or crystallization behavior was observed between these two melting conditions. In some cases repeated melts were made in the same crucible by the addition of more pellets. In general, this procedure of repeated melts in the same crucible is not recommended because the crucible sometimes cracked and physical and chemical alteration of the melt was observed, perhaps because of the initiation of reactions which resulted in the deposition of tungsten or volatilization of silica from the melt. It was necessary to break the crucibles to remove the melt. The as-melted samples were X-rayed to identify crystalline phases formed on cooling. Additional heat treatments on as-melted material were carried out in air from 1100°–1600°C and followed by phase identification using X-ray diffraction and TEM (transmission electron microscopy).

The compositions melted ranged from 20–40 mol% Y_2O_3 . This compositional range is centered around the lower temperature eutectic region shown in Fig. 3, which is a modified version of the Y_2O_3 - SiO_2 phase diagram without inclusion of the Y_2S_3 phase. This range covers compositions observed in the intergranular glassy grain boundary phase in as-processed NASA Lewis silicon nitride, assuming the absence of nitrogen within the glass. The exact chemical analysis of this phase is difficult to determine because the EDS (energy dispersive spectroscopy) system on the TEM at NASA Lewis has a Be window, which precludes soft X-rays such as those that arise from O or N. In earlier studies on these materials,¹ no crystallization of nitrated crystalline phases was observed. This may have been due to incomplete crystallization for the given heat treatment of the material or to the inherent difficulties of crystallizing small amounts of glassy material.⁷

The primary glass composition studied was designated GSI. This is the eutectic composition between SiO_2 and $Y_2Si_2O_7$, and is similar to the intergranular glassy grain boundary composition without nitrogen in the as-processed 6Y silicon nitride. The formulation and as-melted composition is

given in Table I. The presence of tungsten will be discussed in the results section. Less than 0.2% nitrogen was found, indicating that little nitrogen was dissolved in the melt as a result of the 50 atm nitrogen overpressure. In addition, a GSII composition was melted containing 52 wt% Y_2O_3 and 48% SiO_2 and a $Y_2Si_2O_7$ composition. The GSZ5 and GSZ10 compositions are the same as GSI with 5 and 10 wt% ZrO_2 added as a nucleating agent. A $2Y_2O_3 \cdot 3SiO_2$, (Y2S3), composition was also melted to determine the stability of this crystalline phase.

Results

In all cases X-ray diffraction of the as-quenched melt indicated partial crystallization. The diffraction pattern from the as-melted GSI is shown in Fig. 4. The melt is amorphous but with a considerable amount of δ - $Y_2Si_2O_7$ phase present. Even in the case of sol-gel derived glasses at lower temperatures, partial crystallization was observed. Most of the melts contained the δ phase, as would be expected from a rapid quench of the melts. However, in some cases the γ and β phases were observed. A satisfactory explanation cannot be given. The quench obtained in these melts was not a rapid one—estimated to be $270^\circ/\text{min}$. The furnace did not permit the more rapid quench that might have been obtained, for example, by pouring into a liquid. Exactly what melting and quenching conditions would result in the formation of the lower temperature polymorphs is not known. In some cases reheating of the melt might contribute to the existence of lower temperature polymorphs at higher temperatures, or the presence of tungsten in the melts may serve as a nucleating agent.

The GSII composition was phase separated on melting, which is expected from the phase diagram. The only exception to the partial crystallinity of the as-melted material was the Y2S3 composition which X-rayed amorphous (Fig. 5). Further experiments are being carried out to confirm this result. The GSZ5 and GSZ10 compositions consisted of β - and γ - $Y_2Si_2O_7$, respectively together with cubic ZrO_2 .

The as-melted GSI composition produced β -, γ -, and δ - $Y_2Si_2O_7$ for different melts. Results of heat treatment of these melts are shown in Fig. 6. The X-ray diffraction pattern for a heat treatment of 24 h at 1300°C is given in Fig. 7. In this case it would appear that all of the δ phase did not transform. In Fig. 8, a TEM micrograph of the GSI composition heat treated for 4 h at 1600°C shows the presence of SiO_2 glass and δ - $Y_2Si_2O_7$, as expected from the phase diagram. The temperature range of these heat treatments was 1100° – 1600°C , and times ranged from the initial melt to 43 h. In general, the expected phases were formed, but in some cases metastable phases existed for long periods of time at a given temperature. Cristobalite was not present in sufficient amounts to be observed by X-ray diffraction but was identified by TEM. There was some evidence that the initial crystalline phases formed from the as-quenched melt may have determined the subsequent crystal phases formed. Further work needs to be done to clarify these results.

The results of heat treatment of the GSZ compositions containing 5 and 10 wt% ZrO_2 are shown in Fig. 9. For the GSZ5 composition β - $Y_2Si_2O_7$ was always observed with the cubic ZrO_2 . In GSZ10 various phases crystallized including the γ and δ phases. The YS2 and Y2S3 results are shown in Fig. 10. Crystallization of Y_2SiO_5 and δ - $Y_2Si_2O_7$ at 1600°C are the phases expected from the phase diagram with no formation of crystalline $2Y_2O_3 \cdot 3SiO_2$, as shown

in the diffraction pattern in Fig. 11. Crystallization of a polymorph at temperatures above its conversion temperature is unexplained. It may have been due to formation of crystal nuclei on cooling from the melt and subsequent growth during heat treatment. Further crystallization studies are underway to better define the range of temperature stability of these polymorphs.

One of the more troublesome aspects of this investigation was the presence of tungsten in the melts. Obtaining a satisfactory crucible material was difficult. Materials tried included Pt, Rh, Ir and various alloys of these elements, BN, SiC, and Si₃N₄. None of these materials resulted in melts without dissolution and chemical alteration of the melt or the crucible material. Chemical analysis indicated that tungsten concentrations in the range 0.10–0.80 wt% were dissolved or precipitated in the melts. In some cases, tungsten was deposited on the sides of the crucible or on the melt surface. It is not clear how this formed, but a possible mechanism is oxidation of tungsten to form a vapor which then deposited and decomposed to tungsten. Since little oxidation of tungsten used as shields in the furnace was observed, the concentration of oxygen in the furnace must have been very low. At these temperatures the vapor pressure of tungsten is too low to account for vapor transport of the tungsten metal. It is also possible that tungsten may have dissolved in the melts when liquid.

The TGA scan shown in Fig. 12 for a GSZ5 composition to 1800 °C indicates a 40% weight loss, most likely due to the volatilization of SiO. Melting was indicated at 1750 °C and a crystallization on cooling at 1450 °C. No crystallization or polymorphic inversions were observed on heating nor was there any indication of a glass transition. On cooling again, no polymorphic inversions were observed. Further studies are in progress to see if any crystallization can be detected by heat treatment during a DTA scan or in isothermal holds. DTA results on the GSZ compositions indicated possible crystallization on heating, but these results need to be examined further. It may be of interest to investigate other nucleating agents; however, most would lower the refractoriness of the glassy phase, which would be undesirable in the processing of silicon nitride.

Conclusions

Results of crystallization studies in the Y₂O₃-SiO₂ system have shown that, in general, the expected crystalline phases form when heat treated. It was also found that transformations were sluggish and in some cases phases could exist metastably. When the crystallization studies on the bulk glasses have been completed, the heat-treatment schedules which optimize crystallization will be applied to the 6Y silicon nitride composition to attempt to improve the high-temperature mechanical properties.

Acknowledgement

Research at The Ohio State University was supported on NASA Grant No. NAG 3-824.

References

- ¹W. A. Sanders and D. M. Mieskowski, "Strength and Microstructure of Sintered Si₃N₄ with Rare-Earth-Oxide Additions," *J. Am. Ceram. Soc.*, **64** [2] 304-309 (1985).
- ²L. J. Gauckler, H. Hohnke, and T. Y. Tien, "The System Si₃N₄-SiO₂-Y₂O₃," *J. Am. Ceram. Soc.*, **63** [1-2] 35-37 (1980).
- ³K. Liddell and D. P. Thompson, "X-ray Diffraction Data for Yttrium Silicates," *J. Br. Ceram. Trans.*, **85** 17-22 (1986).



⁴E. M. Levin, C. R. Robbins, and H. F. McMurdie, *Phase Diagrams for Ceramists 1969 Supplement*, The American Ceramic Society, Inc., Columbus, OH; Fig. 2388.

⁵W. E. Lee, C. H. Drummond III, G. E. Hilmas, J. D. Kiser, and W. A. Sanders, "Microstructural Evolution on Crystallizing the Glassy Phase in a 6 Weight % Y_2O_3 - Si_3N_4 Ceramic," these proceedings.

⁶W. A. Sanders and T. P. Herbill, "Characteristics of Si_3N_4 - SiO_2 - Ce_2O_3 Compositions Sintered in High-Pressure Nitrogen," *J. Am. Ceram. Soc.*, **66** [12] 835-41 (1983).

⁷R. Raj and F. F. Lange, "Crystallization of Glass (or a Liquid) Segregated in Grain Boundaries," *Acta Met.*, **201** 1993-2000 (1981) and R. Raj, "Morphology and Stability of the Glass Phase in Glass-Ceramic Systems," *J. Am. Ceram. Soc.*, **64** [5] 245-48 (1981).

Table I. Chemical Analysis of GSI

	As Formulated (wt%)	As Melted
SiO_2	40.6	39.94
Y_2O_3	59.4	60.96
WO_3		0.92
N		0.12
		<u>101.94</u>

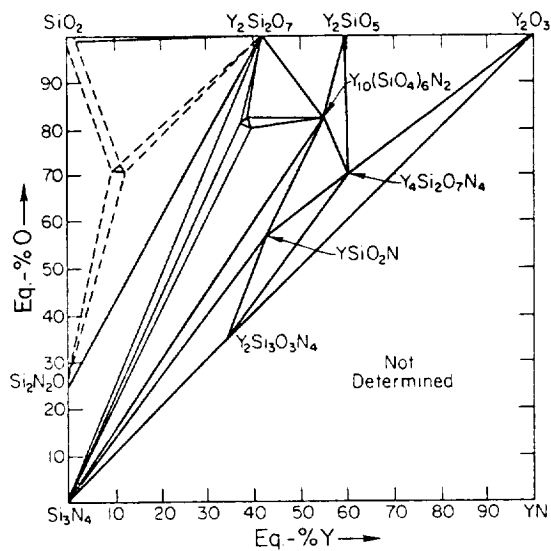
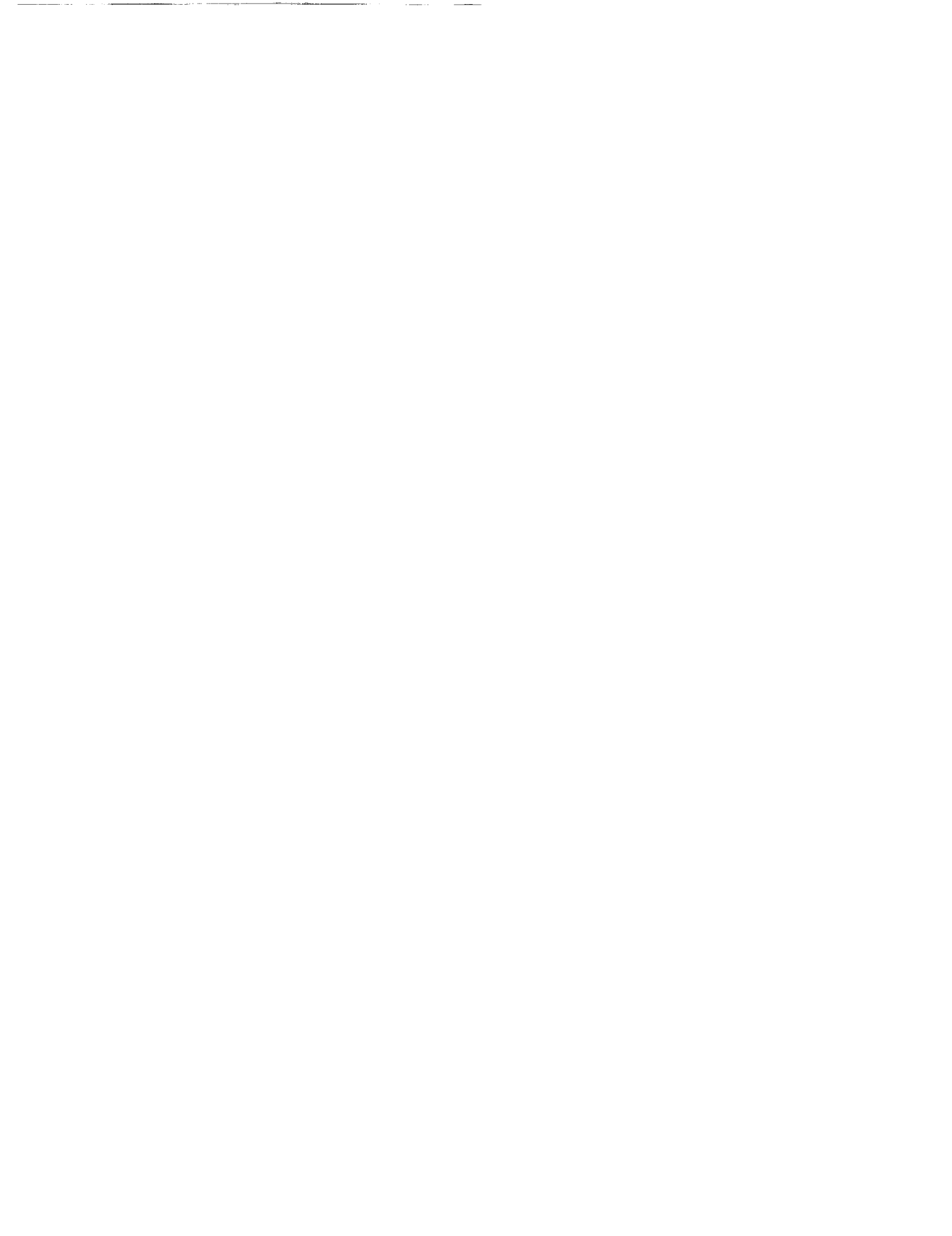


Fig. 1. Isothermal section of the system Si_3N_4 - SiO_2 - Y_2O_3 at 1500° .



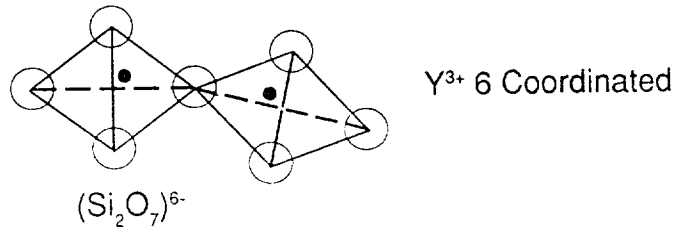
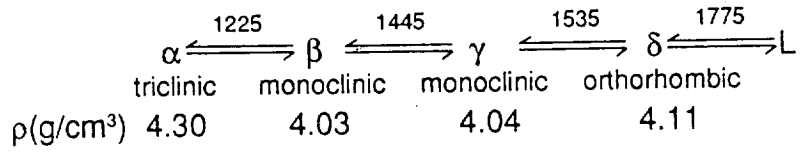


Fig. 2. Polymorphs of $\text{Y}_2\text{Si}_2\text{O}_7$.

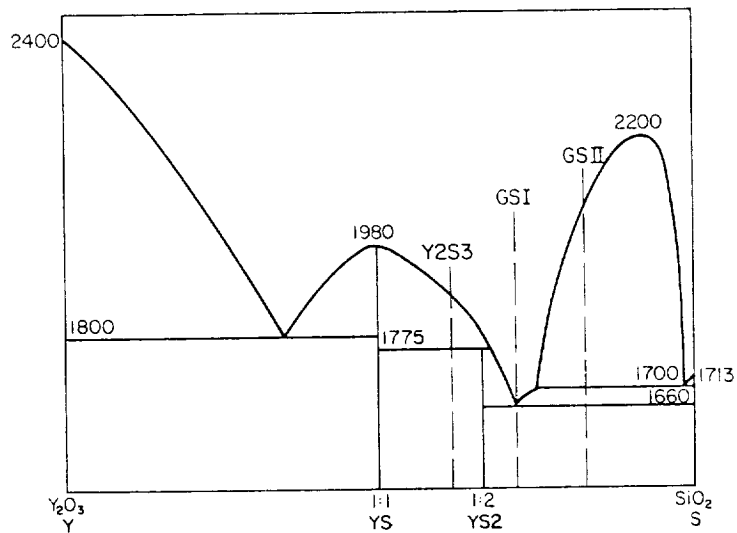


Fig. 3. Y_2O_3 - SiO_2 phase diagram.



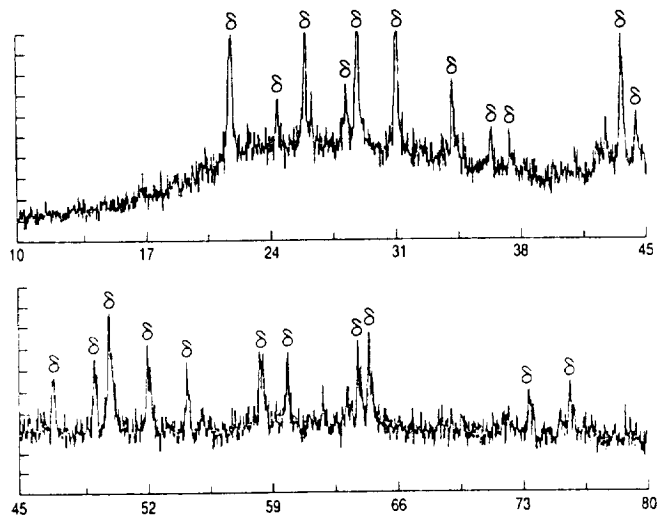


Fig. 4. X-ray pattern of as-melted GSI with δ - $Y_2Si_2O_7$.

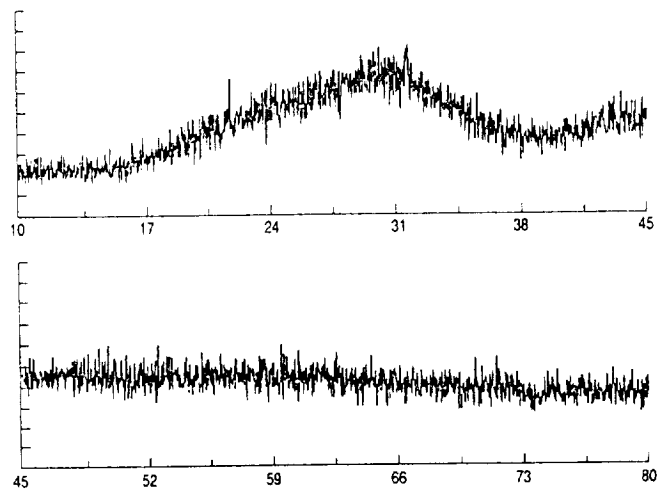


Fig. 5. X-ray pattern of as-melted $2Y_2O_3 \cdot 3SiO_2$.



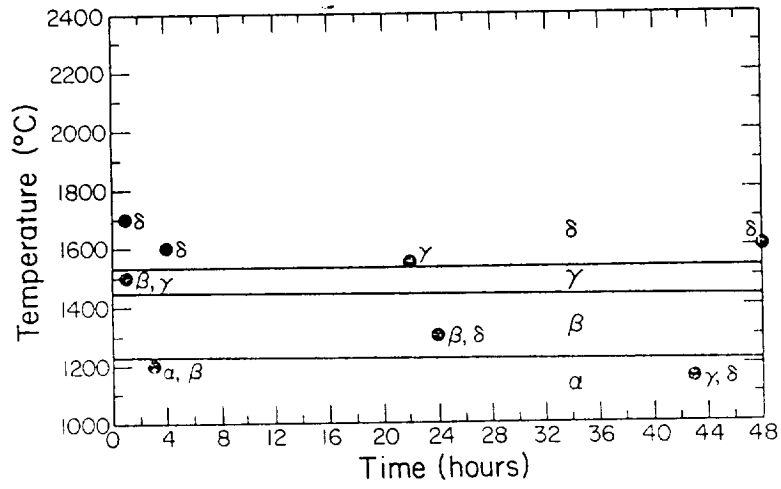


Fig. 6. Heat treatment studies of GSI.

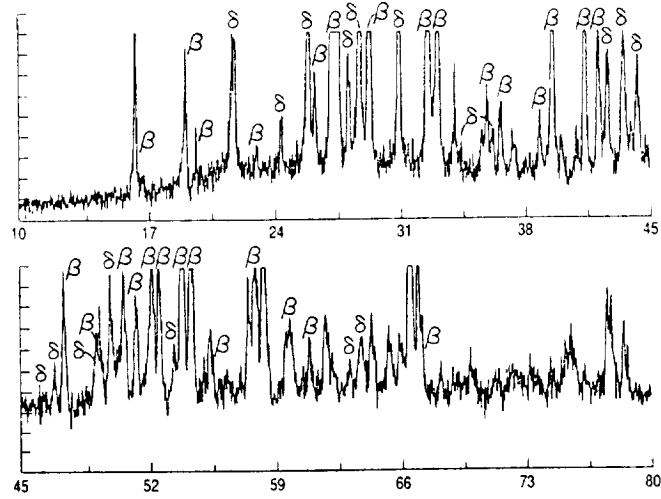


Fig. 7. X-ray pattern of GSI heat treated at 1300°C for 24 h with β and δ - $Y_2Si_2O_7$.



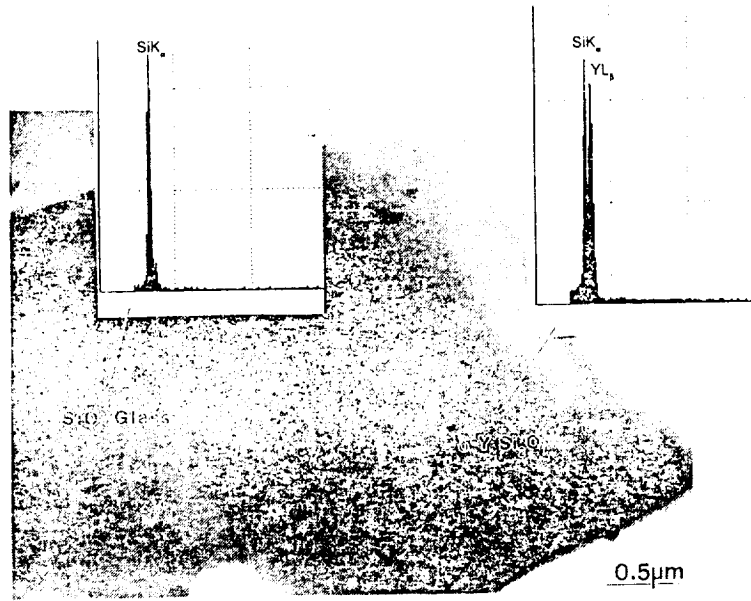


Fig. 8. TEM and AES of GSI heat treated at 1600°C for 4 h.

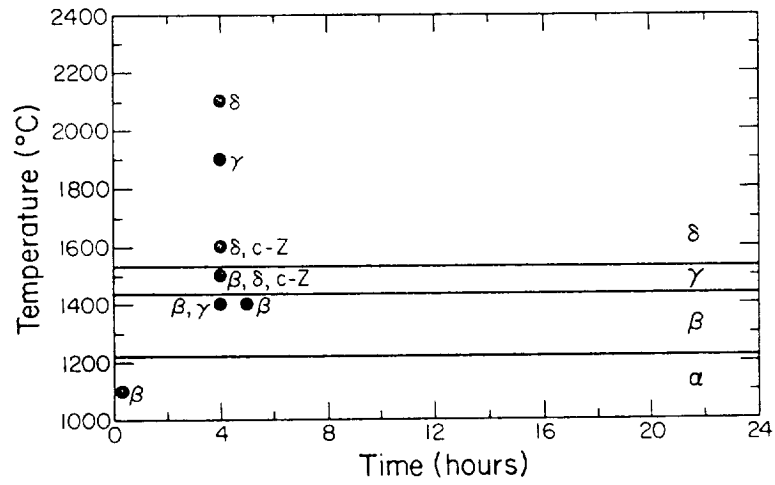


Fig. 9. Heat treatment studies of GSZ compositions.

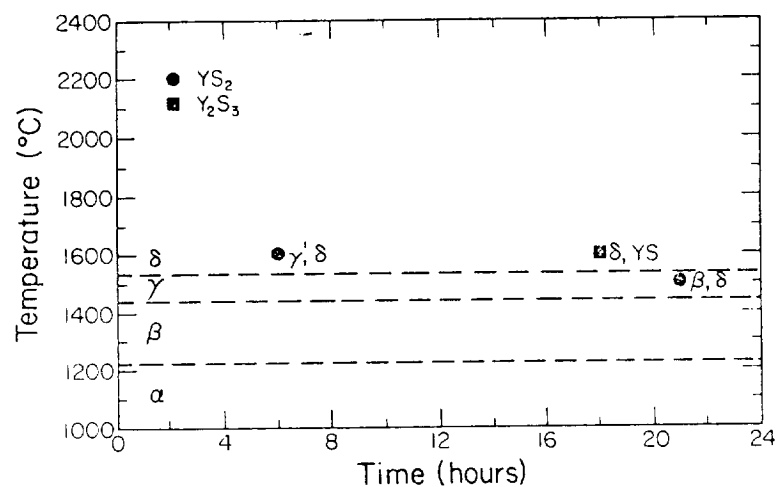


Fig. 10. Heat treatment studies of YS_2 and Y_2S_3 compositions.

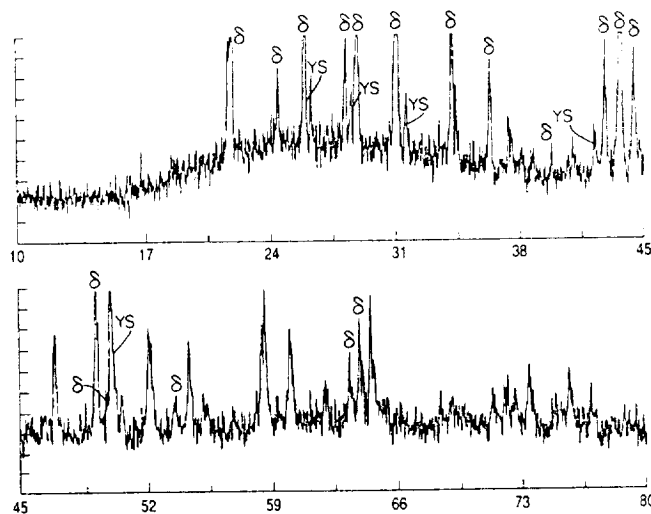


Fig. 11. X-ray pattern of $2Y_2O_3 \cdot 3SiO_2$ heat treated at 1600°C for 18 h with $\delta-Y_2Si_2O_7$ and Y_2SiO_5 .

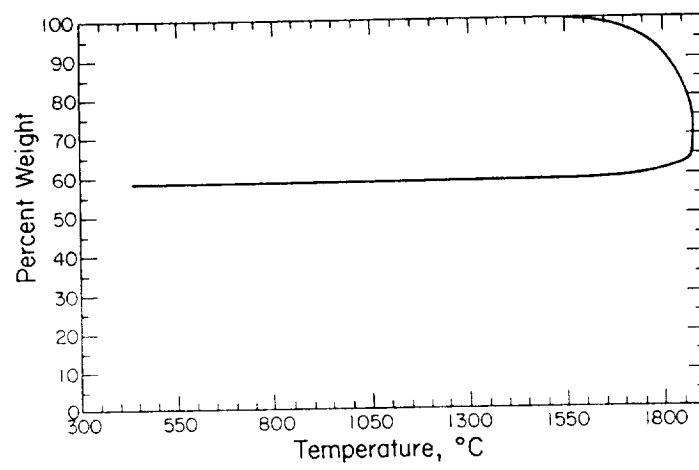


Fig. 12. TGA scan of GSZ5.



Microstructural Evolution on Crystallizing the Glassy Phase in a 6 Weight % Y_2O_3 - Si_3N_4 Ceramic

W. E. LEE, C. H. DRUMMOND III, AND G. E. HILMAS

Department of Ceramic Engineering
The Ohio State University
Columbus, OH 43210

J. D. KISER AND W. A. SANDERS

NASA Lewis Research Center
Cleveland, OH 44135

X-Ray diffraction and analytical electron microscopy have been used to study the crystallization of the grain-boundary glass in a 6 wt% Y_2O_3 - Si_3N_4 ceramic. Upon crystallization, high densities of dislocations formed in the Si_3N_4 grains and remained after 5 h at temperature. However, prolonged holds at the crystallization temperature effectively annealed out the dislocations. Other features present in the microstructure are characterized.

Introduction

Microstructural characterizations of liquid-phase sintered Si_3N_4 have frequently been performed using scanning electron microscopy (SEM) to study fracture surfaces and identify failure sites.¹⁻³ Lattice or structure imaging in the high resolution transmission electron microscope (TEM) has been carried out to detect small quantities of grain boundary glass.⁴⁻⁵ Other techniques such as energy dispersive spectroscopy (EDS) and energy loss spectroscopy (ELS) in the analytical electron microscope (AEM) have been used to quantitatively determine the chemical constituents of this glassy phase.⁶⁻⁷ Impurity phases in hot-pressed Si_3N_4 were carefully analyzed by Lou et al.⁸ Only recently, however, have microstructural studies been extended to examine the evolution of the microstructure with time and temperature upon crystallizing the glass. Bonnell et al.⁹⁻¹⁰ examined crystallization of cordierite ($Mg_2Al_4Si_2O_{14}$) and garnet ($Y_3Al_5O_{12}$) from MgO- and Y_2O_3 -containing SiAlONs respectively. In the present work SEM, AEM, and optical microscopy have been utilized to examine the microstructures in NASA-6Y (6 wt% Y_2O_3) composition Si_3N_4 in the as-sintered condition and after a crystallizing heat treatment in N_2 at 1500 °C for times from 5-20 h. We report here the results of AEM analysis.

Experimental

Materials and Sample Fabrication

Details of the starting powders and processing are given in a previous publication¹¹ and are summarized in Table I. Two series of bars were examined: series A using GTE SN502 Si_3N_4 powder and series B using KBI-AME Si_3N_4 powder. Series A was sintered and crystallized in 25 atm N_2 ; series B was sintered and crystallized in 50 atm N_2 .



Characterization

X-ray diffraction (XRD) of the as-treated surface of the $3 \times 0.56 \times 0.28$ cm bars was carried out using a Philips APD 3600 powder diffractometer. AEM was performed on a Philips 400 EM with an Ortec 500 EDS system. The Be window on the EDS X-ray detector precludes detection of any element lighter than Na so that, unfortunately, neither N nor O could be analyzed with this system. Standard ceramographic grinding and polishing techniques were employed finishing with $3 \mu\text{m}$ diamond paste. Three-mm diameter TEM disks were ultrasonically cut from 1-mm thick slices of the bars, ground and polished to about $100 \mu\text{m}$ thickness, dimpled to $20 \mu\text{m}$ center thickness and ion milled to electron transparency using 5 kV Ar ions. Analysis of X-ray and electron diffraction patterns was facilitated by reference 12 for Si_3N_4 and 13 for $\text{Y}_2\text{Si}_2\text{O}_7$.

Results

X-ray Diffraction

Results of XRD analyses are given in Table II. Series A bars contain detectable amounts of Si_2ON_2 in all cases, even in the as-sintered material. This occurred even though series A had a lower starting SiO_2 content because of contamination during the long milling time (300 h), a higher SiO_2 content in the starting Si_3N_4 powder, and because of possible oxidation of Si_3N_4 upon milling. $\beta\text{-Si}_3\text{N}_4$ was the only other phase found in the as-sintered material but on crystallizing at 1500°C for 5–20 hours, $\beta\text{-Y}_2\text{Si}_2\text{O}_7$ peaks were also revealed.

As-sintered series B material was additionally subjected to a bend test in air at 1370°C before characterization which led to the formation of $\text{Y-Y}_2\text{Si}_2\text{O}_7^*$ crystals from the glass. After crystallizing treatments of 5 and 10 h at 1500°C , as in the series A material, only $\beta\text{-Y}_2\text{Si}_2\text{O}_7$ was formed. However, after 20 h at 1500°C , only peaks attributable to a $\alpha\text{-Y}_2\text{Si}_2\text{O}_7$ were detected.

General Microstructure

The same general trends in the microstructural features observed in the TEM were seen for both series A and series B material. The main difference was that greater amounts of Si_2ON_2 were apparent in series A (detected by XRD) than in series B samples (not detected by XRD). However, Si_2ON_2 was frequently detected in the TEM when examining series B material even though the amount present must have been below the limits of detectability of the XRD unit (about 5 vol%).

As-sintered 6Y-Si₃N₄: Figure 1 is a bright-field TEM image of a typical area of the microstructure of 6Y material before crystallization consisting of hexagonal $\beta\text{-Si}_3\text{N}_4$ grains in a glassy matrix. The glass appears dark since it contains high atomic number Y which absorbs many of the electrons so that they do not contribute to the transmitted image. An EDS spectrum from the glass is also shown indicating the presence of Y and Si (O and N are not detected with this system). Low densities of dislocations were observed in about 40% of the Si_3N_4 grains examined (e.g. as arrowed in Figure 1). We intend to carry out ELS analysis of the as-sintered glass to determine the N content (if any) and O content.

*There are five polymorphs of $\text{Y}_2\text{Si}_2\text{O}_7$, as described in reference 22.



After 5 h at 1500°C: All specimens prepared for TEM after this heat treatment were observed to crack on ion milling, a first indication that they were under a large stress. β - $\text{Y}_2\text{Si}_2\text{O}_7$ crystals were seen at the grain boundaries shown as the dark phase in the bright field image of Fig. 2. The EDS spectrum for this phase shows that the Y L_{α} , L_{β} doublet peak is just smaller than the Si K_{α} , K_{β} doublet peak. Note, however that spectra from this phase must be collected from the edge of the sample away from Si_3N_4 grains to stop X-rays generated from the Si in the Si_3N_4 from reaching the detector, otherwise anomalously high Si peaks result. Figure 3 is a dark-field image where a single reflection from the β - $\text{Y}_2\text{Si}_2\text{O}_7$ has illuminated crystalline regions at the same orientation extending over large areas of the microstructure. It appears that most of the material that was glass before this heat treatment has crystallized at this stage although high-resolution lattice imaging is needed to confirm this.

Figure 4 is a low magnification image of the microstructure. Note the large number of strain fields in the Si_3N_4 grains due to the presence of extensive dislocation networks. Dislocations were observed in about 85% of the grains examined and at much higher densities than in the as-sintered material. Determining the presence of dislocations in a particular grain requires extensive tilting to bring the grain to an orientation at which the dislocation is visible. Work is in progress to quantify the dislocation densities and to analyze their habit planes and Burgers vectors. Figure 5 is a weak-beam dark-field image of some of these dislocations using $g = 0002$. This technique is frequently used when examining high densities of dislocations in ceramics since it images only the core of the dislocation and removes the problem of overlapping strain fields seen in conventional bright- or dark-field images.

After 10–20 h at 1500°C: Similar microstructures were observed in these samples as after 5 h at 1500°C except that the dislocation densities were reduced almost to the level of the as-sintered material (Fig. 6). Specimens did not crack on ion milling.

Other Observations

Several other features were observed in the microstructures using TEM and are worthy of note.

α - Si_3N_4 : Rounded grains of α - Si_3N_4 were occasionally observed in all specimens (e.g. arrowed in Fig. 6). Careful analysis of diffraction patterns was required to distinguish these grains from the hexagonally-shaped β - Si_3N_4 grains. The α grains presumably are particles from the original starting powder which did not dissolve during sintering. Observing large numbers of these grains would indicate the need for longer sintering times or higher temperatures although the amounts detected here were small and below the level of detectability of the XRD unit for series B.

Precipitates in the β - Si_3N_4 Grains: Occasionally, small (about 150 nm diameter) crystals were observed inside β - Si_3N_4 grains. EDS analysis of the crystal indicated the presence of silicon, and electron diffraction patterns identified them as being β -SiC, an impurity phase also observed by Lou et al.⁸ in their TEM study of hot-pressing Si_3N_4 . The crystals are faulted on (111) giving rise to the streaks in the microdiffraction pattern of Fig. 7. The starting powders used in the production of these samples are known to contain about 0.1 wt% C¹¹ which apparently forms into SiC during the solution-



precipitation sintering process. This observation has practical significance since it is known that carbon impurities reduce the oxidation resistance of Y_2O_3 - Si_3N_4 ceramics.¹⁴

Si₂ON₂ Crystals: Detecting the presence of silicon oxynitride was relatively straightforward in the TEM due to the presence of stacking faults (and occasionally twins) on (100) planes as observed previously by Lewis et al.¹⁵ However, two distinct morphologies of Si_2ON_2 were seen. Commonly, the Si_2ON_2 crystals occurred as long, orthorhombic-shaped grains with the stacking faults running along the long (100) axis of the crystal (Fig. 8). The presence of streaks in the diffraction patterns was a strong indication that the grain was Si_2ON_2 . Less common was the appearance of some Si_2OH_2 crystallized with the same morphology as the $Y_2Si_2O_7$ phase, i.e. crystallizing around the Si_3N_4 grains (Fig. 9). This morphology was less inclined to contain stacking faults and so was more difficult to detect. EDS was required to distinguish this from Si_2ON_2 from $Y_2Si_2O_7$, as was careful analysis of diffraction patterns. In both morphologies, small crystals were seen inside the grains similar to the observation of β -SiC crystals in β - Si_3N_4 noted above. However, preliminary analysis suggests that these crystals are simply Si_2ON_2 microcrystals at a different orientation to the parent grain and not a second phase.

Discussion

Crystallization of the grain-boundary glass to increase the refractoriness of Si_3N_4 ceramics has been intensively studied since the work of Tsuge et al.¹⁶ in the Y_2O_3 - Si_3N_4 system. The NASA 6Y composition is chosen to lie in the oxidation-resistant Si_2ON_2 - Si_3N_4 - $Y_2Si_2O_7$ triangle of the Si_3N_4 - SiO_2 - Y_2O_3 phase diagram and the microstructural results presented here confirm the presence of these phases along with the occasional impurity grains such as β -SiC (Fig. 7). The increase in dislocation density in the Si_3N_4 grains upon formation of $Y_2Si_2O_7$ after 5 h at 1500°C was unexpected. Cracking of TEM specimens on ion milling is a clear indication that this material's mechanical properties are adversely affected by this strain. The reduction in dislocation densities with prolonged heating at 1500°C, however, suggests that the dislocations can be annealed out without difficulty.

The reason for the appearance of dislocations is likely to be associated with a volume difference between the yttrium silicate glass and the first $Y_2Si_2O_7$ crystals formed or volume differences between some of the $Y_2Si_2O_7$ polymorphs. Alternatively, differences in thermal expansion between the various phases may lead to stress in the system. Densities of the polymorphic forms of $Y_2Si_2O_7$ are available but the density of the glass is not. Experiments are currently being performed to determine the density of glasses with this composition. A volume change (increase or decrease) will impose a strain on the Si_3N_4 grains, deforming them and causing dislocations to form. The dislocation microstructures formed in the crystallized material are typical of deformation-induced microstructures seen in other ceramics.¹⁷ According to Liddell and Thompson,¹³ α - $Y_2Si_2O_7$ transforms to the β form at 1225°C which should transform to γ - $Y_2Si_2O_7$ at 1445°C. Since crystallization was carried out at 1500°C and γ - $Y_2Si_2O_7$ was never observed, the γ to β transformation must be rapid. Since the β to α transformation did not occur when cooling below the β phase field it, however, must be sluggish. The volume change associated with the only polymorphic transformation to occur (γ to β) is small (0.2%) and so the most likely cause(s) of dislocation formation is (are) a volume change



on crystallization from the glass or differences in thermal expansion behavior. However, as stated above, since the dislocations can be annealed out at the crystallization temperature, their formation need not affect the mechanical properties.

Hayashi et al.¹⁸ note a decrease in flexural strength after crystallization in pressureless-sintered $\text{Al}_2\text{O}_3\text{-Y}_2\text{O}_3\text{-Si}_3\text{N}_4$ ceramics which they attribute to a change in specific volume of grain boundary phases and difference of thermal expansion coefficients between Si_3N_4 and the crystallized phases.

While a thorough analysis of the dislocations observed in both as-sintered (presumably simple growth defects) and crystallized Si_3N_4 is not yet complete, a few words concerning previous studies of dislocations in this material seem in order. Studies of dislocations in Si_3N_4 are sparse. Evens and Sharp¹⁹ and Butler²⁰ studied dislocations in hot-pressed and reaction-sintered materials. In both forms most of the dislocations had a $\langle 0001 \rangle$ -type Burgers vector, b , although other types of dislocation were present. Consideration of the strain energy associated with various types of dislocation in Si_3N_4 ¹⁹ indicated that $\langle 0001 \rangle$ was the most stable Burgers vector whereas an analysis of dislocation mobility using the Peierls model suggested they would also be the most mobile with $\{10\bar{1}0\}$ as the primary slip plane.

The observation that $\text{Y}_2\text{Si}_2\text{O}_7$ crystallizes at a single orientation (i.e. as a single crystal) over large distances in the microstructure (Fig. 3) is interesting. Similar behavior was seen by Bonnell et al.¹⁰ in garnet ($\text{Y}_3\text{Al}_5\text{O}_{12}$) crystallized in SiAlON grain boundaries but not when cordierite ($\text{Mg}_2\text{Al}_2\text{Si}_2\text{O}_{10}$) was crystallized. It is suspected that this behavior is a function of the ease or difficulty of nucleating the second phase; the easier nucleation is the less chance of crystals growing around the Si_3N_4 grains. Since crystallization of $\text{Y}_2\text{Si}_2\text{O}_7$ is observed around several Si_3N_4 grains. Since crystallization of $\text{Y}_2\text{Si}_2\text{O}_7$ is observed around several Si_3N_4 grains, it seems likely that complete crystallization of all the glass in that area had occurred even though the very thin intergranular regions were not illuminated in dark-field images. High-resolution TEM is planned to determine the extent of crystallization in this material. The crystallization morphologies of the $\text{Y}_2\text{Si}_2\text{O}_7$ polymorphs formed from bulk glass are currently being studied in several complex systems.²¹⁻²²

References

- ¹W. A. Sanders and D. M. Mieskowski, "Strength and Microstructure of Sintered Si_3N_4 With Rare-Earth-Oxide Additions," *Ceram. Bull.*, **64** [2] 304-309 (1985).
- ²R. K. Govila, "Uniaxial Tensile and Flexural Stress Rupture Strength of Hot-Pressed Si_3N_4 ," *J. Am. Ceram. Soc.*, **65** [1] 15-21 (1982).
- ³D. W. Richerson and J. M. Wimmer, "Properties of Isostatically Hot-Pressed Silicon Nitride," *J. Am. Ceram. Soc.*, **66** C-173-76 (1983).
- ⁴D. R. Clarke, "Direct Observation of Lattice Planes at Grain Boundaries in Silicon Nitride," pp. 433-40 in *Nitrogen Ceramics* Edited by F. L. Riley (Noordhoff, The Netherlands 1977).
- ⁵O. L. Krivanek, T. M. Shaw, and G. Thomas, "Imaging of Thin Intergranular Phases by High-Resolution Electron Microscopy," *J. Appl. Phys.*, **50** [6] 4223-27 (1979).
- ⁶D. R. Clarke, N. J. Zaluzec, and R. W. Carpenter, "The Intergranular Phase in Hot-Pressed Silicon Nitride: I, Elemental Composition," *J. Am. Ceram. Soc.*, **64** [10] 601-7 (1981).
- ⁷S. A. Bradley and K. R. Karasek, "Analysis of Grain Boundaries for Reaction-Bonded Silicon Nitride with Yttria Addition," *J. Mats. Sci. Lett.*, **6** 791-94 (1987).
- ⁸L. K. V. Lou, T. E. Mitchell, and A. H. Heuer, "Impurity Phases in Hot-Pressed Si_3N_4 ," *J. Am. Ceram. Soc.*, **61** [9-10] 392-96 (1978).
- ⁹D. A. Bonnell, M. Ruhle, and T-Y. Tien, "Redistribution of Aluminum Ions During Processing of Sialon Ceramics," *J. Am. Ceram. Soc.*, **69** [8] 623-27 (1986).
- ¹⁰D. A. Bonnell, T-Y. Tien, and M. Ruhle, "Controlled Crystallization of the Amorphous Phase in Silicon Nitride Ceramics," *J. Am. Ceram. Soc.*, **70** [7] 460-65 (1987).



¹¹W. A. Sanders and G. Y. Baaklini, "Correlation of Processing and Sintering Variables With the Strength and Radiography of Silicon Nitride," *Cer. Eng. and Sci. Proc.*, **7** [7-8] 839-59 (1986).

¹²J. V. Sharp, A. G. Evans, and B. Hudson, "Electron Diffraction Data for Silicon Nitride," UKAEA Harwell Report AERE-R7319 (1972).

¹³K. Liddell and D. P. Thompson, "X-ray Diffraction Data for Yttrium Silicates," *Br. Ceram. Trans. J.*, **85** 17-22 (1986).

¹⁴H. Knoch and G. E. Gazza, "Effect of Carbon Impurity on the Thermal Degradation of an Si₃N₄-Y₂O₃ Ceramic," *J. Am. Ceram. Soc.*, **62** [11-12] 634-35 (1979).

¹⁵M. H. Lewis, C. J. Reed, and N. D. Butler, "Pressureless-Sintered Ceramics Based on the Compound Si₃N₄O," *Mats. Sci. and Eng.*, **71** 87-94 (1985).

¹⁶A. Tsuge, K. Nishida, and M. Komatsu, "Effect of Crystallizing the Grain-Boundary Glass Phase on the High-Temperature Strength of Hot-Pressed Si₃N₄ Containing Y₂O₃," *J. Am. Ceram. Soc.*, **58** [7-8] 323-26 (1975).

¹⁷T. E. Mitchell, "Application of Transmission Electron Microscopy to the Study of Deformation in Ceramic Oxides," *J. Am. Ceram. Soc.*, **62** [5-6] 254-67 (1979).

¹⁸T. Hayashi, H. Munakata, H. Suzuki, and H. Saito, "Pressureless Sintering of Si₃N₄ with Y₂O₃ and Al₂O₃," *J. Mat. Sci.*, **21** 3501-3508 (1986).

¹⁹A. G. Evans and J. V. Sharp, "Microstructural Studies in Silicon Nitride," *J. Mats. Sci.*, **6** 1292-1302 (1971).

²⁰E. Butler, "Observations of Dislocations in β -Silicon Nitride," *Phil. Mag.*, **24** 829-34 (1971).

²¹T. R. Dinger, R. S. Rai, and G. Thomas, "Crystallization Behavior of a Glass in the Y₂O₃-SiO₂-AlN System," *J. Am. Ceram. Soc.*, **71** [4] 236-44 (1988).

²²C. H. Drummond III, W. E. Lee, W. A. Sanders, and J. D. Kiser, "Crystallization and Characterization of Y₂O₃-SiO₂ Glasses," these proceedings.

Table I. Powders and Processing Conditions

	Powder	Mill charge (wt%)	Mill time (h)	Sintering			Crystallizing
				Temp. (°C)	Time (h)	N ₂ pressure (atm)	N ₂ pressure (atm)
Series A	Si ₃ N ₄ *	95.4	300	2140	1	25	25
	SiO ₂ †	0					
	Y ₂ O ₃ ‡	4.6					
Series B	Si ₃ N ₄ §	90.0	100	2140	4	50	50
	SiO ₂	3.6					
	Y ₂ O ₃	6.4					

*GTE SN 502 99.95% purity, 71.5% α , 1.5% β , 27% amorphous.

†Apache Chemicals Inc., Code 6846, 99.99%.

‡Molycorp. 5600, 99.9%.

§KBI-AME high purity, 99.5%, 83.7% α , 15.7% β , 0.6% Si.

Table II. XRD Results

Crystallizing Time (h)	Phases Present	
	Series A	Series B
0	β -Si ₃ N ₄ , Si ₂ N ₂ O*	β -Si ₃ N ₄ , Y-Y ₂ Si ₂ O ₇ †
5	β -Si ₃ N ₄ , Si ₂ N ₂ O β -Y ₂ Si ₂ O ₇	β -Si ₃ N ₄ , β -Y ₂ Si ₂ O ₇
10	β -Si ₃ N ₄ , Si ₂ N ₂ O, β -Y ₂ Si ₂ O ₇	B-Si ₃ N ₄ , β -Y ₂ Si ₂ O ₇
15	β -Si ₃ N ₄ , Si ₂ N ₂ O, β -Y ₂ Si ₂ O ₇	No data
20	β -Si ₃ N ₄ , Si ₂ N ₂ O, β -Y ₂ Si ₂ O ₇	β -Si ₃ N ₄ , α -Y ₂ Si ₂ O ₇ ‡

*High SiO₂ content due to contamination from milling media, high SiO₂ in Si₃N₄ powder, and possible oxidation on milling.

†Formed during bend test in air at 1370°C.

‡Identified from 2 peaks only.

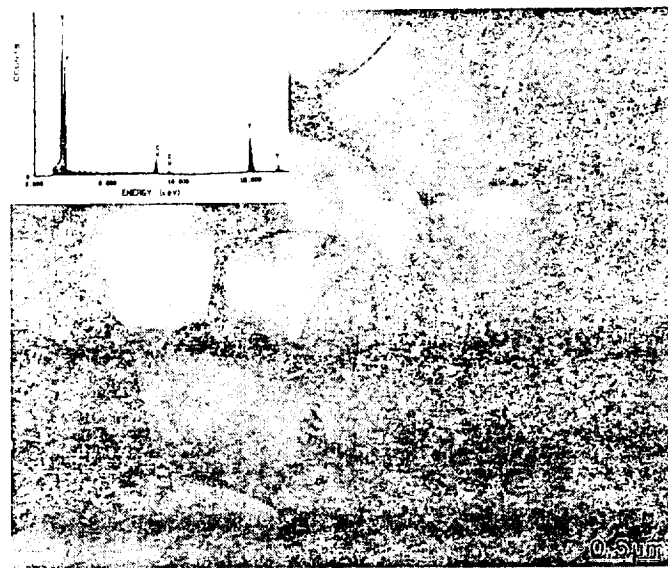


Fig. 1. Bright-field TEM image of as-sintered Si₃N₄. Inset is an EDS spectrum from the glassy phase.



Fig. 2. Bright-field TEM image of Si₃N₄ after crystallization for 5 h at 1500 °C. Inset is an EDS spectrum from Y₂Si₂O₇.

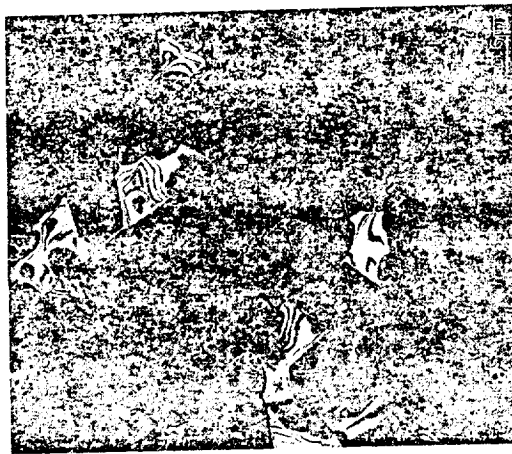


Fig. 3. Dark-field TEM image of β-Y₂Si₂O₇ at a single orientation.





Fig. 4. Bright-field TEM image showing large amounts of strain in Si_3N_4 grains after 5 h at 1500 °C.



Fig. 5. Weak-beam dark-field TEM image of a dislocation network in a Si_3N_4 grain.



Fig. 6. Bright-field TEM image showing reduced dislocation density after 20 h at 1500°C. Arrows indicate α - Si_3N_4 grains.

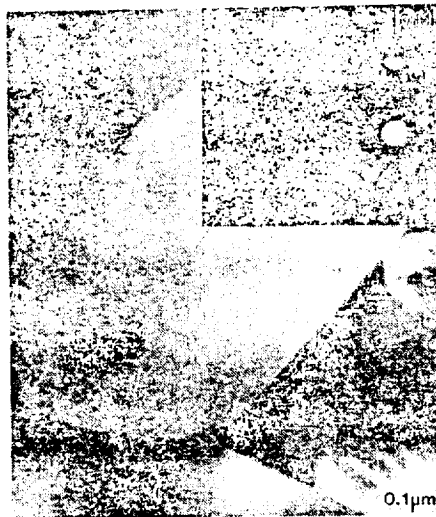


Fig. 7. β -SiC precipitate in Si_3N_4 grain. Inset is a microdiffraction pattern from β -SiC grain with streaking along (111).

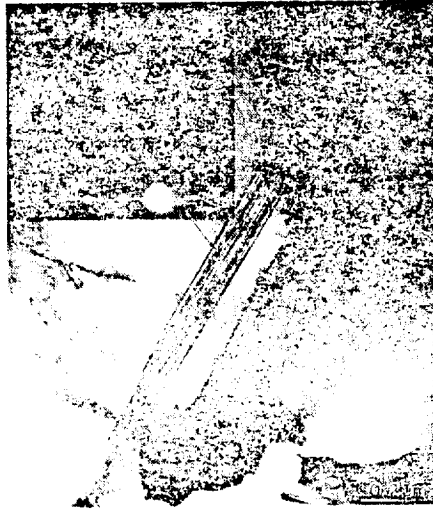


Fig. 8. Orthorhombic Si_2ON_2 grain with stacking faults on (100). Inset diffraction pattern showing streaks on (100).



Fig. 9. Si_2ON_2 grain crystallizing around Si_3N_4 grains.



Microstructural Changes in β -Silicon Nitride Grains upon Crystallizing the Grain-Boundary Glass

William E. Lee** and Gregory E. Hilmas*†

Department of Materials Science and Engineering, The Ohio State University, Columbus, Ohio 43210-1178

CF 1000 QUALITY

Crystallizing the grain-boundary glass of a liquid-phase-sintered Si_3N_4 ceramic for 2 h or less at 1500°C led to formation of $\delta\text{-Y}_2\text{Si}_2\text{O}_7$. After 5 h at 1500°C , the $\delta\text{-Y}_2\text{Si}_2\text{O}_7$ had transformed to $\beta\text{-Y}_2\text{Si}_2\text{O}_7$, with a concurrent dramatic increase in dislocation density within $\beta\text{-Si}_3\text{N}_4$ grains. Reasons for the increased dislocation density are discussed. Annealing for 20 h at 1500°C reduced dislocation densities to the levels found in as-sintered material. [Key words: silicon nitride, microstructure, grain boundaries, grains, glass.]

I. Introduction

THE predominantly covalent nature of the atomic bonds in Si_3N_4 hinders atom migration so that the solid-state sintering (below the decomposition temperature (1878°C at atmospheric pressure in air¹)) is limited. Fabrication of structural components may therefore be facilitated by adding one or more oxides to the Si_3N_4 powder (e.g., Refs. 2 and 3), which combine with surface and (occasionally) added SiO_2 to form a low-melting-point silicate liquid. Liquid-phase sintering (LPS) occurs by a solution-reprecipitation mechanism as originally proposed by Drew and Lewis.⁴ In this process the $\alpha\text{-Si}_3\text{N}_4$ starting powder dissolves in the silicate liquid and is precipitated out as $\beta\text{-Si}_3\text{N}_4$, with the silicate liquid solidifying as a glass at the grain boundaries of the final product. Unfortunately, the low melting point of the silicate phase used to advantage during sintering is detrimental to the mechanical properties of the monolithic material at high temperatures, since the glass typically begins to soften at relatively low temperatures (about 1000°C).

One method of improving the high-temperature mechanical strength is to alter the glass composition to increase its softening point (e.g., Ref. 5). Another technique is to use a postsinter heat treatment to crystallize the glass to a more refractory phase. In a recent study⁶ we employed the latter technique for Si_3N_4 fabricated with a Y_2O_3 sintering aid and crystallized $\text{Y}_2\text{Si}_2\text{O}_7$ at the grain boundaries. We present here observations of the effect of this crystallizing treatment on the microstructure of the $\beta\text{-Si}_3\text{N}_4$ grains.

F. F. Lange—contributing editor

Manuscript No. 198720. Received December 29, 1988; approved February 10, 1989.

Supported by NASA Lewis Research Center, Cleveland, OH, on NASA Grant No. 3-824. Parts of this research were performed while W. E. Lee was a CCFP Summer Faculty Fellow at NASA Lewis Research Center.

*Member, American Ceramic Society.

†Present address: School of Materials, The University of Sheffield, Sheffield S102TZ, UK.

**Present address: Department of Materials Science and Engineering, University of Michigan, Ann Arbor, MI.

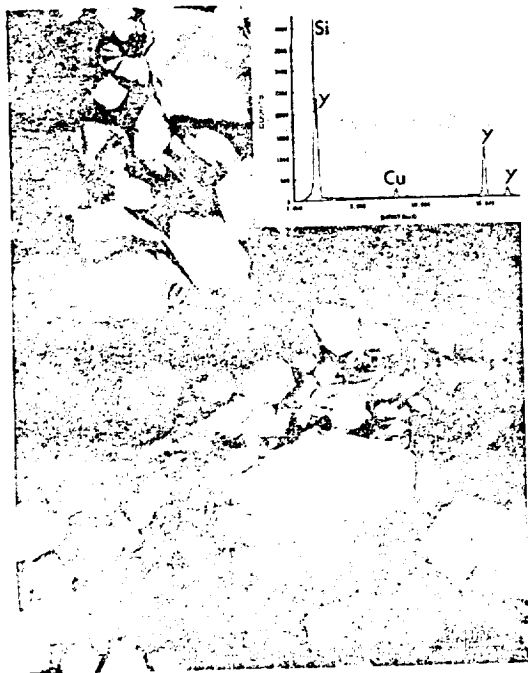


Fig. 1. Bright-field (BF) TEM image of the general microstructure of as-sintered Si_3N_4 with (inset) EDS spectrum from glassy phase.

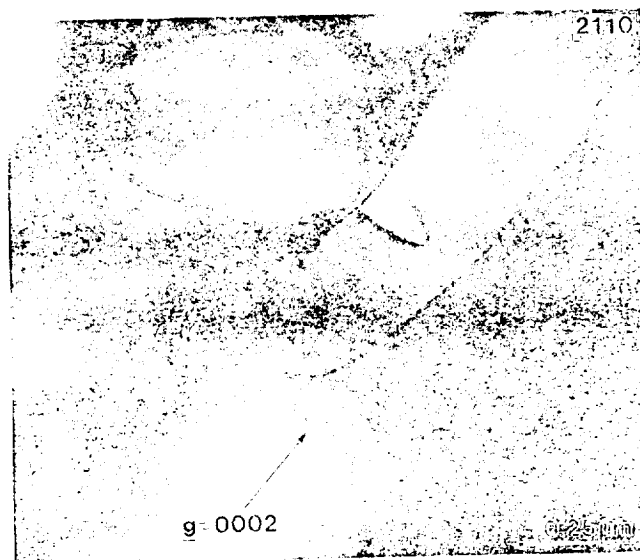


Fig. 2. BF TEM image of a group of $b = (0001)$ dislocations in a $\beta\text{-Si}_3\text{N}_4$ grain of as-sintered material.

II. Experimental Procedure

The starting powders were Si_3N_4 (83.7 wt% α , 15.7 wt% β , and 0.6 wt% Si), Y_2O_3 ,⁵ and SiO_2 .⁶ The powders were mixed in the ratio 90:6.4:3.6 wt%, respectively, and milled as 100-g charges in 1-L Si_3N_4 mills using high-purity Si_3N_4 milling media and ethanol. After oven drying under vacuum, the powders were die-pressed into bars at 21 MPa followed by cold isostatic pressing at 414 MPa. These bars were then sintered at 2140°C for 4 h under 50 atm ($\approx 5 \times 10^6$ Pa) of N_2 . The crystallizing anneal was performed at 1500°C for times of 0.5, 2, 5, 10, and 20 h, again under 50 atm of N_2 . The heating rate from room temperature to 1500°C was 42°C/min, while the cooling rate after switching off the furnace was 130°C/min.

Electron microscopy was performed using either of two TEM units** equipped with an EDS** system. TEM specimens were prepared using standard ceramographic techniques. First, 3-mm-diameter disks were ultrasonically cut from 1-mm-thick slices of the bars and ground and polished to 100 μm before dimpling to 20- μm -center thickness. Final polishing and dimpling was done with 3- μm diamond paste. Ion milling was performed using 6-kV Ar^+ ions. Dislocation Burgers vectors were determined using the $\mathbf{g} \cdot \mathbf{b} = 0$ invisibility criterion⁷ where \mathbf{g} is the operating reflection and \mathbf{b} the Burgers vector of the dislocation. With this technique, dislocations must go out of contrast for two nonparallel reflections, and while the invisibility criterion is strictly valid only for pure screw dislocations, it is commonly applied to those containing an edge component where the contrast at the $\mathbf{g} \cdot \mathbf{b} = 0$ but $\mathbf{g} \cdot \mathbf{b} \times \mathbf{u} \neq 0$ condition is minimal. Residual contrast can arise from the $\mathbf{g} \cdot \mathbf{b} \times \mathbf{u}$ term and/or from elastic anisotropy and in some cases requires image-contrast calculations⁸ to determine \mathbf{b} . Image-matching calculations were not attempted here. Weak-

beam dark-field (WBDF) imaging was necessary when examining dislocations in Si_3N_4 . This technique⁹ images only the dislocation core and enables high densities of dislocations to be studied. In conventional bright-field (BF) and dark-field (DF) images, the overlapping strain fields of the dislocations make analysis of them impossible. Diffraction patterns for Si_3N_4 were solved with the assistance of Ref. 10.

Dislocation densities for 100 adjacent grains were determined in each sample, using the method of counting intersections of dislocations with drawn circles as described in Ref. 7. Convergent beam electron diffraction¹¹ was used to measure the thickness of representative grains and an average value of 200 nm used in all density calculations. This will introduce some error in the dislocation density measurements. Further error is introduced because the technique of Hirsch *et al.*⁷ leads to an underestimate of dislocation density, since at all orientations some dislocations will be out of contrast. This error was minimized by using $\mathbf{g} = 0002$ at the $[\bar{1}210]$ zone axis whenever possible in images used for density determinations. At this orientation the majority of dislocations with $\mathbf{b} = (0001)$ or with c and a components in their \mathbf{b} are in contrast but not those with $\mathbf{b} = \frac{1}{3}[\bar{1}210]$. The maximum total error associated with this procedure for dislocation densities is expected to be on the order of 25%.

III. Results

(I) As-Sintered Microstructure

A BF TEM image of the general microstructure is shown in Fig. 1. Hexagonal β - Si_3N_4 grains are contained in a glue of yttrium silicate glass. Other minor phases occasionally observed in the microstructure include α - Si_3N_4 , β -SiC, and up to 5 vol% $\text{Si}_2\text{N}_2\text{O}$. An EDS spectrum from the glass is shown inset in Fig. 1. More detailed BF examination of the silicon nitride grains shows that some of them contain dislocations (Fig. 2) which we assume are simply "grown in" during the reprecipitation process. The distribution of dislocation densities in β - Si_3N_4 grains (Fig. 3(a)) reveals that about 60% of the grains do not contain dislocations and the maximum dislocation density observed in any grain is $31 \times 10^9/\text{cm}^2$. Burgers vector (\mathbf{b}) analysis on

⁵Kawecki Beryllco, Inc.—Advanced Materials Engineering, Ltd., Reading, PA.
⁶5600, Molycorp, Inc., White Plains, NY.
⁷Code 6846, Apache Chemicals, Seward, IL.
^{**}Model 200 CX, JEOL, USA, Inc., Peabody, MA.; Model 400, Philips Electronics, Inc., Mahwah, NJ.
[†]Ortec 5000 System, Ortec Inc., Oak Ridge, TN (with Philips 400); TN 2000 System, Tracor Northern, Middleton, WI (with JEOL 200 CX).

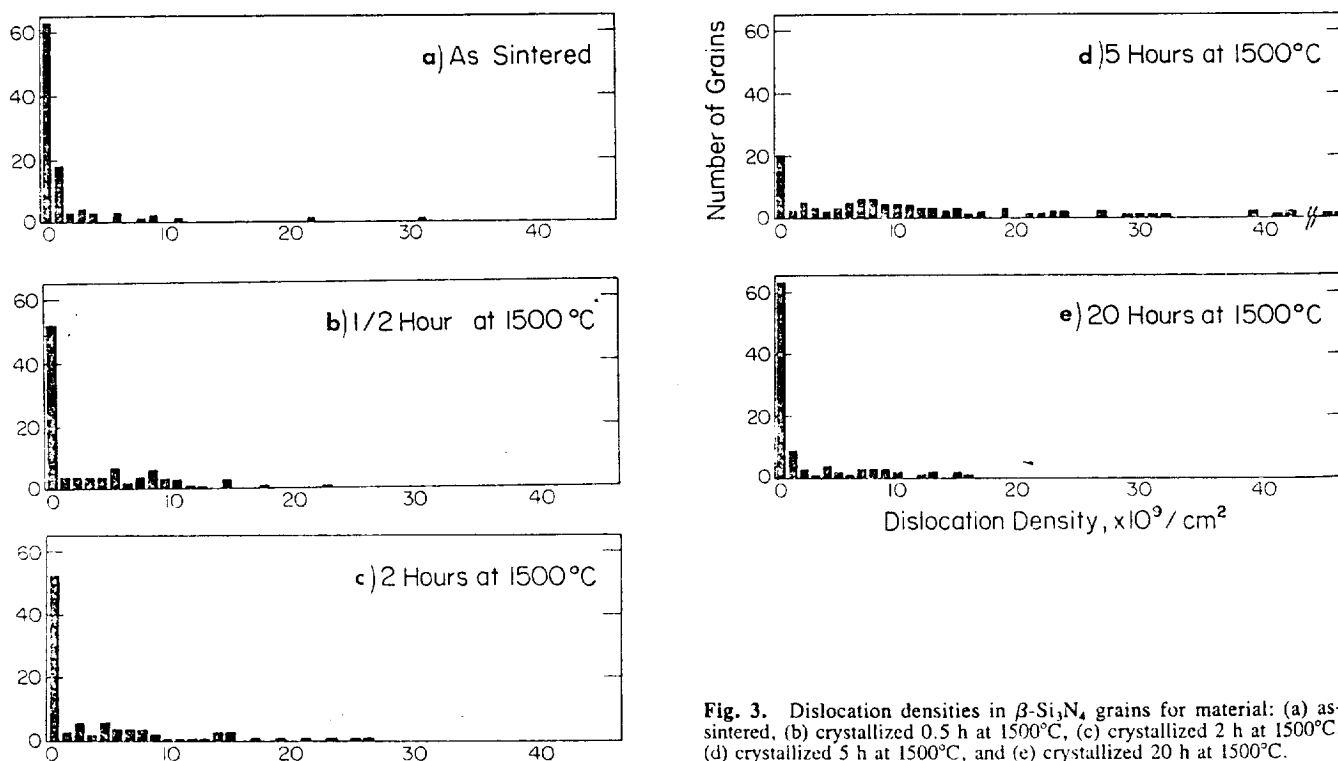


Fig. 3. Dislocation densities in β - Si_3N_4 grains for material: (a) as-sintered, (b) crystallized 0.5 h at 1500°C, (c) crystallized 2 h at 1500°C, (d) crystallized 5 h at 1500°C, and (e) crystallized 20 h at 1500°C.





Fig. 4. BF image of mottled morphology of δ - $\text{Y}_2\text{Si}_2\text{O}_7$ crystallized after 2 h at 1500°C . Inset is the $[010]$ zone axis for δ - $\text{Y}_2\text{Si}_2\text{O}_7$; extra spots arise from other microcrystals included in the selected area aperture.

ORIGINAL PAGE IS
OF POOR QUALITY



Fig. 5. BF image showing highly stressed microstructure of Si_3N_4 after 5 h at 1500°C . β - $\text{Y}_2\text{Si}_2\text{O}_7$ crystallizes at the grain boundaries. The $[001]$ zone axis for β - $\text{Y}_2\text{Si}_2\text{O}_7$ is inset.

selected dislocations indicates that the vast majority of the dislocations have $\mathbf{b} = \langle 0001 \rangle$. However, dislocations having other \mathbf{b} 's were occasionally observed; for example, some dislocations had $\mathbf{b} = \frac{1}{3}\langle 1\bar{2}10 \rangle$.

(2) Microstructure After Heating 0.5 h at 1500°C

After crystallization for only 0.5 h at 1500°C , the microstructure was significantly altered. At the resolution utilized (about 1 nm) the glass had completely crystallized. Electron diffraction patterns matched δ - $\text{Y}_2\text{Si}_2\text{O}_7$ which had a "mottled" morphology in BF, described as "blocky" by Ref. 12, shown in Fig. 4. The dislocation density was slightly higher than in the as-sintered microstructure (Fig. 3(b)), with about 52% of the grains being dislocation-free.

(3) Microstructure After Heating 2 h at 1500°C

The microstructure after 2 h at 1500°C was essentially unchanged from that observed after the 0.5-h crystallizing heat treatment. The dislocation density is given in Fig. 3(c).

(4) Microstructure After Heating 5 h at 1500°C

After a crystallizing heat treatment of 5 h at 1500°C , a highly stressed microstructure is observed (Fig. 5), with large numbers of bend and strain contours visible in the silicon nitride grains. As discussed in Ref. 6, the glassy grain-boundary phase has recrystallized to β - $\text{Y}_2\text{Si}_2\text{O}_7$ after this anneal, with no δ - $\text{Y}_2\text{Si}_2\text{O}_7$ remaining. The inset diffraction pattern in Fig. 5 is the $[001]$ zone for β - $\text{Y}_2\text{Si}_2\text{O}_7$. WBDF imaging reveals that the strain contours arise from complicated and dense dislocation networks and tangles within the β - Si_3N_4 grains (Fig. 6). The distribution of dislocation densities (Fig. 3(d)) shows that now only about 20% of grains are dislocation-free, while the maximum density is $86 \times 10^9/\text{cm}^2$. Again the predominant \mathbf{b} is $\langle 0001 \rangle$, as indicated by the Burgers vector analysis of Fig. 7 (see the $\mathbf{g} \cdot \mathbf{b}$, Table I), in which all dislocations are in contrast for $\mathbf{g} = 0002$ and $0\bar{1}11$ but invisible for $3\bar{6}30$ and $1\bar{3}20$. The heterogeneous nature of the dislocation distribution should be emphasized here in that a dislocation-free grain is often found next to a highly dislocated grain, with no gradual change apparent. Preparation of TEM specimens from material after this treatment was more difficult

than for material given any other treatment: samples invariably cracked on ion thinning.

(5) Microstructure After Heating 20 h at 1500°C

Long heat treatment times at 1500°C led to reduced dislocation densities (Fig. 3(e)), presumably due to the dislocations annealing out. However, the dislocations remaining had undergone extensive rearrangement during the longer heat treatment, giving

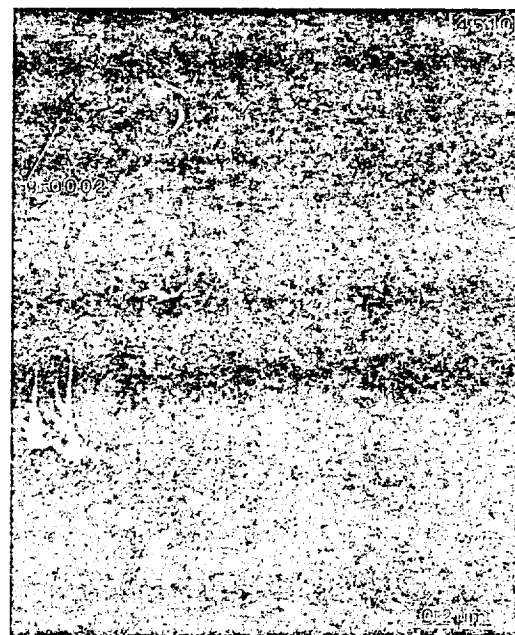


Fig. 6. WBDF image of dense dislocation tangles found after 5 h at 1500°C .



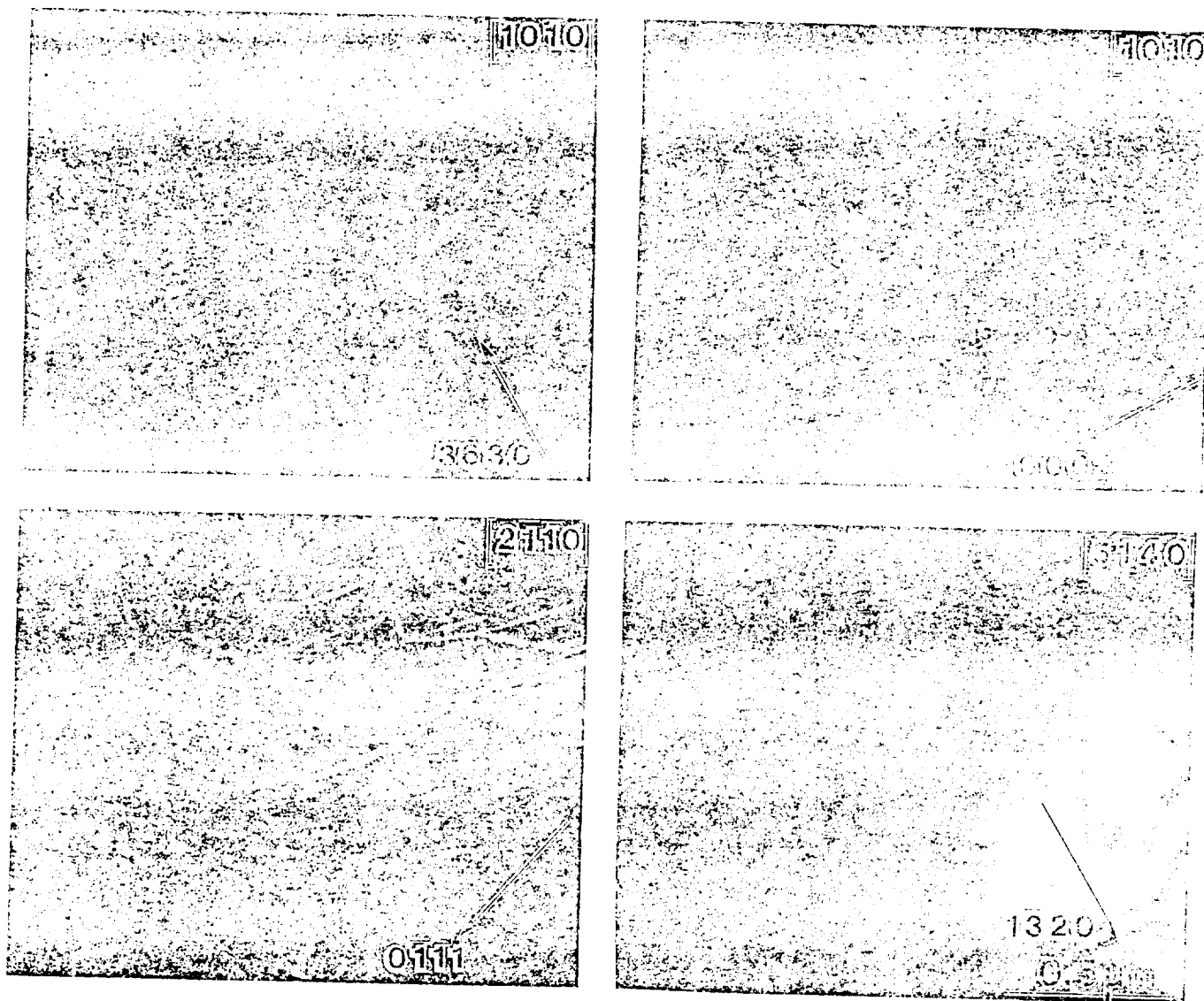


Fig. 7. Burgers vector analysis of dislocations after 5 h at 1500°C using $g = \bar{3}630$ and 0002 from the $[10\bar{1}0]$ zone, $g = 0\bar{1}11$ from $[2\bar{1}10]$, and $g = 1\bar{3}20$ from $[5140]$. All dislocations in this area have $b = \langle 0001 \rangle$.

rise to morphologies such as those of Fig. 8. The Burgers vector analysis illustrated in Fig. 8 suggests that a large number of the dislocations still have $b = \langle 0001 \rangle$, i.e., those in contrast for $g = 0002$ and $0\bar{1}1\bar{1}$ but out for $g = \bar{3}630$ and $02\bar{2}0$, e.g., A. However, dislocations having other b 's are present. If we consider only the perfect dislocation listed for hexagonal structures in Table I, other possible b 's are $\frac{1}{3}[2\bar{1}13]$, e.g., B (in contrast for 0002 , $0\bar{1}1\bar{1}$, and $\bar{3}630$ but out for $02\bar{2}0$), and $\frac{1}{3}[2\bar{1}10]$, e.g., C (in contrast for $g = \bar{3}630$ but out for $0\bar{1}1\bar{1}$, 0002 , and $02\bar{2}0$).

(6) Sub-Grain Boundaries and Polygonized Networks

All samples contained occasional examples of dislocation networks and sub-grain boundaries, e.g., Fig. 9. Initial attempts at b analysis suggest that many of these boundaries are complicated and may require comparison to calculated images for complete interpretation. This is beyond the scope of the present study but will be pursued in the future.

IV. Discussion

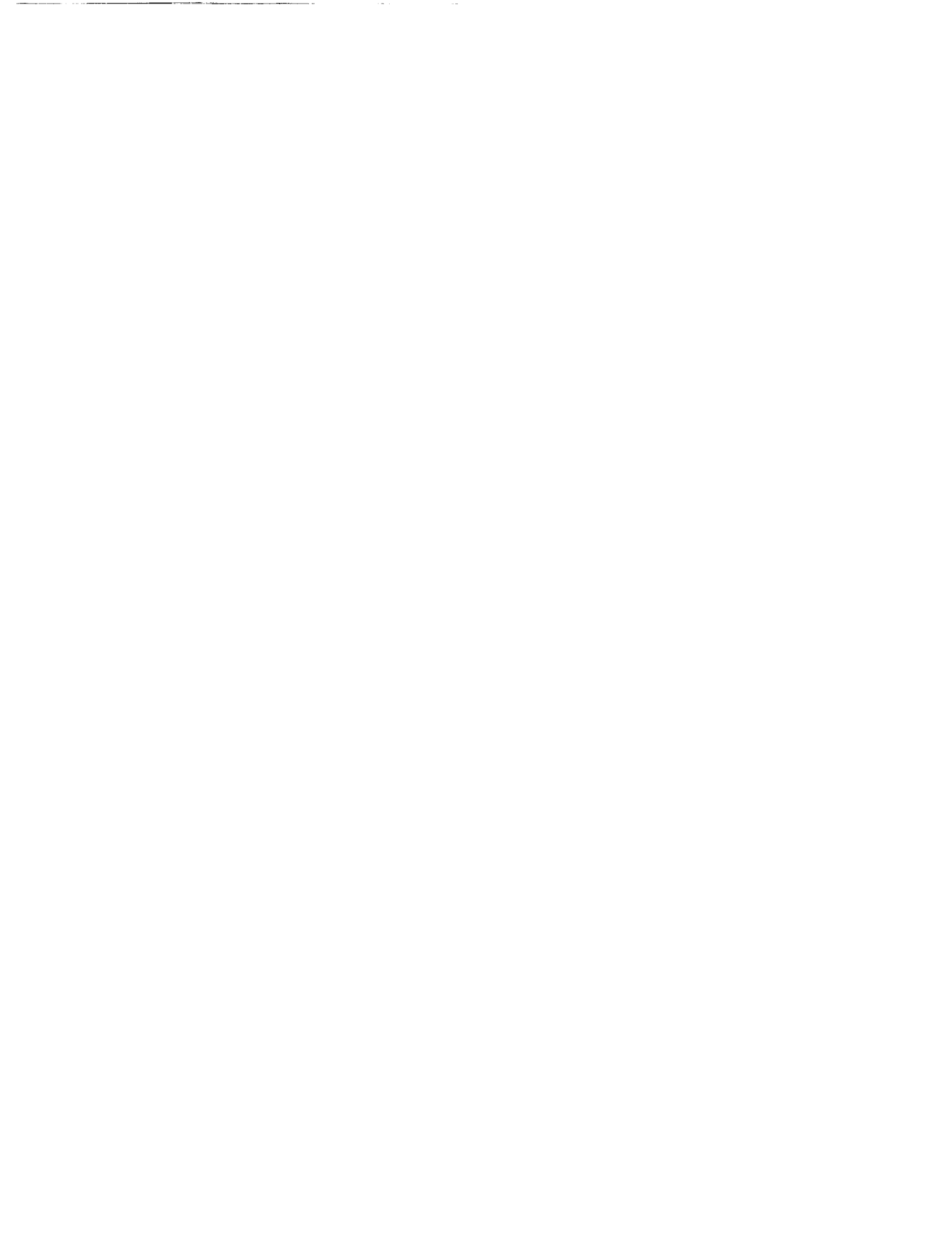
Crystallization of the grain-boundary glass to increase the refractoriness of Si_3N_4 ceramics has been intensively studied since the initial work of Tsuge *et al.*,¹³ also on the $\text{Y}_2\text{O}_3\text{-Si}_3\text{N}_4$ system. However, this is the first observation that crystallization of the

grain-boundary phase may have an effect on the Si_3N_4 grains. While some caution must be heeded with these data in that, because of the complexity of the experiments, only 100 grains were examined in each sample, the trends observed were reproducible. Several explanations can be proffered for the appearance of the dislocations, including a volume change on crystallizing the glass, a volume change upon transformation of one polymorphic form of the crystalline phase to another, or a difference between the thermal expansion coefficient of the phases present.

While the densities of the $\text{Y}_2\text{Si}_2\text{O}_7$ polymorphs are available (see Ref. 14 and Table II), the density of $\text{Y}_2\text{Si}_2\text{O}_7$ glass is not, and experiments to fabricate it and measure its density have been unsuccessful.¹⁵ Crystallization of a glass, however, usually leads to a reduction in volume due to the closer packing of atoms in a crystalline structure, and it seems likely that a volume decrease will occur. Any volume change (increase or decrease) in the grain-boundary phase will impose a strain on the Si_3N_4 grains, deforming them and creating dislocations. The slight increase in dislocation density in the sample crystallized for 0.5 h compared to the as-sintered sample (Figs. 3(a) and (b)) may be attributed to this.

However, the biggest increase in dislocation density occurs between 2 and 5 h at 1500°C (Figs. 3(c) and (d)), during which time, as revealed by electron diffraction analysis, the grain-

ORIGINAL PAGE IS
OF POOR QUALITY



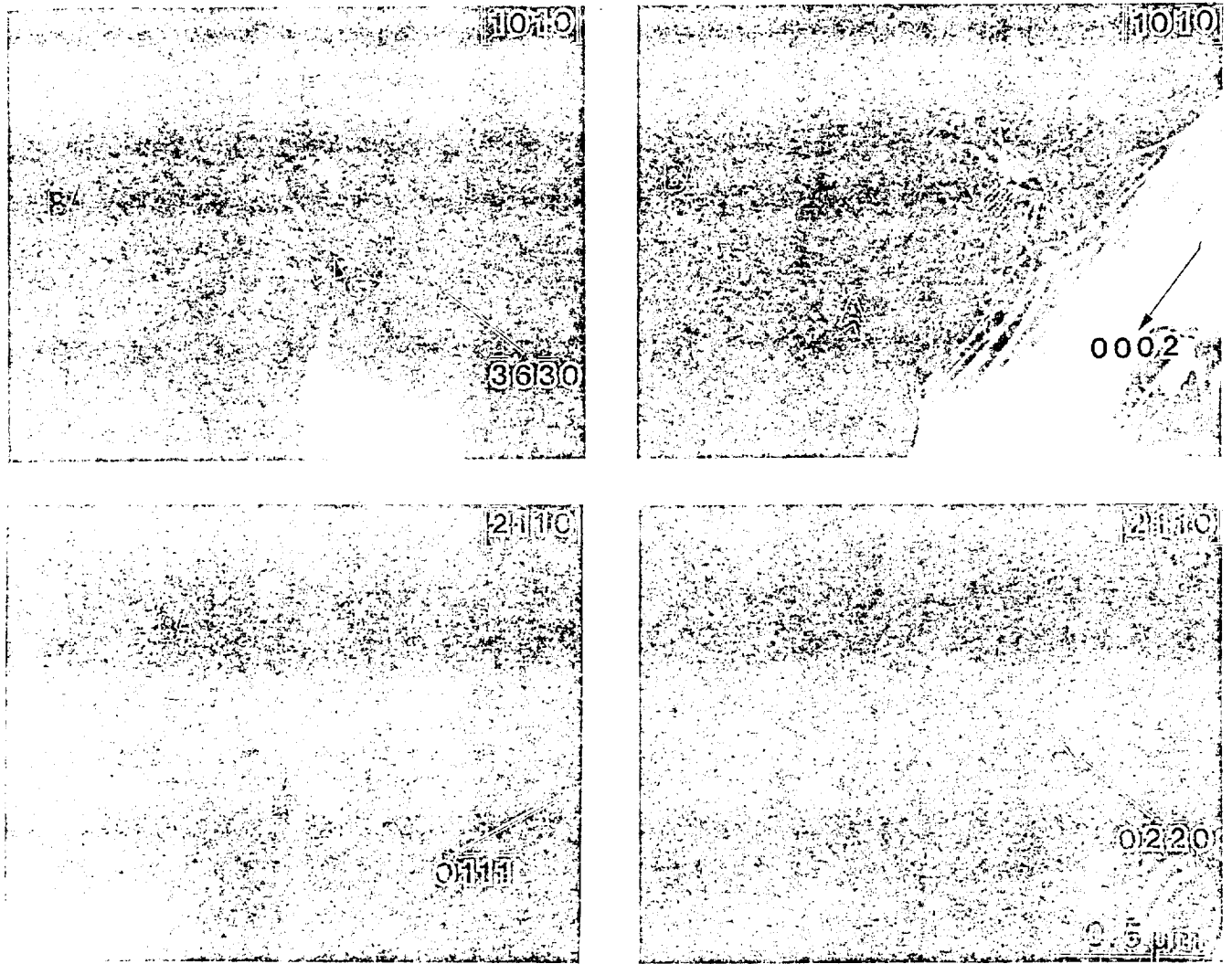


Fig. 8. Partial Burgers vector analysis of dislocations after 20 h at 1500°C using $g = \bar{3}6\bar{3}0$ and 0002 from the $[10\bar{1}0]$ zone and $g = 0\bar{1}\bar{1}\bar{1}$ and $0\bar{2}20$ from $[2\bar{1}10]$. Arrowed dislocations have $b = \langle 0001 \rangle$ (A), $\frac{1}{3}[2\bar{1}\bar{1}3]$ (B), and $\frac{1}{3}[\bar{2}110]$ (C).

boundary phase transforms from δ - to β - $\text{Y}_2\text{Si}_2\text{O}_7$. This strongly suggests that a volume change associated with this transformation is responsible for the observed stress and dislocation formation after 5 h at 1500°C. The volume changes between the polymorphs in $\text{Y}_2\text{Si}_2\text{O}_7$ are given in Table III, calculated from data in Ref. 14. As can be seen, the largest volume change on any transformation is for $\alpha = \beta$. However, the nearly 2% volume change associated with the δ -to- β transition could well generate the stresses necessary to deform the Si_3N_4 grains at 1500°C. Any

shear associated with the δ -to- β transition, which is from orthorhombic to monoclinic symmetry (see Table II), could also contribute to dislocation formation. The dislocation microstructures formed in the crystallized material are typical of those induced in ceramics by high-temperature deformation.¹⁶ The reduced dislocation density after 20 h at 1500°C is due to annealing out of the dislocations by the prolonged heat treatment (Fig. 3(c)).

According to Liddel and Thompson,¹⁴ α - $\text{Y}_2\text{Si}_2\text{O}_7$, the low-temperature form, transforms to β at 1225°C, which should trans-

Table I. Values of $g \cdot b$ for Relevant Reflections in the Hexagonal Crystal Structure for Perfect Dislocations

$b \times 1/3$	$g \cdot b$									
	2020	0220	2200	0002	6330	3630	3360	0111	0111	1320
$\pm[11\bar{2}0]$	∓ 2	∓ 2	0	0	∓ 3	∓ 3	∓ 6	∓ 1	∓ 1	∓ 2
$\pm[1\bar{2}10]$	0	∓ 2	∓ 2	0	∓ 3	∓ 6	∓ 3	∓ 1	∓ 1	∓ 3
$\pm[2110]$	∓ 2	0	∓ 2	0	∓ 6	∓ 3	∓ 3	0	0	∓ 1
$\pm[0003]$	0	0	0	∓ 2	0	0	0	∓ 1	∓ 1	0
$\pm[11\bar{2}3]$	∓ 2	∓ 2	0	∓ 2	∓ 3	∓ 3	∓ 6	0	∓ 2	∓ 2
$\pm[1\bar{2}13]$	0	∓ 2	∓ 2	∓ 2	∓ 3	∓ 6	∓ 3	∓ 2	0	∓ 3
$\pm[2113]$	∓ 2	0	∓ 2	∓ 2	∓ 6	∓ 3	∓ 3	∓ 1	∓ 1	∓ 1
$\pm[11\bar{2}\bar{3}]$	∓ 2	∓ 2	0	∓ 2	∓ 3	∓ 3	∓ 6	∓ 2	0	∓ 2
$\pm[1\bar{2}1\bar{3}]$	0	∓ 2	∓ 2	∓ 2	∓ 3	∓ 6	∓ 3	0	∓ 2	∓ 3
$\pm[211\bar{3}]$	∓ 2	0	∓ 2	∓ 2	∓ 6	∓ 3	∓ 3	∓ 1	∓ 1	∓ 1

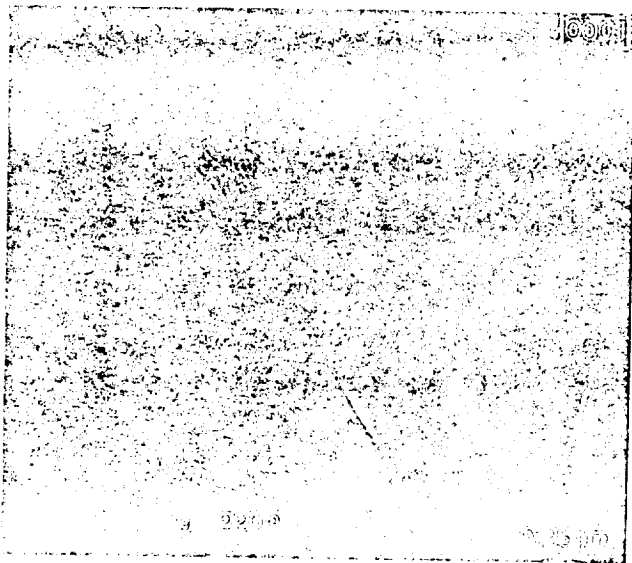


Fig. 9. WBDF image of a sub-grain boundary and a polygonized network (arrowed) in a β - Si_3N_4 grain imaged using $g = 2200$ at the $[0001]$ orientation. The edges of the hexagon are the projections of $\{10\bar{1}0\}$ planes.

ORIGINAL PAGE IS
OF POOR QUALITY

form to γ at 1445°C . Possible reasons for the observation that γ was never detected in the room-temperature microstructure after heat treatment at 1500°C are discussed at length by Lee *et al.*¹⁷

The thermal expansion coefficient of $\text{Y}_2\text{Si}_2\text{O}_7$ is not available, while that of β - Si_3N_4 is known to be low but highly anisotropic.¹⁸ For the temperature range 0° to 1000°C , the thermal expansion coefficient is $3.23 \times 10^{-6}/^\circ\text{C}$ along the a axis and $3.72 \times 10^{-6}/^\circ\text{C}$ along the c axis. This anisotropy is expected to remain at temperatures up to the crystallization temperature used in this study (1500°C) and may cause a significant amount of stress on a local scale, especially if the thermal expansion coefficient of $\text{Y}_2\text{Si}_2\text{O}_7$ is also anisotropic. Thermal expansion mismatch, however, would be expected to lead to similar stress and consequent dislocation formation in all samples regardless of hold time at temperatures, since the stress arises only during the heating and cooling cycle. This cannot, therefore, be invoked to explain the much higher dislocation densities observed after a 5-h crystallization treatment as compared to material receiving other treatments.

Tighe¹⁹ used TEM to examine the surface of Si_3N_4 bars which had been ground with 400-mesh SiC and found high dislocation densities and cracking to a depth of several micrometers. However, after polishing using unreported conditions the damage was substantially reduced. While the possibility exists that some of the dislocations observed in the present study arose from deformation during TEM specimen preparation, it seems unlikely that it could explain the trends observed as a function of heat treatment time, since all samples were prepared in the same manner. The preparation techniques used in the present study did not stop at 400-mesh SiC but continued to 600-mesh SiC followed by polishing with 15-, 9-, and $6\text{-}\mu\text{m}$ diamond paste. The final polish

and dimple then utilized $3\text{-}\mu\text{m}$ diamond paste. This procedure would not be expected to induce severe surface damage in Si_3N_4 at room temperature.

The observation that TEM specimens of the material with high dislocation density fractured on ion thinning is an indication that the room-temperature mechanical properties may be adversely affected by the stress present. However, further mechanical testing of material after the various heat treatments is needed to corroborate this, although the fact that the dislocations anneal out after longer heat treatment times suggests any deterioration may only be temporary. Previous detailed studies of dislocations in Si_3N_4 are sparse, although many authors have commented on the presence of dislocations in Si_3N_4 samples (e.g., Ref. 20). Evans and Sharp,^{21,22} Butler,²³ and Kossowsky²⁴ analyzed the Burgers vectors of dislocations in hot-pressed and reaction-bonded materials. In both forms, most of the dislocations had a $\langle 0001 \rangle$ -type b , although other types of dislocation containing an $a + c$ axis component b were present, tentatively identified as having b approximately $\frac{1}{3}\langle 11\bar{2}3 \rangle$ by Evans and Sharp.²¹ Consideration of the strain energy associated with various types of dislocation in Si_3N_4 ²² indicated that $\langle 0001 \rangle$ was the most stable b , whereas an analysis of dislocation mobility using the Peierls model suggested they would also be the most mobile, with $\{10\bar{1}0\}$ as the primary slip plane. The highly anisotropic slip on systems with a $\langle 0001 \rangle$ Burgers vector in Si_3N_4 ²¹ could be used to explain the inhomogeneity of observations of grains containing dislocations. The observation of $\frac{1}{3}\langle 1\bar{2}10 \rangle$ and $\frac{1}{3}\langle 11\bar{2}3 \rangle$ -type b dislocations in the present study is interesting, and further study of dislocation reactions in this system seem warranted. Kossowsky *et al.*²⁵ suggested that dislocation motion was unlikely at temperatures $< 1700^\circ\text{C}$ in Si_3N_4 and, therefore, their contribution to, for example, creep mechanisms would be small. Evans and Sharp,²¹ however, identified dislocation motion associated with plastic deformation at 1400°C in reaction-bonded Si_3N_4 . More recently Clarke²⁶ has detected increased dislocation densities in material that had undergone a creep test. We feel that more detailed analysis of the dislocations in Si_3N_4 is important since dislocations may well play an active role in high-temperature deformation mechanisms in both monolithic and composite Si_3N_4 -containing materials.

V. Summary and Conclusions

Crystallizing the grain-boundary glass in a Si_3N_4 ceramic containing 6 wt% Y_2O_3 led to the formation of δ - $\text{Y}_2\text{Si}_2\text{O}_7$ after 0.5- or 2-h anneals at 1500°C . A slight increase in dislocation density in the β - Si_3N_4 grains was noted after crystallization. However, after a 5-h anneal at 1500°C the δ - $\text{Y}_2\text{Si}_2\text{O}_7$ had transformed to β - $\text{Y}_2\text{Si}_2\text{O}_7$, and associated with the transition was a dramatic increase in dislocation density in the β - Si_3N_4 grains. The most likely origin for the deformation of the silicon nitride grains is the volume change accompanying the δ -to- β - $\text{Y}_2\text{Si}_2\text{O}_7$ transition. Longer anneals at 1500°C for times up to 20 h reduced the dislocation density to the levels observed in as-sintered materials, suggesting that any effect on the mechanical properties of the silicon nitride may be removed.

Table II. Space Groups, Specific Volumes, and Densities for the $\text{Y}_2\text{Si}_2\text{O}_7$ Polymorphs

Polymorph	Space group	Specific vol (nm^3)	Density (g/cm^3)
γ	Monoclinic $P2_1/m^*$	0.1407	4.083
α	Triclinic $P\bar{1}$	0.1336	4.300
β	Monoclinic $C2/m$	0.1425	4.032
γ	Monoclinic $P2_1/n$	0.1422	4.040
δ	Orthorhombic $Pna2_1$	0.1398	4.110

*Determined as $Aba2$ by Ref. 12.



Table III. Volume Changes Associated with Transformations between $\text{Y}_2\text{Si}_2\text{O}_7$ Polymorphs on Heating

Polymorphs	Vol change (%)
$\alpha \rightarrow \beta$	+6.233
$\beta \rightarrow \gamma$	-0.198
$\gamma \rightarrow \delta$	-1.733
$\beta \rightarrow \delta$	-1.984

References

- ¹S. C. Singhal, "Thermodynamic Analysis of the High-Temperature Stability of Si_3N_4 and SiC ," *Ceramurgia Int.*, **2** [3] 123-30 (1976).
- ²G. G. Deeley, J. M. Herbert, and N. C. Moore, "Dense Silicon Nitride," *Powder Metall.*, **8**, 145-51 (1961).
- ³A. Tsuge and K. Nishida, "High Strength Hot-Pressed Si_3N_4 with Concurrent Y_2O_3 and Al_2O_3 Additions," *Am. Ceram. Soc. Bull.*, **57** [4] 424-26, 431 (1978).
- ⁴P. Drew and M. H. Lewis, "The Microstructures of Silicon Nitride Ceramics During Hot-Pressing Transformations," *J. Mater. Sci.*, **9**, 261-69 (1974).
- ⁵R. E. Loehman, "Preparation and Properties of Yttrium-Silicon-Aluminum Oxynitride Glasses," *J. Am. Ceram. Soc.*, **62** [9-10] 491-94 (1979).
- ⁶W. E. Lee, C. H. Drummond III, G. E. Hilmas, J. D. Kiser, and W. A. Sanders, "Microstructural Evolution on Crystallizing the Glassy Phase in a 6 wt% Y_2O_3 - Si_3N_4 Ceramic," *Ceram. Eng. Sci. Proc.*, **9** [9-10] 1355-66 (1988).
- ⁷P. B. Hirsch, A. Howie, R. B. Nicholson, D. W. Pashley, and M. J. Whelan, *Electron Microscopy of Thin Crystals*. Kreiger, New York, 1977.
- ⁸A. K. Head, P. Humble, L. M. Clareborough, A. J. Morton, and C. T. Forwood, *Computed Electron Micrographs and Defect Identification*. North-Holland, Amsterdam, 1973.
- ⁹D. J. H. Cockayne, I. L. F. Ray, and M. J. Whelan, "Investigations of Dislocation Strain Fields Using Weak Beams," *Philos. Mag.*, **20** [168] 1265-70 (1969).
- ¹⁰J. V. Sharp, A. G. Evans, and B. Hudson, "Electron Diffraction Data for Silicon Nitride," Harwell Research Report AERL-R7319, 1972.
- ¹¹S. A. Allen, "Foil Thickness Measurements from Convergent-Beam Diffraction Patterns," *Philos. Mag. A*, **43** [2] 325-35 (1981).
- ¹²T. R. Dinger, R. S. Rai, and G. Thomas, "Crystallization Behavior of a Glass in the Y_2O_3 - SiO_2 - AlN System," *J. Am. Ceram. Soc.*, **71** [4] 236-44 (1988).
- ¹³A. Tsuge, K. Nishida, and M. Komatsu, "Effect of Crystallizing the Grain-Boundary Glass Phase on the High-Temperature Strength of Hot-Pressed Si_3N_4 Containing Y_2O_3 ," *J. Am. Ceram. Soc.*, **58** [7-8] 323-26 (1975).
- ¹⁴K. Liddel and D. P. Thompson, "X-ray Diffraction Data for Yttrium Silicates," *Br. Ceram. Trans. J.*, **85**, 17-22 (1986).
- ¹⁵M. Long; private communication.
- ¹⁶T. E. Mitchell, "Application of Transmission Electron Microscopy to the Study of Deformation in Ceramic Oxides," *J. Am. Ceram. Soc.*, **62** [5-6] 254-67 (1979).
- ¹⁷W. E. Lee, C. H. Drummond III, G. E. Hilmas, and S. Kumar, "A Comparison of the Crystallization Behavior of Y_2O_3 - SiO_2 Glass as Bulk Material and as an Intergranular Phase in Si_3N_4 ," unpublished work.
- ¹⁸C. M. B. Henderson and D. Taylor, "Thermal Expansion of the Nitrides and Oxynitride of Silicon in Relation to Their Structures," *Br. Ceram. Trans. J.*, **74**, 49-53 (1975).
- ¹⁹N. J. Tighe, "Characterization of Flaws Produced by Mechanical Grinding of Si_3N_4 ," pp. 144-45 in Proceedings of the 35th Annual Meeting of the Electron Microscopy Society of America (EMSA). San Francisco Press, San Francisco, CA, 1977.
- ²⁰H. Makino, N. Kamiya, and S. Wada, "Strength Degradation of Si_3N_4 by Contact Stress," *J. Mater. Sci. Lett.*, **7**, 475-76 (1988).
- ²¹A. G. Evans and J. V. Sharp, "Transmission Electron Microscopy of Silicon Nitride," pp. 1141-53 in *Electron Microscopy and Structure of Materials*, Edited by G. Thomas, R. M. Fulrath, and R. M. Fisher. California Press, Berkeley, CA, 1972.
- ²²A. G. Evans and J. V. Sharp, "Microstructural Studies on Silicon Nitride," *J. Mater. Sci.*, **6**, 1292-302 (1971).
- ²³E. Butler, "Observations of Dislocations in β -Silicon Nitride," *Philos. Mag.*, **24**, 829-34 (1971).
- ²⁴R. Kossowsky, "The Microstructure of Hot-Pressed Silicon Nitride," *J. Mater. Sci.*, **8**, 1603-15 (1973).
- ²⁵R. Kossowsky, D. G. Miller, and E. S. Diaz, "Tensile and Creep Strengths of Hot-Pressed Si_3N_4 ," *J. Mater. Sci.*, **10**, 983-97 (1975).
- ²⁶D. R. Clarke; private communication. □

ORIGINAL PAGE IS
OF POOR QUALITY

Microstructural Evolution in Near-Eutectic Yttrium Silicate Compositions Fabricated from a Bulk Melt and as an Intergranular Phase in Silicon Nitride

William E. Lee,** Charles H. Drummond III,* Gregory E. Hilmas,*† and Suresh Kumar*‡

Department of Materials Science and Engineering, The Ohio State University, Columbus, Ohio 43210

Near-eutectic composition $Y_2O_3-SiO_2$ melts were formed as bulk samples or as an intergranular phase in Si_3N_4 . Upon cooling to room temperature the bulk material partially crystallized to $\delta-Y_2Si_2O_7$, whereas the intergranular phase was glass. On heat-treating at $1500^\circ C$ the bulk material transformed to $\gamma-Y_2Si_2O_7$, whereas the intergranular glass crystallized first to $\delta-Y_2Si_2O_7$, and then to $\beta-Y_2Si_2O_7$. Possible reasons for the different behavior are discussed. [Key words: crystallization, glass, yttria, silica, silicon nitride.]

I. Introduction

TO FACILITATE liquid-phase sintering (LPS) a metal oxide, or a mixture of oxides, is added to $\alpha-Si_3N_4$ powder. The ubiquitous silica film present on the nitride particles (occasionally with added silica powder) combines with the oxide to form a low melting temperature liquid phase which is the host for the solution-precipitation sintering mechanism¹ known to occur in this material. The liquid composition influences its viscosity and hence the kinetics of sintering.^{2,3} Sintering is carried out at high temperatures ($>1700^\circ C$) in nitrogen atmospheres to retard decomposition of silicon nitride. Upon cooling to room temperature the silicate liquid has usually solidified to a glass and the $\alpha-Si_3N_4$ powder has converted to $\beta-Si_3N_4$ during the solution-precipitation process. Unfortunately, the low melting temperature of the silicate phase, used to advantage during sintering, is detrimental to the mechanical properties of the monolithic material at elevated use temperatures since the glass begins to soften. This softening can promote grain-boundary sliding, cavitation creep, and sub-critical crack growth at relatively low temperatures (about $1000^\circ C$).

The compositions of intergranular silicate glasses formed with various oxide additions have been examined using a range of analytical techniques such as analytical electron microscopy,^{1,4,6} electron probe microanalysis,⁷ and Auger electron spectroscopy.^{7,8} Several authors⁸⁻¹⁰ have even attempted to examine the properties of bulk glass fabricated with the approximate composition of the intergranular glass. These studies indicate that the presence of nitrogen not only increases the viscosity of the melt but also increases the glass transition temperature, hardness, density, and fracture toughness of the bulk glass at room temperature. Consequently, ni-

trogen incorporation in the intergranular silicate phase is envisaged as a route to improved high-temperature properties in silicon nitride based ceramics. Crystallization of the intergranular glass by pre-¹¹ or postsinter¹²⁻¹⁴ heat treatments can also lead to improved high-temperature behavior by formation of a more refractory phase at the grain boundaries. No studies, however, have been made of the crystallization behavior of intergranular glass and bulk glass of the same composition. Microstructural characterizations of the crystallization of large volumes of bulk glass are more straightforward since the very high resolution analytical techniques (such as convergent beam electron diffraction, structure imaging, and field emission energy dispersive spectroscopy) needed to study small intergranular phases may be avoided. If the microstructural evolution of intergranular and bulk material can be shown to be equivalent, then use of the latter for phase stability studies is envisaged. This communication reports an attempt to compare the crystallization of an yttrium silicate melt in bulk form and as an intergranular phase in LPS silicon nitride.

II. Experimental Procedure

Bulk melts were prepared from 50-g batches of Y_2O_3 [§] and SiO_2 [¶] powder which were wet ball-milled in silicon nitride mills for 4 h using high-purity Si_3N_4 milling media and ethanol. After drying and dry milling for 2 h the batch was pressed into pellets at 10.3 MPa and melted in W crucibles at $2100^\circ C$ for 4 h under 50 atm (about 5 MPa) of nitrogen. The heating rate was $45^\circ C/min$ and the cooling rate was $520^\circ C/min$ for the first minute after switching off the furnace and $170^\circ C/min$ averaged over the next 10 min. The melt composition was chosen to be at the eutectic in the $Y_2O_3-SiO_2$ phase diagram. NASA 6Y composition silicon nitride samples¹⁵ were prepared from Si_3N_4 ,** Y_2O_3 ,[§] and SiO_2 ^{¶¶} powders mixed in the weight ratio 90:6.4:3.6, respectively, and 100-g batches were milled for 300 h in 1-L silicon nitride ball mills again using high-purity Si_3N_4 milling media and ethanol. This milling process is known to increase SiO_2 content by about 1 to 2 wt% because of the oxidation of silicon nitride.¹⁵ After drying, the powders were die-pressed into 3 cm \times 0.56 cm \times 0.28 cm bars at 21 MPa, cold isostatically pressed at 414 MPa, and sintered at $2140^\circ C$ for 4 h under 50 atm (about 5 MPa) of nitrogen. Heating and cooling rates were the same as for the bulk material. Crystallizing anneals at $1500^\circ C$ were in air for the bulk material (heating rate $10^\circ C/min$, cooling rate $20^\circ C/min$) but 50 atm of N_2 for the silicon nitride (heating and cooling rates as for sintering).

The elemental content of the bulk material (Table I) was determined by X-ray fluorescence (XRF) for all elements except N, which was determined by inert gas fusion (IGF). The composition of the intergranular glass was calculated from

G. H. Beall—contributing editor

Manuscript No. 197876. Received December 26, 1989; approved August 15, 1990.

*Member, American Ceramic Society.

†Present address: School of Materials, University of Sheffield, Sheffield, S1 3JD, U. K.

‡Present address: Department of Materials Science and Engineering, University of Michigan, Ann Arbor, MI 48109.

§Present address: Department of Materials Science and Engineering, Pennsylvania State University, University Park, PA 16802.

§99.99% pure Y_2O_3 Molycorp Inc., White Plains, N.Y.

¶Reagent-grade, Alpha Products, Danvers, MA.

**KBI-AME, Reading, PA.

¶¶Apache Chemicals, Seward, IL.

Table I. Chemical Composition of the Bulk and Intergranular Glass

	Composition (wt%)			
	Y ₂ O ₃	SiO ₂	WO ₃ /W	N
As-mixed powder (bulk glass)	59.4	40.6	0	0
As-melted bulk glass by XRF and IGF*	60.96	39.94	0.92/0.73	0.12
As-mixed powder (intergranular) [†]	64.0	36.0	0	0

*Values total 101.75%, indicating a small error associated with the analytical techniques. [†]Not including oxide impurity and oxidation of Si₃N₄ powder during milling.

the starting powders (Table I). Allowing for SiO₂ impurity and oxidation of Si₃N₄ during milling, the final composition is expected to be close to the eutectic. Intergranular glass composition was also determined using energy dispersive X-ray spectroscopy (EDS) assuming oxides and ignoring the presence of N, which cannot be detected with a Be-window EDS detector. Microstructural and crystallographic analysis was performed using a transmission electron microscope[‡] (TEM) equipped with a Be-window EDS detector[§] and an X-ray powder diffractometer[¶] using CuK α radiation. Electron energy loss spectroscopy^{***} (ELS) was carried out at NASA Lewis Research Center.

III. Results and Discussion

(I) Bulk and Intergranular Melts on Cooling

After bulk powders were melted (at 2100°C) and Si₃N₄ bars were sintered (at 2140°C), furnace-cooled samples were examined using XRD. The bulk powders partially crystallized to δ -Y₂Si₂O₇ (Fig. 1(a)), the highest-temperature polymorph according to Refs. 16 and 17 (Table II). Some remnant silica glass is expected since this eutectic composition is richer in silica than pure Y₂Si₂O₇. Dinger *et al.*¹⁸ found crystals of δ - or β -Y₂Si₂O₇ in as-melted bulk material of similar composition near the Y₂O₃-SiO₂ binary in their study of Y₂O₃-SiO₂-AlN glasses. The as-melted bulk sample contained about 0.73 wt% W (presumably present as WO₃) and a small amount (0.12 wt%) of nitrogen (Table I), attributed to contamination by container and nitrogen atmosphere, respectively.

The 6Y composition Si₃N₄, however, only contained XRD peaks from β -Si₃N₄. Electron diffraction and EDS analysis in the TEM confirmed that the intergranular phase was amorphous with a Si/Y ratio similar to that obtained by XRF for

the eutectic composition bulk material (Table I). ELS analysis for nitrogen in the intergranular glass was inconclusive since the nitrogen edge could not be clearly distinguished from the background. This suggests that nitrogen is not present in large (i.e., >10 atom%) quantities upon cooling the melt to room temperature. Nitrogen will, however, be present in the liquid at high temperatures from solution of α -Si₃N₄ powder and it is not surprising that many (determined at about 2 vol% from TEM images) lath-shaped Si₂N₂O grains were also detected in the as-sintered Si₃N₄ (Fig. 2). Si₂N₂O crystals, distinguishable by characteristic stacking faults along (100) planes,¹⁹ reprecipitate along with β -Si₃N₄ grains. No evidence of any other devitrification was observed in the intergranular phase.

Assuming that the nitrogen content of the bulk material is low in the melt (otherwise Si₂N₂O would also have formed on cooling or high nitrogen contents would be present) the major chemical differences between the two melts are nitrogen content (higher in the intergranular melt) and the W/WO₃ impurity in the bulk melt. Oxynitride silicate melts are more viscous than the corresponding oxide melts. This is thought to be due to the incorporation of nitrogen capable of bridging three network tetrahedral groups replacing oxygen which is only capable of bridging two.²⁰ The higher viscosity of the intergranular melt may kinetically hinder crystallization of Y₂Si₂O₇ whereas the greater fluidity and presence of W/WO₃ in the bulk melt sample may tend to increase crystallization rates upon cooling. Neither the Si₃N₄ crystals nor any impurities scavenged by the silicate liquid² below the detection limit of EDS appear to facilitate crystallization of the intergranular glass on cooling.

The nitrogen contents are low in both bulk material (Table I) and intergranular glass (indicated by ELS analysis). Consequently, in the following discussion we will consider only the binary system Y₂O₃-SiO₂. In contrast to the yttrium SiAlONs, very little work has been published on the Y-Si-O-N system because of the difficulty of forming glasses. Drew *et al.*⁹ obtained bloating and high weight loss due to nitrogen evolution when attempting to form glasses in this system, suggesting nitrogen incorporation in the glass, as opposed to the melt, is difficult.

(2) Heat Treatment at 1500°C

After 5 h at 1500°C δ -Y₂Si₂O₇ in the partially crystallized bulk sample had transformed to γ -Y₂Si₂O₇ (Fig. 1(b)) consistent with the polymorphism of Y₂Si₂O₇ given in Table II.

The 6Y-Si₃N₄ behaved very differently. After 2 h at 1500°C it had completely crystallized to δ -Y₂Si₂O₇ (Fig. 3), which is expected since crystallization of glasses often begins with metastable formation of the highest-temperature polymorph even at temperatures below its equilibrium field of stability.²¹ Additional Si₂N₂O was also detected in the 6Y-Si₃N₄ after crystallization but with a different morphology than in as-sintered material (Fig. 4). In this case the Si₂N₂O is not present as lath-shaped grains but crystallized around Si₃N₄ grains although still with the characteristic (100) stacking faults and streaks in electron diffraction patterns. This crystallization and the observed morphology may result from formation of Y₂Si₂O₇, leaving a nitrogen-containing silica-rich glass which itself crystallized as Si₂N₂O. This result indicates that some nitrogen remained in the intergranular glass after cooling from the sintering temperature and was only incorporated

[‡]Model 200CX, JEOL USA, Inc., Peabody, MA.
[§]TN 2000, Tracor Northern, Middleton, WI.
[¶]XRG 3100, Philips Electronics Inc., Mahwah, NJ.
^{***}Model 607 Gatan Inc., Warrendale, PA.

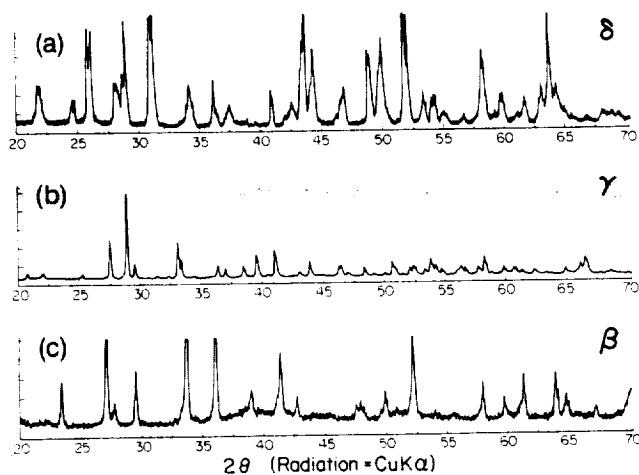


Fig. 1. XRD spectra for (a) as-melted bulk sample, (b) bulk melt after 5 h at 1500°C in air, (c) intergranular glass after 5 h at 1500°C in 50 atm of nitrogen.

Table II. Physical and Crystallographic Data for the Polymorphs of $Y_2Si_2O_7$ *

	Field of stability (°C)	Crystal system	Space group	a (nm)	b (nm)	c (nm)	α	β	γ	JCPDS file	Density ($g \cdot cm^{-3}$)
α	RT to 1225	Triclinic	$P\bar{1}$	0.659	0.664	1.225	94.0	89.2	93.1	21-1457	4.300
β	1225-1445	Monoclinic	$C2/m$	0.688	0.897	0.472	90	101.7	90	22-1103	4.032
γ	1445-1535	Monoclinic	$P2_1/n$	0.558	1.086	0.47	90	96.0	90	20-1436	4.040
δ	1535-1775	Orthorhombic	$Pna2_1$ [†]	1.366	0.502	0.815	90	90	90	22-1460	4.110
Y	Impurity stabilized	Monoclinic	$P2_1/m$ [‡]	0.75	0.806	0.502	90	112	90	32-1448	4.083

*Adapted from Refs. 16 and 17. †Reference 18 lists two δ polymorphs, δ_1 and δ_2 , with δ_2 having space group $Pna2_1$. ‡Determined as $Aba2$ by Ref. 18 using convergent beam electron diffraction.

into Si_2N_2O crystallized with this morphology during heat treatment at 1500°C.

After 5 h at 1500°C the δ - $Y_2Si_2O_7$ had transformed to β - $Y_2Si_2O_7$ (Figs. 1(c) and 5), which remained even after 20 h at 1500°C. The 1.931% positive volume change associated with this transformation is thought to be responsible for the generation of large numbers of dislocations in the Si_3N_4 grains.²² Transformation to β is unexpected since, according to the data in Table II, 1500°C is outside the field of stability of the β polymorph; instead δ would be expected to transform to γ at this temperature. As well as the differing initial phase assemblages, empirical differences between the crystallizing heat treatments for bulk and intergranular material include atmosphere (air and 50 atm of nitrogen, respectively) and quench rate (20° and 170°C/min, respectively). To test that these variables were not significant, bars of 6Y- Si_3N_4 were crystallized at 1500°C in the same furnace as the bulk glass, i.e., in air and with 20°C/min cooling rate. The $Y_2Si_2O_7$ polymorphs formed were the same as with the nitrogen atmosphere and the rapid quench rate.

While it may not be possible to state explicitly the reasons for the difference in behavior of the bulk and intergranular glass during postmelt heat treatments, several significant factors can be considered, such as impurity content, atmosphere, quench rate, crystal nucleation, the characteristics of the polymorphic transitions, and the presence or absence of quench crystals of δ - $Y_2Si_2O_7$. Admittedly much of what follows is conjecture since the information required to fully interpret the results is not available. For example, the effect of impurity ions on the polymorphism of $Y_2Si_2O_7$ has not been clarified and interfacial free energies are not available. However, the

following factors are expected to influence the crystallization behavior.

Intergranular glass in Si_3N_4 is known to scavenge impurity cations from the starting powders.² These impurities outdiffuse along the grain boundaries during elevated-temperature treatments. Falk²³ detected β - $Y_2Si_2O_7$ in grain boundaries at the near surface regions of Si_3N_4 bars but α in grain boundaries at depths near the bar center after 7 h at 1400°C in air. She attributes this result to stabilization of β by impurity cations outdiffusing during the heat treatment but also suggests that the annealing atmosphere may play a role in determining the particular polymorph which forms during crystallization. However, unpublished work by Kumar and Drummond found that the quench rate of melts was a more significant variable than nitrogen pressure. Melts in 1- or 50-atm nitrogen overpressures and quenched at different rates (110° and 170°C/min, respectively) contained similar amounts of nitrogen (about 0.1 wt%) but crystallized to the γ and δ polymorphs of $Y_2Si_2O_7$, respectively. As discussed above, the atmosphere and quench rate have less effect once crystals have formed. Incorporation of impurity cations is known to stabilize the Y form of $Y_2Si_2O_7$, which forms on oxidation of Y_2O_3 - SiO_2 glasses²⁴ and β may be similarly stabilized. The observation that δ forms before β suggests that it too may be impurity stabilized.

Dinger *et al.*¹⁸ found that Y- $S_2Si_2O_7$ nucleated on Fe-Si impurity particles in bulk glass and then transformed to δ - $Y_2Si_2O_7$ although they found two closely related but different polymorphs by HREM designated δ_1 and δ_2 . Their results are also inconsistent with the stability fields of Ref. 17. This may



Fig. 2. Lath-shaped Si_2N_2O crystals in as-sintered 6Y- Si_3N_4 .



Fig. 3. Dark-field TEM image of δ - $Y_2Si_2O_7$ crystals as intergranular phase in 6Y- Si_3N_4 after 2 h at 1500°C.



Fig. 4. Si₂N₂O crystallized around Si₃N₄ grains in 6Y-Si₃N₄ after 5 h at 1500°C.

be due to the formation of metastable phases. The nucleation of crystals on impurities such as Fe-Si or W/WO₃ depends upon many factors, such as contact angle between nucleus and impurity substrate; impurity surface area, shape, and dispersion in the glass; lattice mismatch and interfacial free energy between the impurity and the nucleating crystal.²⁵ However, we observed no such microcrystals which might act as nucleants in the bulk melt glass of this study. In the intergranular glass the polymorph with the lowest interfacial free energy difference with respect to β-Si₃N₄ will crystallize as a transient or metastable phase if Y₂Si₂O₇ nucleates on Si₃N₄ grains. Support for the suggestion that β-Si₃N₄ favors the nucleation of β-Y₂Si₂O₇ was obtained by melting the eutectic glass composition at 2100°C for 4 h in 50 atm of nitrogen with a



Fig. 5. Dark-field TEM image of β-Y₂Si₂O₇ crystals as intergranular phase in 6Y-Si₃N₄ after 5 h at 1500°C.

6Y-Si₃N₄ bar and quenching. The resulting melt contained dissolved silicon nitride and only β-Y₂Si₂O₇.

The volume change on cooling associated with the δ-to-β transformation is 1.931% whereas it is 1.733% for the δ-to-γ transition so that it is unlikely that the volumetric constraint imposed by the Si₃N₄ grains would restrict one transformation in favor of the other. It is also unlikely that β is forming as a metastable phase en route to forming γ after sufficient time at temperature since β is a lower temperature polymorph and therefore less stable than γ at this temperature (Table II).

Some information on polymorphic transitions in other grain-boundary phases may also be gained from this study. The first polymorph to form upon crystallization, δ, has a characteristic mottled morphology and a small grain size, about 1 μm (Fig. 3), suggesting many nucleation sites are available (similar to cordierite crystallized in SiAlON grain boundaries¹²). However, after continued annealing at 1500°C the δ transforms to β with concurrent grain growth so that single grains of β-Y₂Si₂O₇ (about 10-μm diameter) extend over large volumes around many Si₃N₄ grains (Fig. 5). The greater grain size of β compared to δ suggests few β nuclei and/or rapid growth rates of the β nuclei present. If, as seems likely, the β grains nucleate on the δ grain boundaries, then rapid grain growth must be occurring. The large grains of garnet in SiAlON grain boundaries¹² may have formed in a similar manner.

IV. Summary and Conclusions

Attempts to form glass of identical composition from bulk melts and as an intergranular phase in Si₃N₄ were unsuccessful. While the intergranular material was amorphous, the bulk material contained crystals of δ-Y₂Si₂O₇ and a silicate glass at room temperature. On heat-treating at 1500°C the bulk material transformed to γ-Y₂Si₂O₇, whereas the intergranular glass crystallized first to δ-Y₂Si₂O₇ and then to β-Y₂Si₂O₇. Variables discussed which may explain the different behavior include impurity ions, impurity phases, and crystallographic factors. Quench rate and nitrogen content in the crystallization atmosphere were less significant variables.

Si₂N₂O forms in Si₃N₄ with two morphologies: as lath-shaped grains arising from nitrogen solution in as-sintered material (Fig. 2) and also crystallized around Si₃N₄ grains (Fig. 4) after a postsinter heat treatment. The latter morphology may arise since crystallization of Y₂Si₂O₇ leaves a N-containing silica-rich glass which itself crystallizes as Si₂N₂O.

References

- ¹P. Drew and M. H. Lewis, "The Microstructures of Silicon Nitride Ceramics During Hot-Pressing Transformations," *J. Mater. Sci.*, **9**, 261-69 (1974).
- ²M. H. Lewis and R. J. Lumby, "Nitrogen Ceramics: Liquid Phase Sintering," *Powder Metall.*, **26** [2] 73-81 (1983).
- ³S. Hampshire and K. H. Jack, "The Kinetics of Densification and Phase Transformation of Nitrogen Ceramics," *Proc. Br. Ceram. Soc.*, **31** [6] 37-49 (1981).
- ⁴R. Kossowsky, "The Microstructure of Hot-Pressed Silicon Nitride," *J. Mater. Sci.*, **8**, 1603-15 (1973).
- ⁵D. R. Clarke, N. J. Zaluzec, and R. W. Carpenter, "The Intergranular Phase in Hot-Pressed Silicon Nitride: I. Elemental Composition," *J. Am. Ceram. Soc.*, **64** [10] 601-607 (1981).
- ⁶C. C. Ahn and G. Thomas, "Microstructure and Grain-Boundary Composition of Hot-Pressed Silicon Nitride with Yttria and Alumina," *J. Am. Ceram. Soc.*, **66** [1] 14-17 (1983).
- ⁷R. Kossowsky and S. C. Singhal, p. 275 in *Grain Boundaries in Engineering Materials*. Edited by J. L. Walter, J. H. Westbrook, and D. A. Woodford. Gaitors, Baton Rouge, LA, 1975.
- ⁸B. D. Powell and P. Drew, "The Identification of a Grain Boundary Phase in Hot-Pressed Silicon Nitride by Auger Electron Spectroscopy," *J. Mater. Sci.*, **9**, 1867-70 (1974).
- ⁹R. A. L. Drew, S. Hampshire, and K. H. Jack, "Nitrogen Glasses," *Br. Ceram. Soc. Proc.*, **31**, 119-32 (1981).
- ¹⁰R. E. Loehman, "Preparation and Properties of Yttrium-Silicon-Aluminum Oxynitride Glasses," *J. Am. Ceram. Soc.*, **62** [9-10] 491-94 (1979).

- ¹¹A. Tsuge, K. Nishida, and M. Komatsu, "Effect of Crystallizing the Grain-Boundary Glass Phase on the High-Temperature Strength of Hot-Pressed Si_3N_4 Containing Y_2O_3 ," *J. Am. Ceram. Soc.*, **58** [7-8] 323-26 (1975).
- ¹²D. A. Bonnell, T.-Y. Tien, and M. Rühle, "Controlled Crystallization of the Amorphous Phase in Silicon Nitride Ceramics," *J. Am. Ceram. Soc.*, **70** [7] 460-65 (1987).
- ¹³L. K. L. Falk and G. L. Dunlop, "Crystallization of the Glassy Phase in an Si_3N_4 Material by Post-sintering Heat Treatments," *J. Mater. Sci.*, **22**, 4369-76 (1987).
- ¹⁴W. E. Lee, C. H. Drummond III, G. E. Hilmas, J. D. Kiser, and W. A. Sanders, "Microstructural Evolution on Crystallizing the Glassy Phase in a 6 wt% Y_2O_3 - Si_3N_4 Ceramic," *Ceram. Eng. Sci. Proc.*, **9** [9-10] 1355-66 (1988).
- ¹⁵W. A. Sanders and G. Y. Baaklini, "Correlation of Processing and Sintering Variables with the Strength and Radiography of Silicon Nitride," *Ceram. Eng. Sci. Proc.*, **7** [7-8] 839-59 (1986).
- ¹⁶K. Liddell and D. P. Thompson, "X-ray Diffraction Data for Yttrium Silicates," *Trans. J. Br. Ceram. Soc.*, **85**, 17-22 (1986).
- ¹⁷J. Ito and H. Johnson, "Synthesis and Study of Yttrialite," *Am. Mineral.*, **53**, 1940-52 (1968).
- ¹⁸T. R. Dinger, R. S. Rai, and G. Thomas, "Crystallization Behavior of a Glass in the Y_2O_3 - SiO_2 - AlN System," *J. Am. Ceram. Soc.*, **71** [4] 236-44 (1988).
- ¹⁹M. H. Lewis, C. J. Reed, and N. D. Butler, "Pressureless-Sintered Ceramics Based on the Compound $\text{Si}_2\text{N}_2\text{O}$," *Mater. Sci. Eng.*, **71**, 87-94 (1985).
- ²⁰R. E. Loehman, "Oxynitride Glasses," *Mater. Res. Bull.*, **12** [5] 26-30 (1987).
- ²¹G. O. Jones; p. 32 in *Glass*. Methuen, London, 1956.
- ²²W. E. Lee and G. E. Hilmas, "Microstructural Changes in β -Silicon Nitride Grains upon Crystallizing the Grain-Boundary Glass," *J. Am. Ceram. Soc.*, **72** [10] 1931-37 (1989).
- ²³L. K. L. Falk and G. L. Dunlop, "Crystallization of the Glassy Phase in an Si_3N_4 Material by Post-sintering Heat Treatments," *J. Mater. Sci.*, **22**, 4369-76 (1987).
- ²⁴J. T. Smith, "Temperature and Compositional Stability of a $\text{Y}_6\text{Si}_6\text{O}_{21}$ Phase in Oxidized Si_3N_4 ," *J. Am. Ceram. Soc.*, **60** [9-10] 465-66 (1977).
- ²⁵P. F. James, "Volume Nucleation in Silicate Glasses," pp. 59-105 in *Glasses and Glass-Ceramics*. Edited by M. H. Lewis. Chapman and Hall, London, 1989. □



GLASS FORMATION AND CRYSTALLIZATION IN HIGH-TEMPERATURE GLASS-CERAMICS AND Si_3N_4

Charles H. DRUMMOND III

Department of Materials Science and Engineering, The Ohio State University, 2041 College Rd, Columbus, OH 43210, USA

The softening of glassy grain boundaries in ceramic matrix composites and silicon nitride at high temperatures reduces mechanical strength and the upper-use temperature. By crystallizing this glass to more refractory crystalline phases, a material which performs at higher temperatures may result. Three systems were examined: a cordierite composition with zirconia as a nucleating agent; celsian compositions; and yttrium silicate glasses both in bulk and intergranular in silicon nitride. For the cordierite compositions, a series of metastable phases was obtained. The crystallization of these compositions was summarized in terms of metastable ternary isothermal sections. Zircon formed at the expense of zirconia and spinel. In SiC composites the transformations were slower. In celsian, two polymorphs were crystallized. One phase, hexacelsian, which always crystallized, even when metastable, had an undesirable volume change. The other phase, celsian, was very difficult to crystallize. In yttrium silicate bulk glasses, similar in composition to the intergranular glass in silicon nitride, a number of polymorphs of $\text{Y}_2\text{Si}_2\text{O}_7$ were crystallized. The conditions under which these polymorphs formed are compared with crystallization in silicon nitride.

1. Introduction

The increased demand for high-temperature materials for aerospace applications has recently provided the impetus for the development of materials which can withstand higher operating temperatures. Potential uses include high-temperature structural materials for high-efficiency, high-performance engines in aerospace propulsion and power systems. The properties required in some applications also include oxidation resistance and the ability to withstand thermal cycling to these temperatures. Glass-ceramics and silicon nitride, which maintain their structural integrity above 1200°C , are two materials which may meet some or all of these requirements.

Glass-ceramics, like ceramics in general, exhibit brittle fracture behavior. Improved mechanical behavior can be obtained if a second phase, capable of withstanding high tensile loads, can be embedded in the glass-ceramic matrix [1,2]. The use of materials at higher temperatures requires not only a refractory matrix composition, but also a microstructure which does not soften due to the presence of the glassy phase usually in the grain boundary of such systems.

Two ways to eliminate the glassy phase from the final microstructure are by crystallization [3-5] and by alteration of the glass composition to increase the ease of crystallization. The result is an improvement in the high-temperature properties, in particular, the mechanical properties such as creep and strength. Various models including microcrack growth and cavitation [6-9] have been proposed to explain this improved mechanical behavior at high temperature.

The results of crystallization of two glass-ceramic matrix compositions and of the glassy phase in silicon nitride densified by solution-precipitation are presented. Two key factors addressed are the complete crystallization of the glassy phase and the formation of metastable crystalline phases. The crystallization of metastable phases may not be desirable depending on the properties of these phases.

In general, crystalline phases melt at significantly higher temperatures than the softening temperature of a glass of the same composition. Superior properties may be obtained if the more refractory crystalline phases are formed. For example, the four-point flexural strength of hot-pressed silicon nitride, in which the intergranular

glassy phase of a different composition was partially crystallized [3], showed a significant increase in strength and a higher temperature for the initiation of slow crack growth. Specifically, at 1275°C the strength was 50% greater for the crystallized grain boundary and the temperature of initiation of slow crack growth was increased from 1200 to 1300°C.

The final application of these materials will probably require the addition of a second phase in the form of fibers, whiskers or particulates to achieve desired properties. However, composite processing (except for one example) and an evaluation of the mechanical properties of these materials will not be presented in this paper.

Three examples in which the crystallization of an intergranular phase could significantly affect the properties of the matrix are discussed: (1) ceramic matrix composites based on metal alkoxide-derived cordierite compositions with and without SiC fibers; (2) melt-quenched barium-aluminosilicate compositions; and (3) silicon nitride with yttria added as a sintering aid.

1.1. Crystallization of intergranular glassy grain boundaries

The crystallization of an intergranular glassy grain boundary has been treated by Raj [10]. He concluded that it may not be possible to completely crystallize glass segregated at thin grain boundaries on the order of 10A or triple-junction nodes. These small volumes of glass may be thermodynamically stable due to strain energy arising from a volume change upon crystallization generating a hydrostatic stress which cannot be released by fluid flow. Experimental evidence for this conclusion is not possible since the optimum heat treatment that could result in complete crystallization may never be achieved.

Certainly, a number of microstructures have been reported in which complete crystallization of the grain boundaries has not occurred. What has been observed is that crystallization occurs first at triple-junction nodes with the very thin intergranular phase boundaries being the last portions of the microstructure to crystallize.

If complete crystallization of the glassy intergranular phase is not possible from a theoretical standpoint or if it cannot be achieved by heat treatment for a given system, the high-temperature properties are limited by this glassy phase, which softens in a temperature range determined by the glass composition. By altering the composition, the refractoriness may be increased. However, since most compositions are silicates with at least some additional oxides, the maximum temperature of use for such systems is not significantly higher than 1500°C and in fact could be much lower. The addition of nucleating agents can increase the amount and ease of crystallization, but still may not lead to complete crystallization.

1.2. Zirconia / magnesium-aluminosilicate glass-ceramics

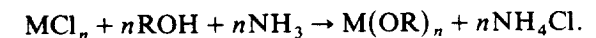
Cordierite, $2MgO \cdot 2Al_2O_3 \cdot 5SiO_2$, glass-ceramics have higher mechanical strength than other glass-ceramics [2] and are able to withstand higher temperatures than other compositions, such as lithium-aluminosilicates. The microstructure of magnesium-aluminosilicates (MAS) contains minerals that form platy and elongated grains. The interweaving structure produces enhanced strength and toughness [11] over the same mineral phases developed with lower aspect ratios. Cordierite is an example of a mineral capable of forming such a microstructure.

Zirconia was used as a nucleating agent to avoid problems with TiO_2 , which has been shown to be detrimental in composite systems. The compositions were modified by the addition of Nb_2O_5 . It has been shown [2] that Nb_2O_5 precipitates as NbC on or near the surface of the fibers. The NbC may then form a protective coating and a diffusion barrier between the fiber and the matrix.

Cordierite glass-ceramics were synthesized from metal alkoxides [12]. The general form of the reaction is



or



The advantage of the metal alkoxide synthesis method for this study was a lower processing temperature. By coating the fibers with a slurry of the matrix prior to hot-pressing, a composite was formed at temperatures lower than those required to process a glass frit. This avoided the degradation of the fibers [13]. In addition, precursor material in the form of fine-grained ($< 10\text{A}$) amorphous powders of higher purity than those from conventional processing [14] were obtained.

Since partially stabilized zirconia exhibits excellent fracture toughness and high strength, zirconia up to 30 wt% was added. In this study, however, the grain size of the zirconia was not optimized to obtain transformation toughening. Additional MgO was added to stabilize the high-temperature tetragonal form and prevent the transformation to the low-temperature, monoclinic form which results in microcracking due to the volume change.

1.3. Crystallization of barium-aluminosilicate glasses

Some of the most refractory ceramic matrix compositions are in the barium-aluminosilicate (BAS) system [15]. Celsian, $\text{BaO} \cdot \text{Al}_2\text{O}_3 \cdot 2\text{SiO}_2$, has a melting temperature of 1760°C . For use at high temperatures, complete crystallization of the glass is necessary. Any remaining silica rich glass will soften below the melting point of celsian, perhaps as low as 1200°C . Even with complete crystallization, compositions with cristobalite present would be expected to have poor room temperature mechanical properties because of the α - β cristobalite transition and the subsequent volume change during temperature cycling.

An additional problem in this system is that celsian has two polymorphs - celsian and hexacelsian. The high-temperature polymorph, hexacelsian, undergoes a rapid, reversible transformation at 300°C from the low-temperature hexagonal hexacelsian (β) to an orthorhombic form (α) with a volume change of 3% or greater. For BAS matrix compositions subjected to temperature cycling, this phase transformation in hexacelsian would be detrimental. Monoclinic celsian does not undergo such a volume change.

The details of the structures of hexacelsian and celsian and the kinetics of the transformation between these two polymorphs have been summarized [16]. Unfortunately, hexacelsian, the metastable phase below 1590°C , is always the first phase to crystallize at all temperatures. Further, the transformation to celsian is very slow. Without the addition of a mineralizer, such as Li_2O [17] or CaF_2 [18] or a nucleating agent, complete transformation of -200 mesh hexacelsian powder required 60 h at 1250°C [19]. Time-temperature requirements such as these would be unacceptable for composite processing.

1.4. Crystallization of yttrium silicates

Yttrium silicate compositions were studied in bulk, because such glasses were formed when yttria was used at NASA Lewis [20,21] as a sintering aid for the densification of silicon nitride. Silica present on the surface of the silicon nitride grains and formed by oxidation during processing, combined with the added silica and yttria. A silicate glass forms when these powders are sintered or hot-pressed at temperatures in excess of 1700°C . The solution-precipitation of the β - Si_3N_4 and subsequent densification is one common method of formation of dense silicon nitride. If the intergranular glassy silicate phase can be crystallized to form more refractory crystalline phases, an improvement of the high-temperature mechanical properties of silicon nitride is expected.

There are a number of crystalline phases in the Y_2O_3 - SiO_2 system which are important in this study. Four polymorphs of $\text{Y}_2\text{Si}_2\text{O}_7$, designated α , β , γ and δ exist. The diffraction data for these polymorphs have been summarized by Liddel and Thompson [22]. The transformation temperatures, densities and the crystal class of each polymorph are given in fig. 1.

The structure of all polymorphs consists of $\text{Si}_2\text{O}_7^{6-}$ units with the Y^{3+} connecting these units. The volume change associated with the polymorphic inversions of $\text{Y}_2\text{Si}_2\text{O}_7$ is as large as 6.7% and may be significant in the crystallization of intergranular glassy grain boundary phases in silicon nitride [23,24]. Densities of these glasses have not been reported. The several polymorphs of YSiO_5

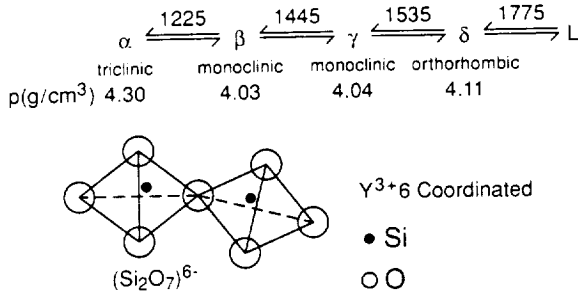


Fig. 1. Polymorphs of $Y_2Si_2O_7$.

have been discussed by Liddel and Thompson [22]. The existence of the $2Y_2O_3 \cdot 3SiO_2$ phase as shown in the published phase diagram [25] has not been confirmed and, in fact, the existence of such a phase has been questioned [22].

2. Experimental procedure

2.1. Zirconia / magnesium-aluminosilicate glass-ceramics

The compositions studied were nominally cordierite in the stable phase fields of spinel and mullite. Five different cordierite compositions were synthesized from metal alkoxides. These compositions are shown in fig. 2 and are denoted MAS (2% ZrO_2), ZMAS (25% ZrO_2), ZCOR (15 and 25% ZrO_2), ZSPIN (30% ZrO_2).

For these syntheses, commercial grade tetraethoxysilane (TEOS), $Si(OC_2H_5)_4$, was used but the other alkoxides were synthesized from high-purity metals or anhydrous metal chlorides. The

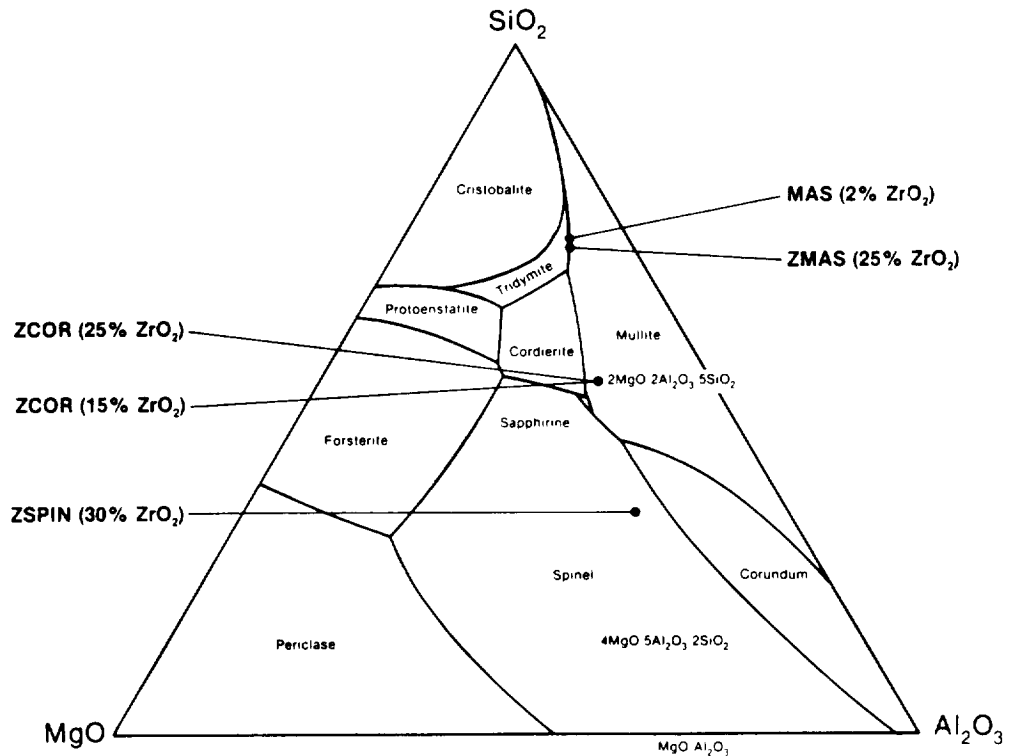
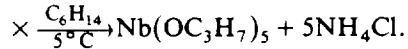
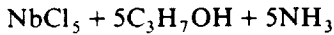
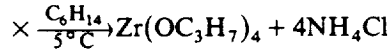
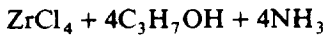
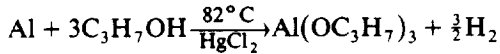
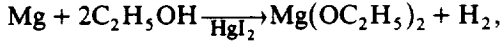
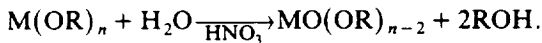


Fig. 2. ZrO_2 /cordierite composites synthesized.

following reactions gave metal alkoxides of Mg, Al, Zr and Nb:



Quantities of metal alkoxides solutions to give the desired nominal composition were combined in a dry box, refluxed to give a homogeneous solution, and dropwise acid-hydrolyzed using water and nitric acid. The general reaction is:



The mixture, after being stirred and allowed to stand overnight, was made basic with NH_4OH .

The resulting hydroxide slurry was concentrated to dryness by roto-evaporation and vacuum dried. The dried powder was ground in a B_4C mortar to comminute the larger agglomerates before calcining. The as-prepared fine powders, as well as the powder calcined at $500^\circ C$, were amorphous as determined by X-ray diffraction (XRD). The hydroxide slurry and calcined powder were used in the fabrication of the matrix and composites.

Matrix samples were prepared by vacuum hot-pressing the calcined material into 25-mm round discs under pressures up to 41.5 MPa (6000 psi) at temperatures up to $1500^\circ C$. The samples were X-rayed, chemically analyzed and the strength measured in four-point loading with the surface polished to $3 \mu m$.

Composites were fabricated by slurry-coating fibers which were then dried and calcined to $450^\circ C$ prior to vacuum hot-pressing. The final composite contained between 30 and 50 vol.% fibers. The continuous fibers were ceramic-grade SiC Nicalon[®] and approximately $13 \mu m$ in diame-

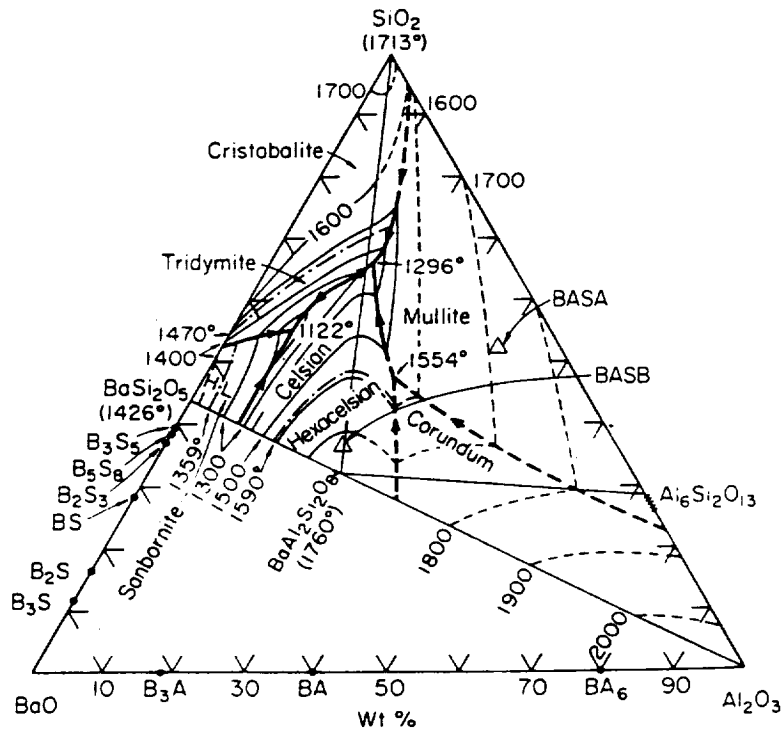


Fig. 3. Celsius compositions synthesized.

ter. The as-received fibers were coated with a sizing. The sizing was removed by a rapid heat treatment at $< 600^\circ\text{C}$ before slurry coating the matrix material onto the fibers. The heat treatment time was < 1 min in an air atmosphere. Tapes of the slurry-coated fibers were stacked and vacuum hot-pressed at temperatures and pressures similar to those for the matrix. The diffraction patterns of these composite samples were evaluated.

2.2. Crystallization of barium-aluminosilicate glasses

Composition BASB in the celsian phase field shown in fig. 3 and a stoichiometric composition BASC were melted in a small commercial electric furnace with Mo electrodes at $2000\text{--}2100^\circ\text{C}$. Reagent grade BaCO_3 , Al_2O_3 and SiO_2 were used. The liquid was roller quenched from flakes of homogeneous glass. The BSAB composition was melted with MoO_3 added as a nucleating agent. The as-batched composition was $\text{BaO}: 39.0$, $\text{Al}_2\text{O}_3: 25.0$, $\text{SiO}_2: 35.0$ and $\text{MoO}_3: 1.0$ wt%. The analyzed composition was $\text{BaO}: 36.7$, $\text{Al}_2\text{O}_3: 26.2$, $\text{SiO}_2: 34.0$ and $\text{MoO}_3: 1.0$ wt%. The crystal phases expected with complete crystallization were celsian, mullite and cristobalite for BASB and only celsian for BASC.

Heat treatments were performed in air using a programmable Linberg box furnace. The temperature was controlled to $\pm 5^\circ\text{C}$. Samples were nucleated for 1 h at the following temperatures: 850 , 900 and 950°C and grown for 4 h at 1080 , 1150 , 1220 and 290°C . Additional heat treatments were 1 h at 800°C followed by 48 h at 1000°C . Details of the chemical analysis, XRD, and electron microscopy are given elsewhere [16,26]. Standard techniques were employed.

2.3. Crystallization of yttrium silicates

Reagent grade silica and yttrium oxide were ball milled for 4 h with silicon nitride grinding media in dry alcohol and dried. The powder was dry milled for 2 h then pressed into pellets and placed in tungsten crucibles for melting in a high-pressure nitrogen furnace [21,27]. Powders were

melted at temperatures ranging from 1900 to 2100°C , depending on composition, and were held for 4 h under 50 atm nitrogen. Additional melts were also made in 1 atm nitrogen. No difference in properties or crystallization behavior was observed between these two melting conditions. It was necessary to break the crucibles to remove the melt. The X-ray diffraction patterns of the as-melted samples identified the crystalline phases formed on cooling. Additional heat treatments of as-melted material were carried out in air from $1100\text{--}1600^\circ\text{C}$ and followed by phase identification by XRD and transmission electron microscopy (TEM).

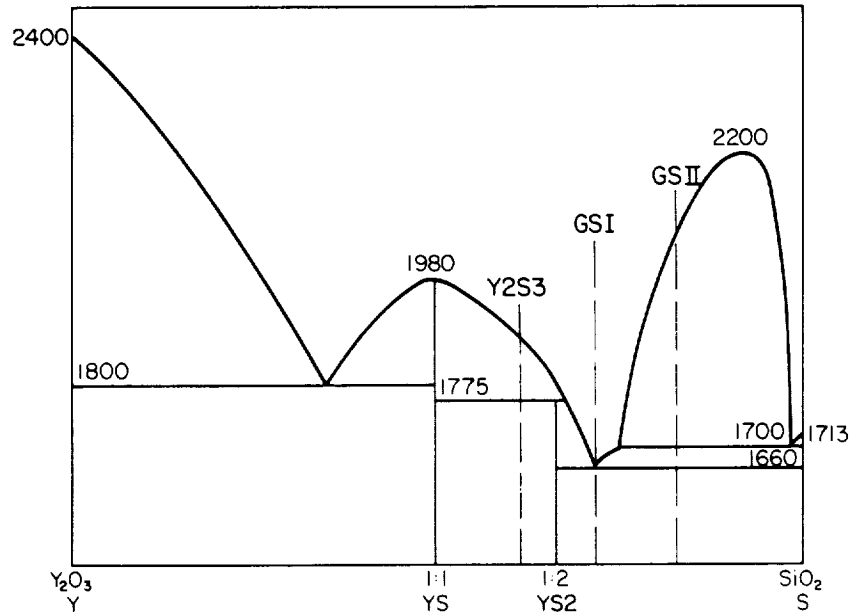
The primary glass composition studied was the eutectic composition between SiO_2 and $\text{Y}_2\text{Si}_2\text{O}_7$ which is similar to the intergranular, glassy grain boundary composition without nitrogen in the as-processed silicon nitride. This material has been designated as 6Y by NASA Lewis since it contains a 6.6 wt% yttria addition as the sintering aid. This composition lies in the oxidation-resistant $\text{Si}_3\text{N}_4\text{--Y}_2\text{Si}_2\text{O}_7\text{--Si}_2\text{N}_2\text{O}$ triangle.

The formulated and as-melted bulk glass compositions are given in table 1. The 1 indicates that the melt was made under one atm nitrogen and 50 denotes 50 atm nitrogen. Additional compositions melted ranged from 20–40 mol% Y_2O_3 . This compositional range is centered around the lower temperature eutectic region shown in fig. 4, which is a modified version of the $\text{Y}_2\text{O}_3\text{--SiO}_2$ phase diagram [25] without the inclusion of the Y_2S_3 phase.

A small amount of tungsten was found due to the fact that the melts were made in tungsten crucibles. Less than 0.2% nitrogen was found, indicating that little nitrogen was dissolved in the melt as a result of the 50 atm nitrogen overpressure. The exact chemical analysis was difficult to

Table 1
Bulk yttrium silicate glass compositions

	wt%		mol%	
	SiO_2	Y_2O_3	SiO_2	Y_2O_3
GS1, GS50	59.4	40.6	28.0	72.0
$\text{Y}_2\text{Si}_2\text{O}_7$	65.3	34.7	33.3	66.7
Y_2S_3	71.5	28.5	40.0	60.0

Fig. 4. Revised phase diagram Y_2O_3 - SiO_2 .

determine because the energy dispersive spectroscopy (EDS) system on the TEM had a Be window, which precluded soft X-rays such as those that arise from O or N.

3. Results

3.1. Zirconia / magnesium aluminosilicate glass-ceramics

Complete crystallization of the glassy phase was not attempted or confirmed. However, because of the ease of crystallization of these compositions and the presence of zirconia as a nucleating agent, nearly complete crystallization was probably achieved.

The crystalline phases developed were metastable but partially transformed to the equilibrium phases, as shown in fig. 5. A composition midway between cordierite and spinel with 30% zirconia, ZSPIN, crystallized at 600°C as spinel ($\text{Mg}_2\text{Al}_2\text{O}_4$), sapphirine (a spinel-type structure with the formula $\text{Mg}_7\text{Al}_{18}\text{Si}_3\text{O}_{40}$) and tetragonal zirconia. Crystallization at 1300°C or greater resulted in zircon and cordierite formation, with the amount

of zircon increasing and zirconia decreasing with time.

The formation of zircon and cordierite was at the expense of sapphirine. The crystallization of zircon with a 20% density increase over sapphirine resulted in the formation of significant flaws and lower four-point bend strengths. The zircon for-

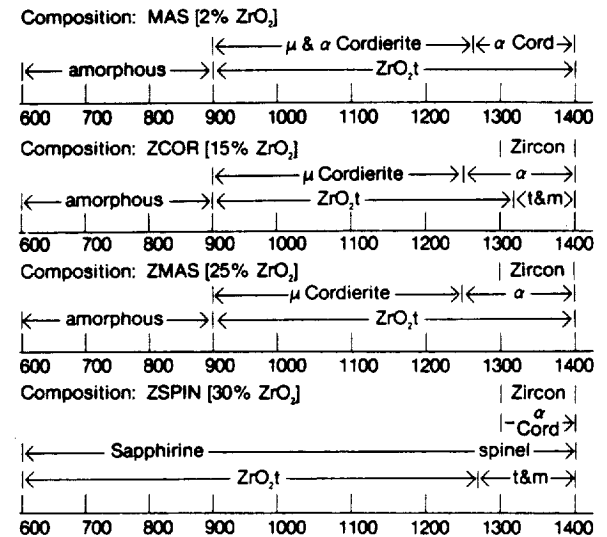


Fig. 5. Crystallization sequence for cordierite compositions.

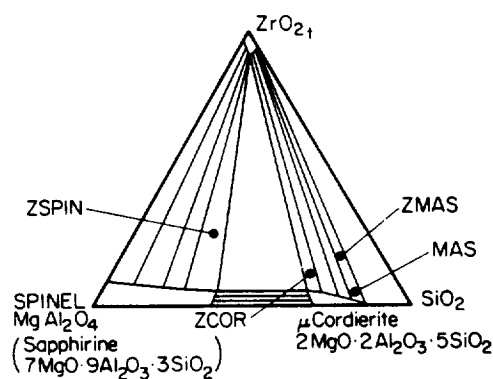
mation is consistent with phase formation in a glass-ceramic with 10 wt% ZrO_2 and magnesium-aluminosilicate composition between ZSPIN and ZCOR [28].

The ZCOR and ZMAS compositions contained primarily cordierite with tetragonal zirconia. At 1300°C and above, zircon began to form as earlier work showed [28]. The zircon formation was not sensitive to modest variations in the zirconia or silica content. In addition to zircon formation, cordierite transformed from the μ to the α phase and sapphirine disappeared. Some tetragonal

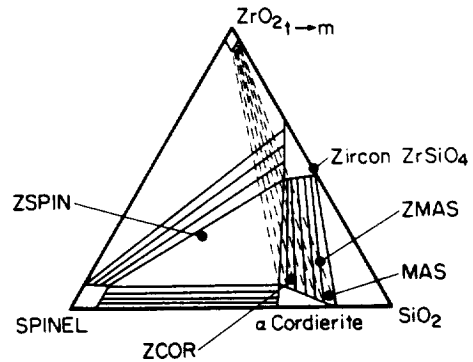
zirconia remained, since the reaction to form zircon was sluggish.

Not only was the amount of tetragonal zirconia decreased with the zircon formation, but also a portion of the tetragonal phase destabilized and monoclinic zirconia formed. The monoclinic zirconia formation at 1300°C corresponded to the disappearance of sapphirine and the formation of spinel as the ternary component.

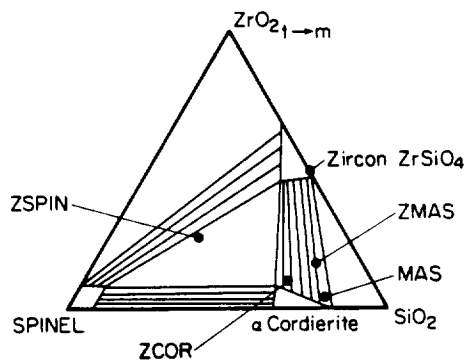
Spinel contains a higher magnesia content than sapphirine. A portion of the magnesia stabilizing the tetragonal zirconia probably reacted with sap-



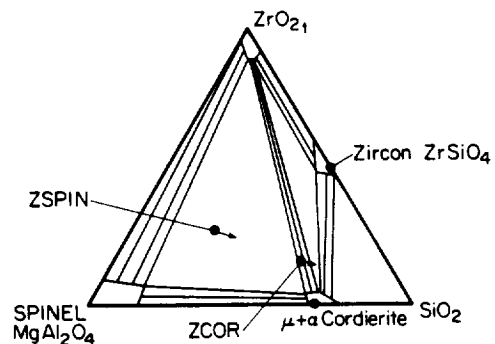
Matrix at 1250°C,
15 min.



Matrix at 1300°C,
15 min.



Matrix at 1300°C,
Extended time



Composite at
1300°C, 15 min.

Fig. 6. Crystalline phases for cordierite compositions formed at various temperatures.

phirine, forming spinel and freeing silica for zircon formation.

With the addition of Nicalon[®] SiC fibers, the phase development was more sluggish with the transformation of α to μ cordierite and zircon formation retarded. This result suggests that phase transformations in the matrix may be altered, or at least slowed, as a result of the addition of a second, nonreacting phase. The major phases developed in the composites are shown in fig. 6. The matrix composition in the composites appeared to contain a higher silica content than the matrix material alone. Since the fibers used contained a

significant SiO_2 fraction, the higher content silica matrix was not surprising.

3.2. Crystallization of barium-aluminosilicate glasses

In this study complete transformation of hexacelsian to celsian without the addition of a flux or a nucleating agent was never achieved. As-quenched BASB and samples nucleated below $950^\circ C$ were amorphous, as shown by XRD in fig. 7. Various heat treatments and the phase identification by XRD are also shown in fig. 7. Results of

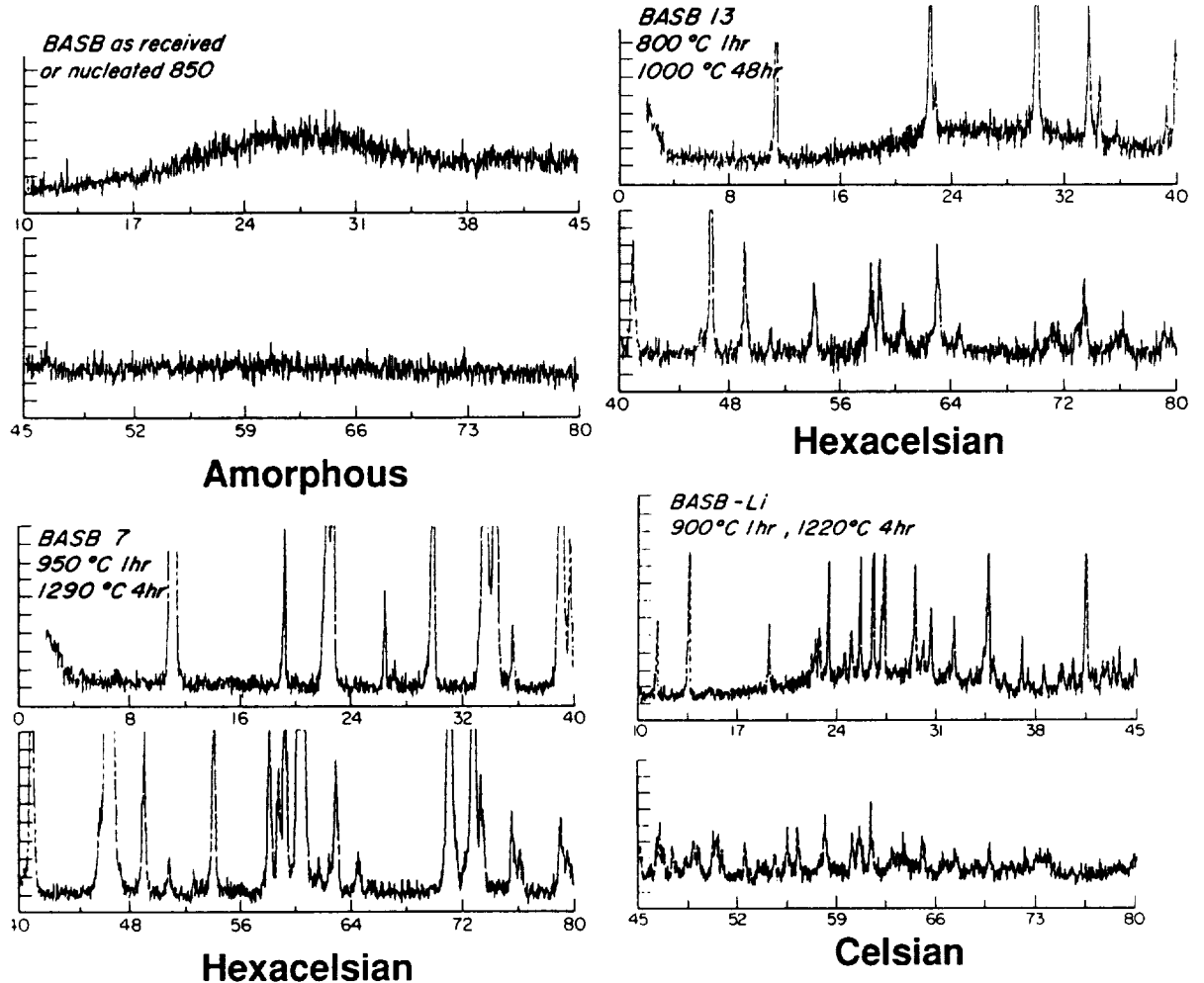


Fig. 7. X-ray diffraction data for celsian compositions for heat treatments indicated with phase identification.

these heat treatments and others not shown indicate that regardless of the crystallization temperature hexacelsian always forms when MoO_3 is used as a nucleating agent. Further studies [26] have shown that stoichiometric celsian, BASC, does not crystallize as celsian with various heat treatments.

The microstructure of a heat-treated glass

(BASB 13, fig. 7) is shown in fig. 8. Both hexacelsian grains, all with the same orientation, and mullite crystallized in the apparent grain boundaries. The single orientation of the grains may be the result of recrystallization or a slow growth rate. The phases were identified by EDS spectra.

With the addition of 5 wt% Li_2O to the BASB

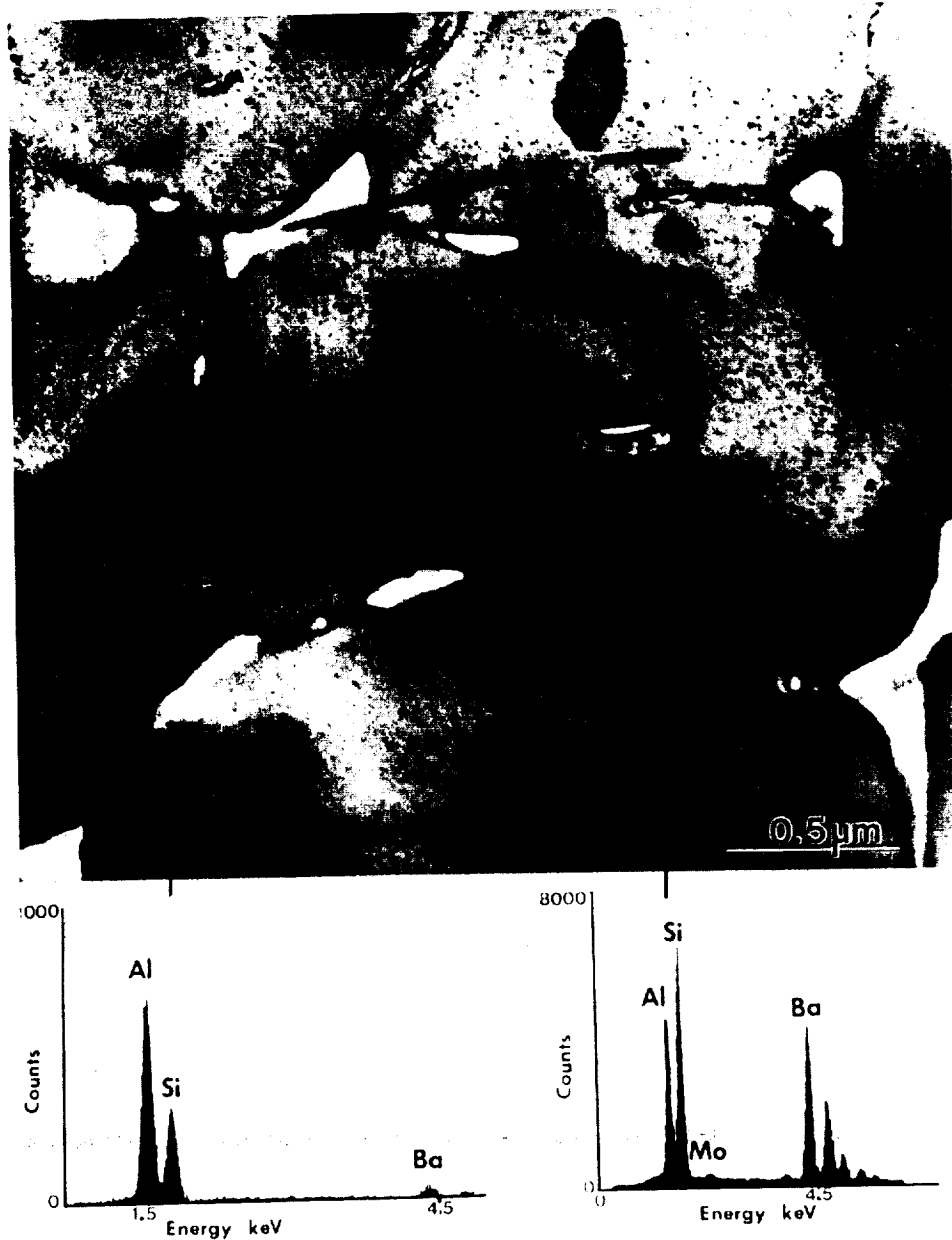


Fig. 8. Micrograph of BASB 13 showing hexacelsian and mullite grains.



Fig. 9. Micrograph of celsian (C) with 5 wt% Li_2O showing Mo rich glass (G) and mullite (M).

composition, the as-quenched sample was amorphous. When nucleated at $900^\circ C$ and grown at $1220^\circ C$ for 4 h, celsian crystallized as shown in fig. 7. The micrograph in fig. 9 shows the complex microstructure formed with the addition of the mineralizer, Li_2O . Bands of a Mo rich glass alternated with bands of mullite and bands of celsian. Although MoO_3 was added as a nucleating agent, it was not effective for the crystallization of celsian.

3.3. Crystallization of yttrium silicates

The bulk glass compositions, GS1 or GS50, similar to the intergranular glassy composition,

have been shown [29] to have a minimal amount of nitrogen dissolved in the glass. In other studies [20,23] on the 6Y composition, no crystallization of yttrium containing nitrides was observed. Thus, the results of crystallization studies on bulk glass with minimal nitrogen content may be used to optimize crystallization of the intergranular glassy phase in silicon nitride.

In all cases, XRD results of the as-quenched melt indicated partial crystallization. Most of the melts contained $\delta-Y_2Si_2O_7$. The quench rate obtained in these melts was not a rapid one: it was estimated to be $270^\circ C/min$. The furnace did not permit a more rapid rate. In the bulk glass material the γ or δ polymorphs were observed. The dif-

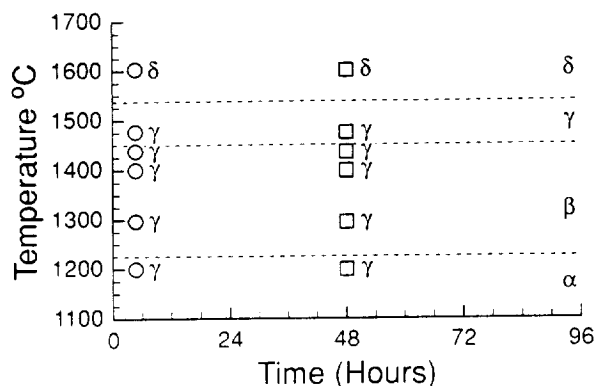
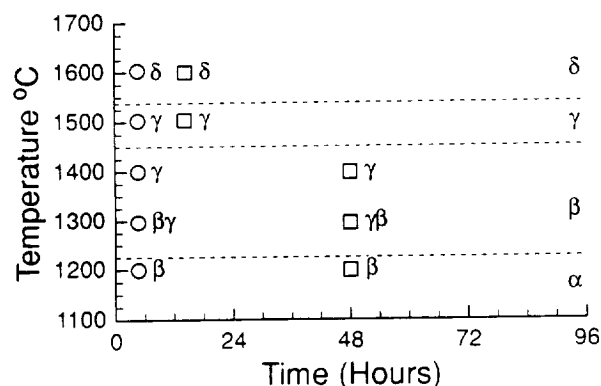


Fig. 10. XRD results for bulk sample GS1.

Fig. 12. XRD results of bulk sample $\text{Y}_2\text{Si}_2\text{O}_7$.

ference was probably due to different quench rates in the two furnaces used.

In the as-processed silicon nitride, the crystalline phase formed was β or δ , depending on the heat treatment [24]. The difference between bulk glass samples and the glassy phase in silicon nitride may have been due to the presence of nucleating agents, perhaps silicon nitride itself, since in bulk glass samples with the addition of zirconia as a nucleating agent the β polymorph is formed.

The Y_2S_3 composition did not crystallize when quenched in the bulk. All other compositions in this study were partially crystallized. Differential thermal analysis results showed an exothermic peak at 1400°C , corresponding to the crystallization of $\text{Y}_2\text{Si}_2\text{O}_7$. The previously observed [30]

crystalline phase of the Y_2S_3 composition was not observed.

The results of these crystallization studies are shown in figs. 10–13. The X_1 denotes a polymorph of YSiO_5 , and the u an unidentified phase (fig. 13). The expected transformation temperatures are shown by the horizontal dashed lines with the expected phases shown on the right in each figure. When more than one phase is shown at a particular time and temperature, both phases were detected by XRD. The α phase was never observed. In the GS1 sample the melt was γ as quenched and in the GS50 melt it was δ . Over time at various temperatures polymorphic changes occurred, but not always the expected one. For example, the γ phase formed in some cases instead of the reported stable phase β .

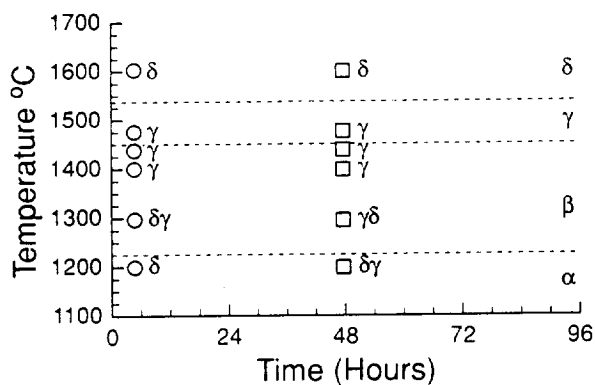
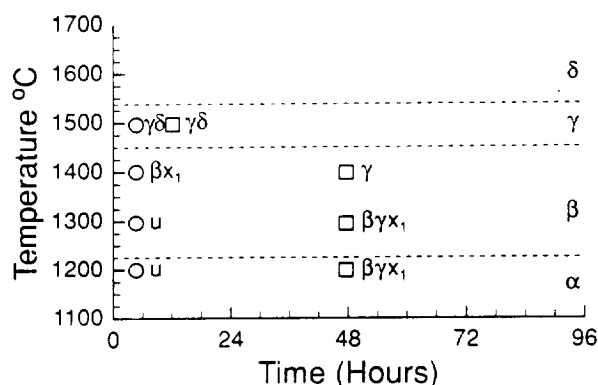


Fig. 11. XRD results of bulk sample GS50.

Fig. 13. XRD results of bulk sample Y_2S_3 .

4. Discussion

4.1. Zirconia / magnesium-aluminosilicate glass-ceramics

Cordierite compositions with excess silica and 10 or 15 wt% zirconia crystallized as primarily cordierite and tetragonal zirconia with conversion to zircon at higher temperatures. These results can be explained in terms of a simplified non-equilibrium isothermal ternary section (fig. 6). They suggest that the zircon formation is not sensitive to variations in zirconia and silica contents.

With MgAl_2O_4 being considered as a single component and with the aid of the ZrO_2 - SiO_2 phase diagram [31], these compositions and their resulting phases can be illustrated semiquantitatively. Figure 6 illustrates the spinel-zirconia-silica non-equilibrium ternary isothermal section at 1250 and 1300°C. Sapphire cannot be properly depicted as a component on the 1250°C metastable ternary. However, since at 1250°C a combination of spinel and sapphire was present and structurally and compositionally they are very similar, sapphire is included on the isothermal section with spinel. This modified ternary provides a useful tool in visualizing the phase development of these materials.

The composition ZSPIN was unable to form cordierite and spinel with tetragonal zirconia as shown in the metastable ternary section in fig. 6. This was without the formation of zircon. A slightly higher silica-content composition than ZSPIN may be out of the two-phase region between spinel and zirconia observed at 1250°C. Examination of the diagram implies that a metastable coexistence between spinel, cordierite, and zirconia could be achieved with a composition of slightly higher silica content than ZSPIN.

The matrix materials without SiC fiber densified most rapidly at 1200 through 1250°C. The final density depended upon the applied pressure and the rate of temperature increase or hold time in this temperature range. Compositions ZSPIN and ZCOR were the most extensively studied for densification characteristics. ZSPIN densified up to 95% of theoretical when hot-pressed at 10°C/min heating rate and 15 min at 1250°C under 7.6

MPa (1100 psi) applied pressure. Crystalline phase development appeared to be unaffected by the applied pressure when varied from 0 to 7.6 MPa (1100 psi).

Composition ZCOR was extremely difficult to densify. At 11.7 MPa (1700 psi) applied pressure, a 10°C/min heating rate and 15 min at top temperatures of 1250°C and 1300°C, the density appeared to be ~90% of theoretical. Although there may have been some glass remaining in the matrix which would have had a lower density than the crystalline phases, most of the deficiency in density was probably due to porosity. The addition of a flux to the matrix composition would probably aid in densification but would be detrimental to the high-temperature properties.

The phase development in the composites appeared to be sluggish compared to the matrix material without the fibers. Comparing the composite metastable ternary at 1300°C with that of the matrix only material (fig. 6), it is apparent that the μ to α transformation is retarded and the zircon formation region is reduced in the composite materials.

4.2. Crystallization of barium-aluminosilicate glasses

Crystallization of celsian glass-ceramic matrices for composite applications requires not only the complete crystallization of the amorphous phase to avoid softening at high temperature, but also the crystallization of the celsian polymorph. The hexacelsian polymorph is always the first phase to form, even in a temperature range where it is the metastable phase. However, the large volume change at 300°C makes it unsuitable for composite applications.

In this system, unfortunately, the crystallization of cristobalite or hexacelsian will reduce both room and high-temperature mechanical properties. Complete crystallization of the BASC with a nucleating agent resulted in only celsian phase and no cristobalite.

4.3. Crystallization of yttrium silicates

The crystallization of metastable phases which exist above and below their thermodynamically

stable temperature range was a common feature in this system. The polymorphic transformations were also sluggish.

A satisfactory explanation has not been given. It may be due to formation of nuclei on cooling from the melt or during reheating followed by growth. Crystallization from the bulk GS glasses never resulted in the α phase. Either the γ or the δ phase formed in the melt of the GS1 or GS50 compositions with no β formation. This formation is in contrast to the results [24] in the 6Y silicon nitride in which the β phase readily formed in the triple point junctions. In addition, an increase in dislocation density has been found in the crystallized 6Y silicon nitride materials [24].

The reason for the appearance of dislocations is probably associated with a volume difference between the yttrium silicate glass and the first $\text{Y}_2\text{Si}_2\text{O}_7$ crystals formed or with volume differences between some of the $\text{Y}_2\text{Si}_2\text{O}_7$ polymorphs. Alternatively, differences in thermal expansion between the various phases may lead to stress in the system. The dislocation density however was reduced by annealing at 1500°C , thus minimizing the effect on mechanical properties.

Moreover, $\text{Y}_2\text{Si}_2\text{O}_7$ crystallizes at a single orientation over large distances in the microstructure [23,24]. This behavior may be due to the degree of ease of nucleating the second phase: the easier the nucleation, the less the chance of crystals growing around the Si_3N_4 grains. Since crystallization of $\text{Y}_2\text{Si}_2\text{O}_7$ was observed around several Si_3N_4 grains, it seems probable that complete crystallization of all the glass in that area had occurred even though the very thin intergranular regions were not illuminated in dark-field images.

5. Conclusions

For both the glass in a glass-ceramic matrix and as a grain boundary phase in silicon nitride, complete crystallization is required to prevent softening at higher temperatures. With complete crystallization, improvement in mechanical properties such as creep and strength is possible for composite or monolithic materials.

Crystallization studies on three different systems showed that the addition of nucleating agents and heat treatment can result in crystallization of the intergranular glassy phase. Studies on bulk glasses are useful for application to composite materials, but the transformations may be altered by the addition of other components, resulting in different crystalline phases or sluggish transformations. Volume changes upon crystallization or polymorphic changes of crystal phases formed must be considered in optimizing the properties at high temperatures or during thermal cycling.

Portions of this work were supported by NASA grant NAG 3-824 and The Air Force Office of Scientific Research, USAF under contract F49620-85-C-0013, and NASA/ASEE Summer Fellow Program. The collaboration with N.P. Bansal and W.E. Lee and former graduate students V.J. Powers, A.G. Parker, S.K. Kumar and G.E. Hilmas is gratefully acknowledged.

References

- [1] I.W. Donald and P.W. McMillan, *J. Mater. Sci.* 11 (1976) 949.
- [2] J.J. Brennan and K.M. Prewo, *J. Mater. Sci.* 17 (1982) 2371.
- [3] S.H. Knickerbocker, A. Zangvil and S.D. Brown, *J. Am. Ceram. Soc.* 68 (1985) C-99.
- [4] T.R. Dinger, R.S. Rai and G. Thomas, *J. Am. Ceram. Soc.* 7 (1988) 236.
- [5] A. Tsuge, K. Nishida and M. Komatsu, *J. Am. Cer. Soc.* 58 (1975) 323.
- [6] R.K. Govila, *J. Mater. Sci.* 20 (1985) 4345; 23 (1988) 1141.
- [7] F.F. Lange, in: *Progress in Nitrogen Ceramics*, ed. F.L. Riley (Nijhoff, Boston, MA, 1983) p. 467.
- [8] A.G. Evans and A. Rana, *Acta Metall.* 28 (1980) 129.
- [9] J.E. Marion, A.G. Evans, M.D. Drory and D.R. Clarke, *Acta Metall.* 31 (1983) 1445.
- [10] R. Raj, and F.F. Lange, *Acta Metall.* 201 (1981) 1993; R. Raj, *J. Am. Ceram. Soc.* 65 (1981) 245.
- [11] K.T. Faber and A.G. Evans, *Acta Metall.* 31 (1983) 565.
- [12] V.J. Powers and C.H. Drummond III, *Ceram. Eng. Sci. Proc.* 7 (1986) 969.
- [13] T. Mah, N.L. Hecht, D.E. McCullum, J.R. Hoenigman, H.M. Kim, A.P. Katz and K.A. Lipsitt, *J. Mater. Sci.* 19 (1984) 1191.
- [14] K.S. Mazdiyasi, *Ceram. Int.* 8 (1982) 42.
- [15] D. Bahat, *J. Mater. Sci.* 4 (1969) 855.
- [16] C.H. Drummond III, W.E. Lee, N.P. Bansal and M.J. Hyatt, *Ceram. Eng. Sci. Proc.* 10 (1989) 1485.

- [17] M.C.G. Villar, C.G. Monzonis and J.A. Navorro, *Trans. J. Br. Ceram. Soc.* 82 (1983) 67.
- [18] D.P. Lepkova, I.T. Ivanov and L.P. Pavlova, *Dokl. Bolg. Akad. Nauk.* 29 (1976) 1165.
- [19] D. Bahat, *J. Mater. Sci.* 5 (1970) 805.
- [20] W.A. Sanders and D.M. Mieskowski, *J. Am. Ceram. Soc.* 24 (1985) 304.
- [21] W.A. Sanders and G.Y. Baaklini, *Adv. Ceram. Mater.* 3 (1988) 88.
- [22] K. Liddell and D.P. Thompson, *J. Br. Ceram. Trans.* 85 (1986) 17.
- [23] W.E. Lee, C.H. Drummond III, G.E. Hilmas, J.D. Kiser and W.D. Sanders, *Ceram. Eng. Sci. Proc.* 9 (1988) 1355.
- [24] W.E. Lee and G.E. Hilmas, *J. Am. Ceram. Soc.* 72 (1989) 1931.
- [25] N.A. Topopov, in: *Phase Diagrams for Ceramists*, ed. E.M. Levin, C.R. Robbins and H.F. McCurdie, (Am. Ceram. Soc., Columbus, OH, 1969) fig. 2388, p. 107.
- [26] C.H. Drummond III and N.P. Bansal, *Ceram. Eng. Sci. Proc.* 11 (1990) to be published.
- [27] C.H. Drummond III, W.E. Lee, W.A. Sanders and J.D. Kiser, *Ceram. Eng. Sci. Proc.* 9 (1988) 1343.
- [28] M.A. Conrad, *J. Mater. Sci.* 7 (1972) 527.
- [29] W.E. Lee, private communication.
- [30] N.A. Toropov and I.A. Bondar, *Izv. Akad. Nauk. SSSR, Otd. Khim. Nauk.* 4 (1961) 547.
- [31] R.F. Geller and S.M. Lang, in: *Phase Diagrams for Ceramists*, ed. E.M. Levin, C.R. Robbins, H.F. McCurdie and M.K. Reser (Am. Ceram. Soc., Columbus, OH, 1964) fig. 361, p. 141.

TO BE SUBMITTED

24-76
N91-819656

P. 16

INDIRECT MEASUREMENT OF THE VISCOSITY OF THE INTERGRANULAR
GLASS PHASE IN YTTRIA-SINTERED SILICON NITRIDE

Mark B. Dittmar and Charles H. Drummond, III, Dept. of Materials Science and Engineering, The Ohio State University, 143 Fontana Labs, 116 W.19th Ave, Columbus, OH 43210.

ABSTRACT

Dense, sintered Si_3N_4 possesses a residual intergranular glass phase which softens at high temperatures, resulting in degradation of the ceramic's mechanical properties at these temperatures. An important parameter in the determination of the high temperature mechanical properties of sintered Si_3N_4 is the temperature-viscosity relationship of the intergranular glass. In this paper, a method for indirectly measuring the intergranular glass viscosity at a given temperature using physical modelling of a two-phase glass crystal microstructure and beam-bending viscometry measurements of Si_3N_4 is described. Intergranular glass viscosities obtained by this method are presented for a yttria-sintered Si_3N_4 .

INTRODUCTION

Si_3N_4 is a material that has received considerable interest in recent years for use in structural components for high temperature applications, in particular the all-ceramic gas turbine engine. Because of its low self-diffusivity up to its decomposition temperature, Si_3N_4 requires the use of a sintering aid, commonly a metal oxide, for fabrication of fully dense materials. As a result of this processing, a residual glass phase is present at the grain boundaries [1, 2]. At high temperatures, the degradation of mechanical properties, such as flexural strength and creep resistance, has been attributed to the softening of this intergranular glass phase [3]. In a number of investigations, it has been presumed that the temperature-viscosity relationship of the intergranular glass has a direct influence on the mechanical properties above the glass softening point [4, 5]. It has been suggested that improvements in the high temperature mechanical properties can be obtained by either increasing the viscosity of the intergranular glass through suitable compositional changes [6] or by reducing the volume fraction of glass phase present through crystallization heat treatments [7]. Although it has been demonstrated that reduced glass volume fractions do enhance the high temperature mechanical properties [8], it has also been shown that the existence of a very thin amorphous phase may always be present due to thermodynamic constraints [9]. Hence, the physical properties of the glassy phase, in particular the viscosity, may be a limiting factor in the optimization of the high

temperature mechanical properties. Knowledge of the intergranular glass viscosity at a given temperature, along with the appropriate mathematical models, can be useful in the prediction of creep rates, flexural strengths, and times to failure. Therefore, the purpose of the present study is to obtain the viscosity of the intergranular glass phase as a function of temperature in yttria-sintered Si_3N_4 . To accomplish this, physical modelling of a two phase glass/crystal microstructure, coupled with beam bending viscometry measurements of the apparent viscosities of the sintered silicon nitride at various temperatures, were performed.

EXPERIMENTAL PROCEDURES

Direct measurements of the true viscosity of the intergranular glass in dense yttria-sintered Si_3N_4 are not possible due to the polyphase microstructure of dense Si_3N_4 . Any viscosity measurements performed on bulk Si_3N_4 samples will produce an apparent viscosity value, resulting from the viscosity of the parent yttrium-silicate glass and the effect on that viscosity due to the presence of $\beta\text{-Si}_3\text{N}_4$ crystals within the glass. In addition, it is not possible to perform direct viscosity measurements on bulk glass with compositions similar to the intergranular glass in yttria-sintered Si_3N_4 . These glasses will devitrify upon cooling from the melt [10]. Hence, in order to obtain values for the true viscosity of the intergranular glass in yttria-sintered Si_3N_4 , an indirect measurement approach is required. Basically, this approach involves the physical modelling of a two-phase microstructure by fabricating glass/crystal composites containing a parent glass of known temperature-viscosity relationship and crystalline material of known specific volume. The volume fraction of crystalline material is varied in these composites and the effect upon the viscosity of the parent glass is noted as a function of volume fraction crystalline content. A curve is then constructed which relates the volume fraction of crystalline content in the composites to the relative viscosity, η_{rel} , defined as the ratio of the measured composite viscosity to the true glass viscosity at a given temperature. Using values of the relative viscosity obtained from this curve, combined with measurements of the apparent viscosity in the bulk Si_3N_4 , allow the calculation of the true intergranular glass viscosity.

In this study, four different bulk Si_3N_4 compositions were processed. The compositions and sintering conditions are listed in Table 1. Greater than 98% theoretical density was achieved for these compositions, with the exception of the SN60/40, which attained 95% density. The 6Y and SN60/40 were processed so that the intergranular glass phase was silica rich, with a $\text{SiO}_2 : \text{Y}_2\text{O}_3$ molar ratio of $\approx 3.5 : 1$ in the starting powders. The SN84/16 and SN76/24 were processed with a $\text{SiO}_2 : \text{Y}_2\text{O}_3$ ratio of $2 : 1$ in the starting powders. The powder processing and sintering of the green bodies was performed at NASA Lewis Research Center, Cleveland, OH. Details of the processing have been published previously [11]. X-ray diffraction (XRD) of the as-sintered bars was performed both before and after viscosity measurements to check for devitrification of the glass phase. SEM of etched microstructures was performed on each composition and determinations of the glass volume fractions were made using a Zeiss videoplan image analyzer.

The physical modelling was accomplished by fabricating a series of fully dense, hot-pressed composites containing -325 mesh Al_2O_3 and Corning 7761 glass. The volume fractions of Al_2O_3 in the composites were 30, 40, and 50 vol%. The pressing



conditions were at 870 °C and 1000 - 2000 psi for 15 minutes. XRD was performed on each of the composites before and after viscosity measurements to check for devitrification of the glass phase.

Compositions and Sintering Conditions for Si ₃ N ₄				
Composition	Mill charge (wt%)			Sintering Conditions
	Si ₃ N ₄	Y ₂ O ₃	SiO ₂	
6Y	86.52	6.77	6.71	2140 C, 4 hr, 5 MPa N ₂
SN84/16	86.47	8.83	4.70	2140 C, 2 hr, 5 MPa N ₂
SN76/24	79.40	13.45	7.15	2140 C, 4 hr, 5 MPa N ₂
SN60/40	59.37	21.25	19.38	1900 C, 8 hr, 2.5 MPa N ₂

Table 1. Processing and sintering conditions for Si₃N₄.

Viscosity measurements were made using the beam-bending technique as described by Hagy [12]. In this technique, the rate of deflection of a centrally loaded beam in a three-point loading configuration is measured and related to the viscosity by the equation

$$\eta = \frac{gL^3}{2.4I_c v} \left[M + \frac{\rho AL}{1.6} \right], \quad (1)$$

where η = viscosity (poise), $g = 980 \text{ cm/sec}^2$, L = span length, cm, I_c = cross sectional moment of inertia, cm⁴, v = midpoint deflection rate, cm/min, M = applied load, grams, ρ = specimen density, g/cc, and A = cross-sectional area of test beam, cm². In this study, two separate viscometers were employed: for the bulk Si₃N₄ materials, a top loading configuration was used, wherein loads were applied via a SiC

loading rod and deformation of the specimen was detected by a LVDT coupled to the rod. This construction was necessary because of the higher loads required to obtain measurable deformation rates for these materials. The deflection of the specimen was then plotted versus time on a chart recorder. After making necessary corrections to the data to account for transient differential thermal expansion within the apparatus, equation (1) was applied to the deflection data. The other viscometer, which was used with the composites, utilized a .100 inch diameter sapphire rod to load the specimens from the bottom. In either case, the underlying principle of operation was identical. The error in the measured viscosity for either viscometer was $\pm 10\%$, and the error in temperature measurement was ± 1.5 °C. The accuracy of the viscometers was ascertained by checking them against viscosity data for fused silica [13] and National Institute of Standards standard reference material SRM 711 viscosity standard.

RESULTS

SEM and volume fraction determinations

The typical etched microstructures of the sintered Si_3N_4 is shown in figure 1. The microstructures of each composition are basically the same, consisting of elongated, hexagonal, interlocking $\beta\text{-Si}_3\text{N}_4$ crystals. The microstructures were very uniform over the entirety of each sample. The dark regions are the areas where the grain boundary glass has been etched out by the HF acid treatment.

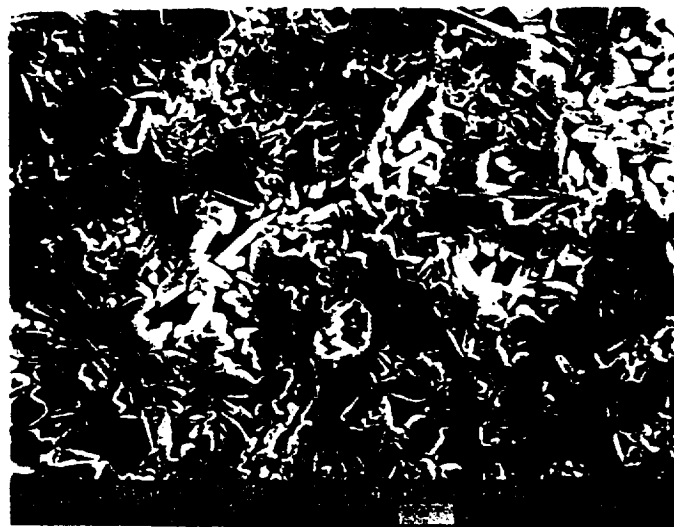


Figure 1. Microstructure of SN84/16 sintered silicon nitride.

To obtain the volume fraction of glass phase present in a given material, the area fraction occupied by the $\beta\text{-Si}_3\text{N}_4$ grains in an etched microstructure was determined and this value subtracted from unity to obtain the area fraction occupied by the glass. The principle of equivalence of area and volume fractions was then employed to obtain the volume fraction of glass phase present. The average measured values, calculated from three micrographs from each composition, were 16.3 ± 3.0 ,

22.3 ± 2.1, 17.3 ± 3.2, and 23.0 ± 1.7 vol% for the 6Y, SN84/16, SN76/24, and SN60/40 compositions respectively.

Composite bar modeling

The curve relating volume fraction of Al₂O₃ in the composites to the average relative viscosity $\eta_{rel,avg}$ was prepared from the composite bar viscosity data. A second degree polynomial curve fit was applied to the data, resulting in the following relation for $\eta_{rel,avg}$:

$$\log_{10} \eta_{rel,avg} = -1.6381 \cdot 10^{-2} + 3.9309V + 5.66768V^2, \quad (2)$$

where V = the volume fraction of Al₂O₃. This curve is shown in figure 2.

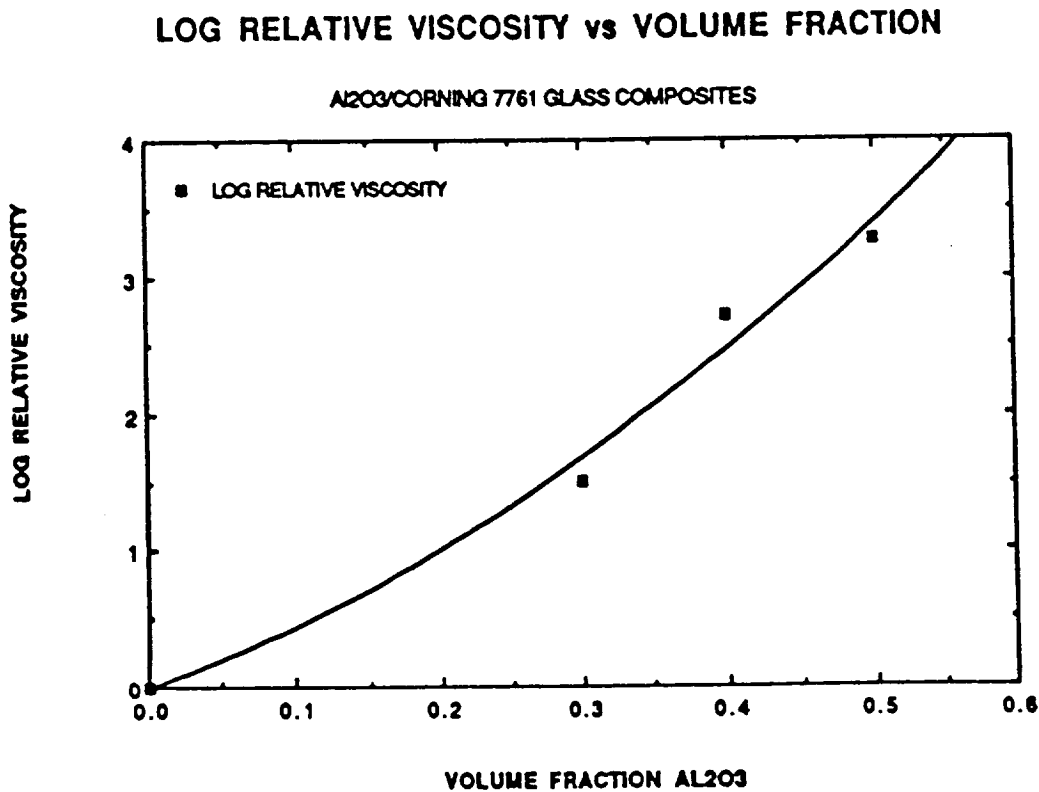


Figure 2. Volume fraction Al₂O₃ vs log₁₀ $\eta_{rel,avg}$

Viscometry of bulk Si_3N_4

All of the corrected deflection vs time curves exhibited two characteristic stages of deformation which are manifested in the slopes of the curves. The first stage, occurring upon the instant of loading, is a region of initial rapid deflection rate which quickly diminishes with time. The second stage is a region of constant deflection rate. A typical curve is shown in figure 3. These curves are structurally similar to creep curves (strain vs time) for similar Si_3N_4 materials [14], as well as the creep curves for other ceramics containing an intergranular glass phase. In this study, the deflection rates corresponding to the constant deflection rate region of the deflection curves were calculated by performing a least-squares fit to the data over this portion. The apparent viscosities of the bulk Si_3N_4 compositions, calculated by applying equation (1) to the deflection rate data, are listed in table 2. In this table, N/A indicates that a viscosity could not be calculated from the data. Also listed in this table are the calculated intergranular viscosities for each listed apparent viscosity value. These values are calculated on the basis of relative viscosity factors obtained from equation (2).

SN76 #6, 1355 C, 281 MPa

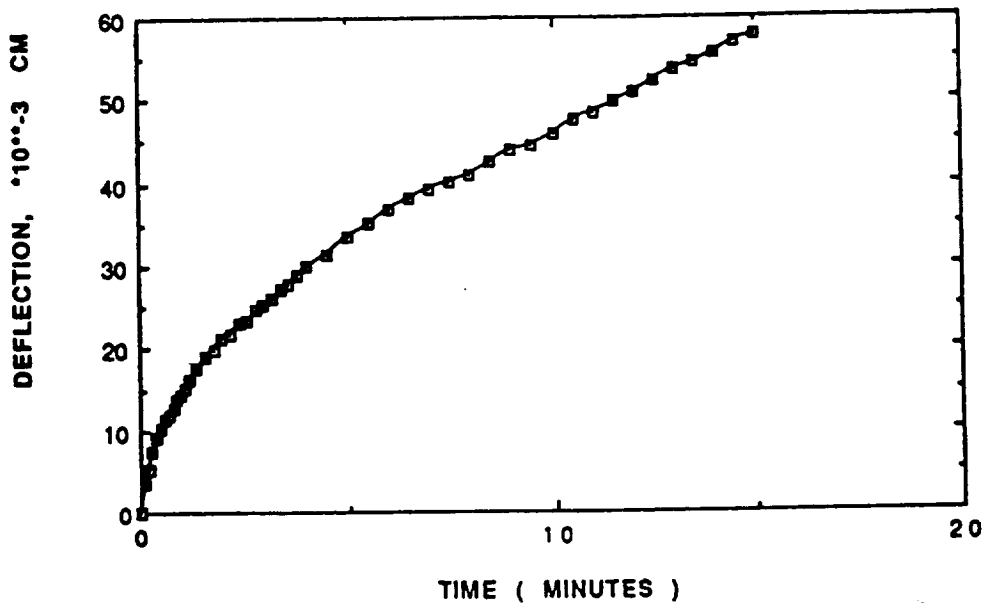


Figure 3. Typical deflection-time curve of sintered silicon nitride

DISCUSSION

The apparent viscosity data is seen to decrease with increasing temperature as expected. For example, the apparent viscosity of SN84/16 decreases from 14.73 \log_{10} Pa s to 13.34 \log_{10} Pa s as the temperature increases from 1305 °C to 1405 °C.

Summary of sintered Si_3N_4 viscosity data.			
composition	T (°C)	$\log_{10} \eta_{\text{app}}$ (\log_{10} Pa s)	$\log_{10} \eta_{\text{int}}$ (\log_{10} Pa s)
6Y(K) #2	1305	N/A	N/A
#5	1330	14.45	7.20 [6.79-7.60]
#3	1355	13.96	6.71 [6.30-7.11]
#6	1405	N/A	N/A
SN84/16 #21	1305	14.73	8.27 [7.99-8.53]
#16	1355	13.79	7.33 [7.05-7.59]
#8	1405	13.34	6.88 [6.60-7.14]
SN76/24 #12	1305	13.66	6.54 [6.11-6.96]
#7	1330	13.62	6.50 [6.07-6.92]
#6	1355	13.40	6.28 [5.85-6.70]
#11	1385	14.01	6.89 [6.46-7.31]
#4	1405	14.40	7.28 [6.85-7.70]
SN60/40 #8	1305	13.83	7.45 [7.24-7.67]
#9	1330	13.98	7.60 [7.39-7.82]
#5	1355	N/A	N/A
#7	1405	N/A	N/A

Table 2. Summary of sintered silicon nitride viscosity data.

Exceptions to this in the viscosity data occur in the SN76/24 and 6Y above 1385 °C and in the SN60/40. The expected decrease in apparent viscosity is observed in the SN76/24 material until 1385 °C is reached, whereupon the apparent viscosity is seen to increase sharply. This is due to crystallization of the glassy phase, thereby increasing the total amount of crystallinity in the material. From equation (2), it is clear that increased crystallinity results in higher values of $\eta_{\text{rel,avg}}$, and therefore increased apparent viscosities. Crystallization of the intergranular glass was observed to occur to some extent during all of the tests. No attempt was made to obtain an estimate of the amount of crystallization. Measurements of the apparent viscosity were made 15 minutes after the furnace reached the desired setpoint. This was done in order to try to minimize the effects of crystallization to the viscosity measurements. Additionally, there is no microstructural evidence to suggest that dissolution of the β - Si_3N_4 into the glass phase occurred.



Average values of the intergranular glass viscosity based on the measured volume fraction were calculated for 1305, 1330, and 1355 °C. These values are plotted vs $1/T$ in figure 4 along with data obtained for Amersil fused silica. The viscosity of the intergranular glass is seen to be ≈ 3 orders of magnitude less than that of fused silica at a given temperature within the range of study. This is as expected, since pure silica possesses the highest viscosity of any glass, which is reduced with the addition of an oxide such as Y_2O_3 . Differences in intergranular glass viscosities at a given temperature may be attributed to differences in the glass compositions or to differences in crystallization behavior among the different compositions. An activation energy was also calculated from the averaged viscosity data assuming an Arrhenius dependence of viscosity on temperature. The value obtained was 631.6 ± 7.6 kJ/mol. This value is consistent with the activation energy for flow of certain silicate glasses, ≈ 600 kJ/mol [15]. The activation energy for viscous flow of the silica glass in figure 3 is ≈ 570 kJ/mol.

INTERGRANULAR GLASS VISCOSITY

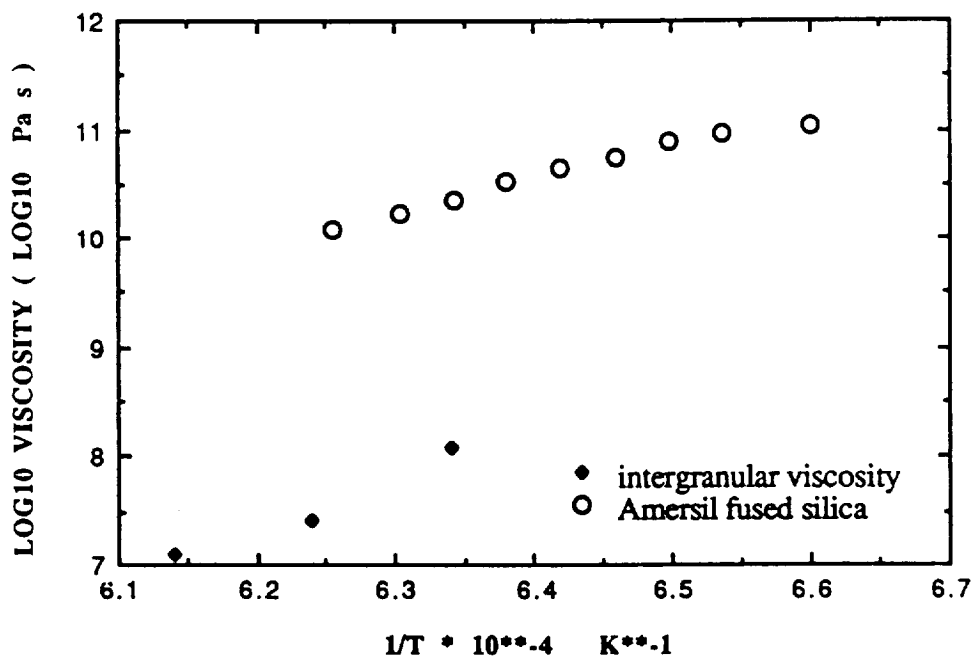


Figure 4. Sintered silicon nitride intergranular glass viscosity.

V. CONCLUSIONS

The viscosity of the intergranular glass in a yttria-sintered Si_3N_4 has been calculated from the apparent viscosity data of the bulk material. Reasonable values for intergranular glass viscosity can be obtained by using the relative viscosity values extrapolated from the physical modeling data. An activation energy for flow of the intergranular glass can be calculated from the data, and the result is comparable to the activation energy for viscous flow of certain silicate glasses.

REFERENCES

1. A.G. Evans and J.V. Sharp, " Microstructural Studies on Silicon Nitride ", J. Mat. Sci. 6 (1971) 1292-1302.
2. D.R. Clarke and G. Thomas, " Microstructure of Y_2O_3 Fluxed Hot-Pressed Silicon Nitride ", J. Am. Cer. Soc. 61 (1978) 114-118.
3. C.L. Quackenbush, J.T. Smith, J.T. Neil, and K.W. French, " Sintering, Properties and Fabrication of $Si_3N_4 + Y_2O_3$ Based Ceramics ", ed. F.L. Riley, Progress in Nitrogen Ceramics, (1983) 669-682.
4. R. Kossowsky, " The Microstructure of Hot Pressed Silicon Nitride ", J. Mat. Sci. 8 (1973) 1603.
5. R. Raj, D. Mosher, and R. Kossowsky, " Measurement of the Viscosity of the Grain Boundary Phase in Hot Pressed Silicon Nitride ", J. Mat. Sci., 11 (1976) 49-53.
6. C.A. Anderson and R. Bratton, " Ceramic Materials for High Temperature Turbines ", Final Technical Report, U.S. Energy Res. Dev. Adm. Contract No. EY-76-C-05-5210, Aug. 1977.
7. A. Tsuge and K. Nishida, " High Strength Hot Pressed Silicon Nitride with Concurrent Y_2O_3 and Al_2O_3 Additions ", Bull. Am. Cer. Soc. 57 (1978) 429-431.
8. F.F. Lange, " High Temperature Deformation and Fracture Phenomena of Polyphase Si_3N_4 Materials ", ed. F.L. Riley, Progress in Nitrogen Ceramics, (1983) 467-489.
9. D.R. Clarke, " On the Equilibrium Thickness of Intergranular Glass Phases in Ceramic Materials ", J. Am. Cer. Soc. 70 (1987) 15-22.
10. S. Kumar, Master's thesis, The Ohio State University, (1989).
11. L. A. Pierce, D. M. Mieskowski, and W.A. Sanders, " Effect of Grain Boundary Crystallization on the High Temperature Strength of Silicon Nitride ", J. Mat. Sci. 21 (1986) 1345-1348.
12. H.E. Hagy, " Experimental Evaluation of Beam Bending Method for Determining glass Viscosities in the Range 10^8 to 10^{15} poises ", J. Am. Cer. Soc. 46 (1963) 93-97.
13. E.H. Fontana and W.A. Plummer, " A Study of Viscosity-Temperature Relationships in the GeO_2 and SiO_2 Systems ", Phys. Chem. Glasses, 7 (1966) 139.
14. J.A. Todd, Zhi-Yue Xu, " The High Temperature Creep Deformation of $Si_3N_4 - 6Y_2O_3 - 2Al_2O_3$ ", J. Mat. Sci. 24 (1989) 4443-4452.
15. G.R. Fonda, " Zinc-Silicate Phosphors ", J. Phys. Chem. 44 (1940) 851.

Crystallization of the Yttria Silicate Intergranular Phase in Silicon Nitride with Zirconia Additions

K. A. Kuechelmann and C. H. Drummond, III
Department of Materials Science and Engineering, The Ohio State University, Columbus, OH 43210

Abstract: Crystallizing the grain boundary glassy phase in liquid-phase sintered Si_3N_4 with zirconia additions has been studied as a function of post-fabricating heat treatment. Delta- $\text{Y}_2\text{Si}_2\text{O}_7$ is crystallized in the grain boundaries after heat treatments for 2 h between 1200 C and 1400 C. Heat treatments at 1500 C and 1600 C result in the crystallization of beta- $\text{Y}_2\text{Si}_2\text{O}_7$. Details of the crystallization behavior of a simulated bulk glass composition with added zirconia is also presented.

I. Introduction

Interest in sintering covalent crystalline solids such as silicon nitride (Si_3N_4) to theoretical density stems from the potentially excellent high temperature properties which would make it suitable for applications in the aerospace industry or in gas turbine engines. In order to achieve dense silicon nitride, oxide sintering aids are generally added [1-3]. However, the glassy phase subsequently formed softens by 1200 C, degrading properties above this temperature sharply [4]. Crystallization of the intergranular phase to a more refractory phase(s) via post-sintering heat treatments is one method by which improvements in mechanical strength may be achieved [5]. The addition of zirconia to silicon nitride has proved to be an effective densifier [6,7], and is also a known nucleating agent in glass ceramics [8,9]. Previous studies [10-12] have shown Si_3N_4 with Y_2O_3 as a sintering aid to crystallize delta- $\text{Y}_2\text{Si}_2\text{O}_7$ after heat treatments for 2 h or less at 1500 C while longer heat treatments at 1500 C resulted in the crystallization of beta- $\text{Y}_2\text{Si}_2\text{O}_7$. Zirconia additions are introduced to enhance crystallization of these yttrium disilicate polymorphs, and perhaps encourage a crystallization sequence more in line with that reported by Ito and Johnson [13].

(1)

II. Experimental Procedure

The initial powders used to fabricate the simulated bulk glass composition consisted of 56.43 wt% Y_2O_3 , 38.57 wt% SiO_2 , and 5.00 wt% zyttrite. Zyttrite is a fine-particulate (0.05 micron) yttria stabilized cubic zirconia (c- ZrO_2) with 6.5 mol% Y_2O_3 . After processing and drying, the material was pressed into pellets, filled into either W or Mo crucibles, and melted at 2100 C for 4 h at either 1 or 25 atm N_2 . Annealing was performed in air at temperatures ranging from 1300 C - 1650 C at 0.5 to 120 h. The heating rate from room temperature to 1500 C was 10 C/min and the cooling rate approximately 15 C/min.

Samples were finely ground to a powder and studied by x-ray diffraction after heat treatment. Analytical electron microscopy was performed. Standard ceramographic techniques were used in the preparation of TEM specimens. Three mm discs were cut ultrasonically and then mechanically wet polished to 100 microns in thickness. Final polishing and dimpling was accomplished sequentially with 15, 6 and 1 micron diamond compounds. Samples were cryomilled (two Ar⁺ beams) to avoid transformations between crystalline and amorphous species. Milling was performed at 6 kV, 1 mA at angles ranging between 15 and 8 degrees. During the last 30 minutes of milling, the settings were decreased to 3 kV and 0.5 mA to remove amorphous layer build-up. Selected area diffraction patterns of yttrium disilicate polymorphs were solved using the computer program DFTools and crystallographic data previously reviewed by Liddel and Thompson [14].

Silicon nitride samples were prepared from initial powders: 92.44 wt% Si₃N₄, 6.96 wt% Y₂O₃, and 0.6 wt% zyttrite. The amount of zyttrite added approximately equaled 5 wt% in the intergranular phase. The powders were milled in high-purity silicon nitride grinding media and ethanol. They were then vacuum dried and die pressed at 21 MPa and subsequently cold isostatically pressed at 50 atm N₂. The samples were heat treated in a nitrogen atmosphere for 2 h at temperatures ranging from 1200 C to 1600 C and at 1500 C for 5 and 20 h. The heating rate from room temperature was 42 C/min and cooling rate approximately 130 C/min upon turning off the furnaces.

X-ray diffraction was performed on solid silicon nitride samples. TEM specimen preparation was similarly performed as described above, however, samples were polished to 60 microns in thickness before dimpling and ion milling. Electron microscopy and EDS analysis were again used to examine the grain boundary phase content.

III. Results

Bulk Glass Composition

(1) As-melted samples

The as-melted samples of the simulated bulk glass composition crystallized beta-Y₂Si₂O₇ regardless of nitrogen partial pressure or melting crucible employed. X-ray diffraction did not indicate any amorphous content, however bright-field TEM (Figure 1) did show silica rich pockets which were determined to be amorphous by characteristic diffuse ring patterns.

(2) Heat Treatments 1300 C - 1425 C

After heat treatments in this temperature range, at times up to 20 h, beta-Y₂Si₂O₇ was consistently determined to be present. At longer heat treatments, 48 to 120 h, gamma-Y₂Si₂O₇ was the predominant phase at 1400 C and above.

(3) Heat Treatments 1425 C - 1600 C

Gamma-Y₂Si₂O₇ was favored in this temperature region for all heat treatments, with exception at very short heat treatment times. At 1500 C and up to one hour heat treatments, beta-

$Y_2Si_2O_7$ remained the major phase present. Delta- $Y_2Si_2O_7$ began to crystallize at about 1600 C for those heat treatments of 5 hours or longer.

(4) Heat Treatments at 1650 C

A mixture of gamma- and delta- $Y_2Si_2O_7$ crystallized after heat treatment at 1650 C for 20 h.

Figure 2 demonstrates schematically the x-ray diffraction results obtained for the bulk glass sample melted at 1 atm N_2 in a W crucible, designated 'GS1/5(W)'. Each letter represents the phase or phases found present after heat treatment. When it was qualitatively determined that one phase predominated over another, an ">" separates them. Traces of phase present are indicated by parentheses. The horizontal lines at 1445 C and 1535 C indicate the temperatures at which the transformations from beta to gamma and gamma to delta have been previously reported.

Analytical electron microscopy performed indicated confirmation of these findings, while the presence of cristobalite as a minor phase was also verified. Zirconia was confirmed to be cubic in structure, as was the initial zyttrite powder.

Figure 3 is a schematic representation of the phase transformations in the simulated bulk glass. These results demonstrate that the transformations are sluggish. The approximate polymorphic transformations of yttrium disilicate from beta to gamma and gamma to delta occur at 1425 C and 1600 C respectively for 20 hour heat treatments. The gamma- phase appears preferentially stabilized as compared with the reported phase stability region by Ito and Johnson.

Silicon Nitride Composition

(1) As-sintered specimen

The as-sintered specimen of the 6Y Si_3N_4 with zirconia additions demonstrated an amorphous grain boundary phase as confirmed by TEM. Figure 4 shows the general morphology of the specimen with the corresponding ring pattern obtained from the intergranular phase. Figure 5 demonstrates both bright field and dark field images of the intergranular phase, the diffuse scattering of electrons again indicating the amorphous nature of the grain boundary region. EDS analysis was performed over four regions of the intergranular phase and weight percents of oxide components were calculated to be: 53.20 wt% Y_2O_3 , 44.16 wt% SiO_2 , and 2.65 wt% ZrO_2 . These results correspond well with the composition of the simulated bulk glass composition.

(2) Heat Treatments 1200 C - 1400 C

Heat treatments for 2 h between 1200 C and 1400 C crystallized delta- $Y_2Si_2O_7$ as the grain boundary phase. The morphology of the yttrium disilicate intergranular phase was characterized by a fine-grained mottled nature as shown in Figure 6.

(3) Heat Treatments 1500 C - 1600 C

An isothermal study at 1500 C for 2, 5, and 20 hour heat treatments revealed that while the yttrium disilicate polymorph crystallized was beta-Y₂Si₂O₇ in all cases, the morphology of the phase changed with increasing heat treatment times. The intergranular beta-yttrium disilicate phase had a larger grain size and appeared interconnected in contrast to the delta-phase. At 2 h heat treatment (Figure 7), beta-Y₂Si₂O₇ appeared at a single orientation, as demonstrated by dark-field images obtained using a spot diffracted by the intergranular phase, over limited areas of the microstructure. After 5 h (shown in Figure 8) and 20 h heat treatments, the beta- phase appeared at a single orientation over 5 microns and 20 microns respectively.

IV. Discussion

Reaction Sequence

a. Bulk Glass Composition

The phases of yttrium disilicate in the GS/5 compositions followed a sequence similar to that reported by Ito and Johnson, with the exception that the alpha-Y₂Si₂O₇ polymorph was never observed. The kinetics of the transformation were sluggish in all cases, the reaction being highly dependent upon time of heat treatment, as shown below:

	1500 C		(0.5 h)	
	1425 C	1600 C	(20 h)	
beta	-----	gamma	-----	delta
	1350 C		(120 h)	

Earlier studies by Kumar and Drummond examined a composition identical to the composition studied here, except that no zirconia was added. Their study revealed that beta-yttrium disilicate was not crystallized upon quenching as it was in this case. Depending upon the cooling rate of the furnace used, either delta- or gamma-Y₂Si₂O₇ crystallized. No beta-Y₂Si₂O₇ was ever observed. The initial yttrium disilicate phase crystallized upon quenching may have affected subsequent phases formed.

b. Silicon Nitride Composition

The observed reaction sequence for the intergranular phase in the 6y Si₃N₄ composition with 0.5 wt% zyttrite added differed from that of the bulk glass significantly. The grain boundary phase was amorphous prior to heat treatment and crystallized delta-Y₂Si₂O₇ and ultimately beta- after higher temperature heat treatments as described below:

	1200 C	1400 C	(2 h)	
amorphous	-----	delta	-----	beta

This reaction sequence does, however, correspond well with studies previously performed on a similar 6Y composition without zirconia performed by Hilmas and Lee. In their study, the grain boundary phase was also amorphous before heat-treatment, and

similarly crystallized delta-yttrium disilicate after heat treatments at 1200 C, 2 h. However, in their study the crystallization of beta- occurred at a higher temperature, 1500 C, after heat treatments of 5 h or longer.

V. Conclusions

The introduction of zirconia to the 6Y silicon nitride composition acted to increase the number of heterogeneous sites for nucleation to accelerate the delta to beta transformation. The zirconia appears to have stabilized the presence of the beta- $Y_2Si_2O_7$ polymorph in both the GS bulk glass composition and the 6Y silicon nitride composition.



REFERENCES

- ¹G. R. Terwillier, F. F. Lange, "Pressureless Sintering of Si_3N_4 ," *J. Mat. Sci.*, **10**, 1169-74 (1975).
- ²N. Hirosaki, A. Okada, and K. Matoba, "Sintering of Si_3N_4 with the Addition of Rare-Earth Oxides," *J. Am. Ceram. Soc.*, **71** [3] C-144-7 (1988).
- ³T. Hayashi, H. Munakata, H. Suzuki, H. Saito, "Pressureless Sintering of Si_3N_4 with Y_2O_3 and Al_2O_3 ," *J. Mat. Sci.*, **21**, 3501-8 (1986).
- ⁴A. Giachello, P. C. Martinengo, G. Tommasini, and P. Popper, "Sintering and Properties of Silicon Nitride Containing Y_2O_3 and MgO ," *Bull. Am. Ceram. Soc.*, **59** [12] 1212-15 (1980).
- ⁵D. R. Clarke, F. F. Lange, and G. D. Schnittgrund, "Strengthening of a Sintered Silicon Nitride by a Post-Fabrication Heat Treatment," *J. Am. Ceram. Soc.*, C-51-2 (1982).
- ⁶W. A. Sanders and D. M. Mieskowski, "Strength and Microstructure of Si_3N_4 Sintered with ZrO_2 Additions," *Adv. Ceram. Mat.*, **1** [2] 166-73 (1986).
- ⁷S. Dutta and B. Buzek, "Microstructure, Strength, and Oxidation of a 10 wt% Zyttrite - Si_3N_4 Ceramic," *J. Am. Ceram. Soc.*, **67** [2] 89-92 (1984).
- ⁸P. F. James, "Nucleation in glass-forming systems - a review"; pp. 1-48 in *Advances in Ceramics 4: Nucleation and Crystallization in Glasses*. Ed. by J. H. Simmons, D. R. Uhlmann, and G. H. Beall. The American Ceramic Society, Inc., Columbus, OH, 1982.
- ⁹P. W. McMillan. *Glass Ceramics*, 2nd ed. Academic Press, London, 1979.
- ¹⁰W. E. Lee and G. E. Hilmas, "Microstructural Changes in Beta-Silicon Nitride Grains upon Crystallizing the Grain-Boundary Glass," *J. Am. Ceram. Soc.*, **72** [10] 1931-7 (1989).
- ¹¹G. E. Hilmas and W. E. Lee, "Crystallizing $\text{Y}_2\text{Si}_2\text{O}_7$ at the Grain Boundaries of a Si_3N_4 Ceramic"; pp. 608-9 in *Proceedings of the 46th Annual Meeting of the Electron Microscopy Society of America*. Ed. by G. W. Bailey. San Francisco Press, Inc., San Francisco, CA 1988.
- ¹²W. E. Lee, C. H. Drummond, III, and G. E. Hilmas, "Microstructural Evolution on Crystallizing the Glassy Phase in a 6 wt% Y_2O_3 - Si_3N_4 Ceramic," *Ceram. Eng. Sci. Proc.*, **9** [9-10] (1988).

¹³J. Ito and H. Johnson, "Synthesis and Study of Yttrialite," Am. Mineralogist, **53**, 1940-52 (1968).

¹⁴K. Liddell and D. P. Thompson, "X-ray Diffraction Data for Yttrium Silicates," Br. Ceram. Trans. J., **85**, 17-22 (1986).

